

Micro-Fabricated Penning Trap Arrays for Quantum Simulation

by

Shreyans Jain

A THESIS SUBMITTED IN PARTIAL FULFILLMENT
OF THE REQUIREMENTS FOR THE DEGREE OF

MASTER OF SCIENCE
PHYSICS
ETH ZÜRICH

APRIL, 2018

MICRO-FABRICATED PENNING TRAP ARRAYS FOR QUANTUM SIMULATION
Shreyans Jain

M.Sc. Thesis

Supervisors: Dr. Joseba Alonso and Prof. Dr. Jonathan Home

Trapped Ion Quantum Information Group
Department of Physics
Eidgenössische Technische Hochschule Zürich

Acknowledgments

First and foremost, I would like to express my heartfelt gratitude to Dr. Joseba Alonso who proposed the topic of this thesis and was an extremely helpful presence throughout what has been a long journey. I could not have asked or hoped for a more exciting, challenging and motivating project. Joseba's contributions to the TIQI group here at ETH Zürich will be deeply missed and I wish him all the luck in his personal and professional life in València. Secondly, I would like to thank Prof. Dr. Jonathan Home for the opportunity to complete my masters thesis along with other research projects in his group. I had the pleasure of having several useful discussions with him, specially over the latter half of this thesis. His physical insight into what appear as merely mathematical formulations and results is unique. I am also grateful to Dr. Matt Grau for helping me with several aspects of this project, and in particular everything to do with normal mode calculations. Finally, a special thanks to all current and past members of the TIQI group for providing a wonderful atmosphere to work in. The kicker breaks initiated more often than not by Oliver have always been very welcome.

Contents

ACKNOWLEDGMENTS	iv
o INTRODUCTION	1
1 PENNING TRAPS	3
1.1 Classical Motion	3
1.2 Quantum Motion	6
1.3 Axialisation drive	9
2 ARRAYS OF PENNING TRAPS	14
2.1 Classical Motion	14
2.2 Quantum Motion	18
2.3 Axialisation drive	21
3 LASER COOLING OF IONS	22
3.1 Doppler Cooling of a Single Ion	22
3.2 Arrays of Traps	25
4 SPIN-SPIN COUPLING	30
5 SURFACE ELECTRODE TRAPS	36
6 BENCHMARKING RESULTS	41
7 CONCLUSIONS AND OUTLOOK	51
APPENDIX A QUADRATIC EIGENVALUE PROBLEM	52
APPENDIX B NORMAL MODE ANALYSIS: CLASSICAL DESCRIPTION	56
APPENDIX C NORMAL MODE ANALYSIS: QUANTUM DESCRIPTION	63
APPENDIX D TRAP IMPERFECTIONS	73
APPENDIX E NORMAL MODES OF A SINGLE ION	76
APPENDIX F NORMAL MODES OF LINEAR CHAINS	80
APPENDIX G DOPPLER COOLING	86
APPENDIX H SPIN-SPIN COUPLING	93
REFERENCES	99

O

Introduction

Simulating quantum mechanical systems is a challenging computational task given the exponential scaling in the number of parameters required to describe the system with increasing system size. This unavoidable problem makes calculations for a few tens of spins already intractable on even the most powerful classical computers in existence¹. It can be possible, however, to simulate a complex quantum system by using another quantum system that can be manipulated more easily, as proposed by Richard Feynman in 1982². While a universal quantum computer would fulfill this requirement³, experimental implementations of such devices are still far off and it would be sufficient to use simpler special-purpose analog devices that can emulate a specific Hamiltonian of interest⁴. Analog quantum simulators would be easier to construct and control and could allow for a better understanding of the evolution of complicated quantum systems such as spin models in condensed-matter physics.

Trapped ions provide an attractive platform for realising quantum simulation⁵ as quantum information can be encoded in the internal energy levels as well as the external motional states of the ions. Ion qubits have long coherence times and strong long range interactions between ions can be mediated through Coulomb repulsion. This makes it possible for state preparation, single and two-qubit gates, and state determination to be performed with high fidelity, as has been demonstrated in laboratory experiments over the last two decades⁶.

To date, most quantum simulation experiments with trapped ions have been performed with radio frequency traps, also called Paul traps⁷, where the system of ions is confined using oscillating electric fields in a single potential well. A recent implementation involving 53 ion spins has been used to study dynamical phase transitions in the transverse-field Ising model⁸, but the ions are restricted to a linear string formation. This is because ions in Paul traps inherently suffer from micromotion⁹ which cannot only limit decoherence rates but also effectively allow an arrangement of ions only along the spatial direction where micromotion is minimised. Penning traps, on the other hand, confine ions with static electric and magnetic fields alone, meaning there is no micromotion

and with a strong magnetic field, high motional frequencies can be achieved¹⁰. The nature of the radial motion in a Penning trap does mean that the laser cooling process is not as straightforward as compared to Paul traps¹¹, but the application of small radio-frequency fields can help combat this problem whilst producing minimal micromotion¹². In fact, the largest quantum-spin simulator built so far consists of hundreds of Beryllium ions arranged on a naturally occurring triangular lattice in a single Penning trap¹³.

While trapped ions are an excellent prospect for quantum information processing, the crucial issue for experiments, as with other proposed platforms, has been scalability. Two-dimensional arrays of microtraps, where each ion is placed in its own harmonic well, show much more promise in this direction as compared to trapping in a common potential¹⁴. Such proposals were initially made for arrays of Paul traps but apply equally well in the case of Penning traps. Planar electrode structures in conjunction with a global magnetic field can be optimised to create arbitrary configurations of trapped ions, allowing for the study of any lattice of choice¹⁵. It would be more straightforward to achieve this in the case of Penning traps as compared to Paul traps since no pseudopotential approximation is required, and with no micromotion the traps are more resilient to stray electric fields. With these miniaturised Penning trap arrays it would be feasible to gain individual control over ions as well as devise tuneable interactions along more than one spatial dimension. Such couplings can be engineered, for instance, through optical dipole forces that create coherent state-dependent displacements and mimic an effective spin Hamiltonian by modifying the Coulomb energy of the ions¹⁶.

In this thesis, work towards implementing a quantum spin simulator using micro-fabricated arrays of Penning traps is organised as follows:

- Chapter 1 discusses the basic trapping mechanism in a Penning trap along with the classical and quantum dynamics of a single trapped ion
- Chapter 2 generalises this discussion to ions in arrays of Penning traps with a complete normal mode analysis in the classical and quantum regimes
- Chapter 3 describes the process of laser cooling ions in Penning traps
- Chapter 4 illustrates the generation of effective Ising-like spin interactions using optical dipole forces
- Chapter 5 summarises the design and optimisation of surface electrode structures to generate suitable trapping potentials
- Chapter 6 characterises the expected performance of the proposed spin simulator based on different ion lattice configurations
- Chapter 7 concludes this thesis and offers an outlook for further research
- Appendices A-H consist of the derivations of all major results presented in the main body of thesis

1

Penning Traps

Trapping a charged particle in space requires a potential minimum in all three dimensions. Electrostatic fields alone, however, cannot confine a charged particle in three dimensions*. The Penning trap uses a quadrupolar electrostatic potential which confines along one of the trap axes but is anti-confining in the other two. Confinement in the plane perpendicular to the trapping axis is achieved through the use of a strong homogeneous magnetic field along this axis. The classical motion of an ion in a Penning trap can be described as follows.

1.1 CLASSICAL MOTION

Assume an ion of mass m and charge $+e$ in an electrostatic potential varying spatially as $V(x, y, z) = \phi_0(z^2 - (x^2 + y^2)/2)$ and a uniform magnetic field $\mathbf{B} = B_0\hat{z}$. Then the equation of motion of the ion is

$$m\ddot{\mathbf{r}} = -e\nabla V + e(\mathbf{v} \times \mathbf{B}), \quad (1.1)$$

which can be written in terms of the three Cartesian components as

$$m\ddot{x} = e\phi_0 x + eB_0\dot{y}, \quad (1.2a)$$

$$m\ddot{y} = e\phi_0 y - eB_0\dot{x}, \quad (1.2b)$$

$$m\ddot{z} = -2e\phi_0 z. \quad (1.2c)$$

*This result is known as Earnshaw's theorem and can be derived by considering the Laplace equation for a charged particle in free space

The general solutions to these equations are

$$x = \frac{r_+}{\sqrt{2}} \cos(\omega_+ t + \delta_+) + \frac{r_-}{\sqrt{2}} \cos(\omega_- t + \delta_-), \quad (1.3a)$$

$$y = -\frac{r_+}{\sqrt{2}} \sin(\omega_+ t + \delta_+) - \frac{r_-}{\sqrt{2}} \sin(\omega_- t + \delta_-), \quad (1.3b)$$

$$z = r_z \cos(\omega_z t + \delta_z), \quad (1.3c)$$

where the amplitudes $\{r_+, r_-, r_z\}^\dagger$ are assumed to be positive and the phases $\{\delta_+, \delta_-, \delta_z\}$ are determined by the initial conditions. The motion comprises of three frequencies, the axial frequency ω_z , the reduced cyclotron frequency ω_+ , and the magnetron frequency ω_- defined as

$$\omega_z = \sqrt{2e\phi_0/m}, \quad (1.4a)$$

$$\omega_\pm = \frac{\omega_c \pm \sqrt{\omega_c^2 - 2\omega_z^2}}{2}, \quad (1.4b)$$

with $\omega_c = eB_0/m$ being the true cyclotron frequency. For stable confinement of the ion we require these frequencies to be real, leading to the stability criterion

$$\omega_z < \omega_c / \sqrt{2}, \quad (1.5)$$

which translates to an upper bound on the potential,

$$\phi_0 < \frac{eB_0^2}{4m}. \quad (1.6)$$

In this sense, the quadrupole potential needs to be weaker than the magnetic potential. Increasing the potential beyond this limit leads to the ion being no longer confined in the radial plane. The axial frequency ω_z can be either higher or lower than ω_+ but is always higher than ω_- . Typically we have the following hierarchy of eigenfrequencies,

$$\omega_- < \omega_z < \omega_+. \quad (1.7)$$

The motion of the ion along the \hat{z} -axis is just simple harmonic motion at the frequency ω_z . The motion along the \hat{x} - and \hat{y} -axes is coupled together and the trajectory of the ion is a superposition of the two circular orbits corresponding to the fast reduced cyclotron motion and the slower magnetron motion in the radial (\hat{x} - \hat{y}) plane. This epicyclic radial motion along with the total trajectory of the ion in three dimensions is depicted in fig. 1.1.

[†]The notation used here for the amplitudes of radial modes differs from the one typically found in other texts (for eg. in ref. ¹¹) by a factor of $\sqrt{2}$. This stems from the fact that the normal mode vectors in this thesis have been normalised. With the notation kept consistent, the same discrepancy will be present in the following chapters

The kinetic and potential energy of the ion are given as

$$E_k \equiv \frac{1}{2}mv^2 = \frac{1}{4}mr_+^2\omega_+^2 + \frac{1}{4}mr_-^2\omega_-^2 + \frac{1}{2}mr_+r_-\omega_+\omega_-\cos(\omega_+t - \omega_-t + \delta_+ - \delta_-) + \frac{1}{2}mr_z^2\omega_z^2\sin^2(\omega_zt + \delta_z), \quad (1.8a)$$

$$E_p \equiv eV(\mathbf{r}) = \frac{1}{2}m\omega_z^2\left\{r_z^2\cos^2(\omega_zt + \delta_z) - \frac{1}{4}(r_+^2 + r_-^2) - \frac{1}{2}r_+r_-\cos(\omega_+t - \omega_-t + \delta_+ - \delta_-)\right\}. \quad (1.8b)$$

Thus the total energy of the system

$$E = E_k + E_p = \frac{1}{2}m\omega_z^2r_z^2 + \frac{1}{2}m\Omega(\omega_+r_+^2 - \omega_-r_-^2) \quad (1.9)$$

is a constant of motion. Here $\Omega = (\omega_+ - \omega_-)/2$. The total energy contained in each mode

$$E_z = \frac{1}{2}m\omega_z^2r_z^2, \quad (1.10a)$$

$$E_+ = \frac{1}{2}m\Omega\omega_+r_+^2, \quad (1.10b)$$

$$E_- = -\frac{1}{2}m\Omega\omega_-r_-^2, \quad (1.10c)$$

is also constant while the time-averaged kinetic energy in each mode is given by

$$\langle E_{kz} \rangle = \frac{1}{4}m\omega_z^2r_z^2, \quad (1.11a)$$

$$\langle E_{k+} \rangle = \frac{1}{4}m\omega_+^2r_+^2, \quad (1.11b)$$

$$\langle E_{k-} \rangle = \frac{1}{4}m\omega_-^2r_-^2. \quad (1.11c)$$

Reducing the amplitude of the axial or reduced cyclotron modes reduces the total energy contained in the mode, and these two modes are stable. On the contrary, the total energy of the magnetron motion is negative and the ion can be seen as sitting on an effective potential hill in the radial plane. An increase in the amplitude r_- , for example due to collisions with background gas, will lead to a decrease in the total energy meaning this motion is unstable, but typically in experiments the magnetron motion is slow and weakly coupled to the environment resulting in storage times long enough for effective stability¹⁰.

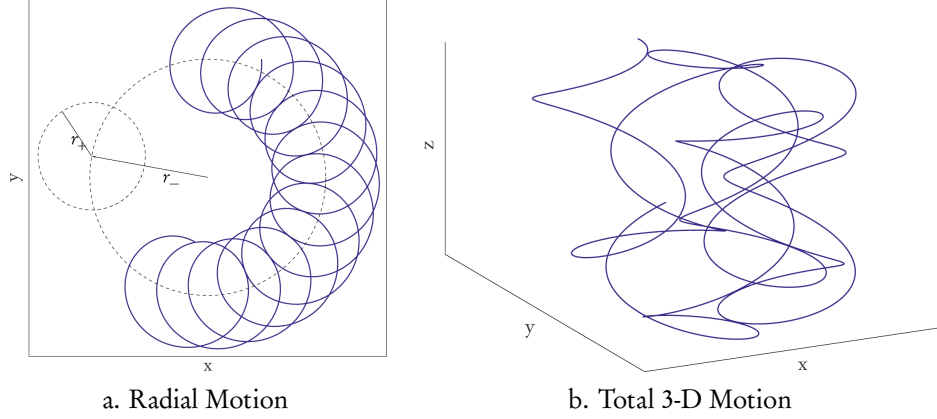


Figure 1.1: Motion of a single ion in a Penning trap

1.2 QUANTUM MOTION

The quantum mechanical treatment of a single ion in the ideal Penning trap discussed can be carried out by constructing the Hamiltonian operator

$$H = \frac{(\mathbf{p} - e\mathbf{A})^2}{2m} + eV(\mathbf{r}) \quad (1.12)$$

in terms of the canonical position and momentum operators \mathbf{r} and \mathbf{p} . In the symmetric gauge the vector potential is given by $\mathbf{A} = \frac{1}{2}(\mathbf{B} \times \mathbf{r})$ and the Hamiltonian can be expressed as $H \equiv H_{xy} + H_z$, where

$$H_{xy} = \frac{p_x^2 + p_y^2}{2m} + \frac{1}{2}m\Omega^2(x^2 + y^2) - \frac{1}{2}\omega_c(xp_y - yp_x) \quad (1.13a)$$

and

$$H_z = \frac{p_z^2}{2m} + \frac{1}{2}m\omega_z^2 z^2 \quad (1.13b)$$

are respectively the radial and axial parts.

The axial part H_z is the Hamiltonian of a simple harmonic oscillator in one dimension and can be written in the second quantised form in terms of the creation and annihilation operators[‡]

$$a_z^\dagger = \sqrt{\frac{1}{2\hbar m \omega_z}} p_z + i \sqrt{\frac{m \omega_z}{2\hbar}} z, \quad (1.14a)$$

[‡]The notation used here for the ladder operators corresponding to all modes is non-standard and differs other texts (for eg. in ref.¹¹ and in ref.¹⁰). A full derivation can be found in the appendices

$$a_z = \sqrt{\frac{1}{2\hbar m\omega_z}} p_z - i\sqrt{\frac{m\omega_z}{2\hbar}} z \quad (1.14b)$$

as

$$H_z = \hbar\omega_z \left(a_z^\dagger a_z + \frac{1}{2} \right). \quad (1.15)$$

With $z_0 = \sqrt{\hbar/(2m\omega_z)}$, the operators z and p_z take the form

$$z = iz_0(a_z - a_z^\dagger), \quad (1.16a)$$

$$p_z = m\omega_z z_0(a_z + a_z^\dagger). \quad (1.16b)$$

The radial part of the Hamiltonian H_{xy} contains a term dependent on the axial component of the angular momentum $L_z = x p_y - y p_x$ in addition to the Hamiltonian of a two-dimensional isotropic simple harmonic oscillator. This term couples the motion in the radial plane. The construction of the operators

$$a_+^\dagger = \sqrt{\frac{1}{4\hbar m\Omega}} (p_x - i p_y) + i\sqrt{\frac{m\Omega}{4\hbar}} (x - iy) \quad (1.17a)$$

$$a_+ = \sqrt{\frac{1}{4\hbar m\Omega}} (p_x + i p_y) - i\sqrt{\frac{m\Omega}{4\hbar}} (x + iy) \quad (1.17b)$$

$$a_-^\dagger = \sqrt{\frac{1}{4\hbar m\Omega}} (p_x + i p_y) + i\sqrt{\frac{m\Omega}{4\hbar}} (x + iy) \quad (1.17c)$$

$$a_- = \sqrt{\frac{1}{4\hbar m\Omega}} (p_x - i p_y) - i\sqrt{\frac{m\Omega}{4\hbar}} (x - iy) \quad (1.17d)$$

allows the radial motion to be decoupled, and reduces the radial Hamiltonian to

$$H_{xy} = \hbar\omega_+ \left(a_+^\dagger a_+ + \frac{1}{2} \right) - \hbar\omega_- \left(a_-^\dagger a_- + \frac{1}{2} \right). \quad (1.18)$$

Defining $r_0 = \sqrt{\hbar/(2m\Omega)}$, the operators x , y , p_x and p_y take the form

$$x = \frac{ir_0}{\sqrt{2}} (a_+ - a_+^\dagger + a_- - a_-^\dagger), \quad (1.19a)$$

$$y = \frac{r_0}{\sqrt{2}} (a_+ + a_+^\dagger - a_- - a_-^\dagger), \quad (1.19b)$$

$$p_x = \frac{m\Omega r_0}{\sqrt{2}} (a_+ + a_+^\dagger + a_- + a_-^\dagger), \quad (1.19c)$$

$$p_y = -\frac{im\Omega r_0}{\sqrt{2}} (a_+ - a_+^\dagger - a_- + a_-^\dagger). \quad (1.19d)$$

The three sets of creation and annihilation operators follow the standard commutation relations

$$[a_j, a_k] = 0, \quad [a_j^\dagger, a_k^\dagger] = 0, \quad [a_j, a_k^\dagger] = \delta_{jk}, \quad (1.20)$$

for $j, k = z, +, -$.

The total Hamiltonian of the system is thus

$$H = \hbar\omega_z \left(N_z + \frac{1}{2} \right) + \hbar\omega_+ \left(N_+ + \frac{1}{2} \right) - \hbar\omega_- \left(N_- + \frac{1}{2} \right), \quad (1.21)$$

where we define the number operators $N_z = a_z^\dagger a_z$, $N_+ = a_+^\dagger a_+$ and $N_- = a_-^\dagger a_-$.

The eigenstates of H are the composite number states $|n_z, n_+, n_- \rangle$

$$H|n_z, n_+, n_- \rangle = \left(\hbar\omega_z \left(n_z + \frac{1}{2} \right) + \hbar\omega_+ \left(n_+ + \frac{1}{2} \right) - \hbar\omega_- \left(n_- + \frac{1}{2} \right) \right) |n_z, n_+, n_- \rangle. \quad (1.22)$$

These can be constructed from the $|0, 0, 0 \rangle$ vacuum state by the application of raising operators

$$|n_z, n_+, n_- \rangle = \frac{1}{\sqrt{n_z! n_+! n_-!}} (a_z^\dagger)^{n_z} (a_+^\dagger)^{n_+} (a_-^\dagger)^{n_-} |0, 0, 0 \rangle \quad (1.23)$$

for any set of three non-negative integers $\{n_z, n_+, n_- \}$.

Comparing the expression for the total classical energy and the quantum Hamiltonian, the classical amplitudes and quantum phonon occupation numbers correspond as

$$r_z^2 \sim 4 \left(n_z + \frac{1}{2} \right) z_0^2, \quad (1.24a)$$

$$r_+^2 \sim 4 \left(n_+ + \frac{1}{2} \right) r_0^2, \quad (1.24b)$$

$$r_-^2 \sim 4 \left(n_- + \frac{1}{2} \right) r_0^2. \quad (1.24c)$$

It is clear from the Hamiltonian that while the reduced cyclotron and axial motion can be described in terms of simple harmonic oscillators, the magnetron motion corresponds to an inverted harmonic oscillator and with increasing n_- (which is the quantum analogue of increasing the classical amplitude r_-) the energy of the system decreases. This contrasting feature of the magnetron mode has implications on laser cooling and will be revisited later.

1.3 AXIALISATION DRIVE

The application of an oscillatory electric field can help control the radial motion of ions in a Penning trap. Driving this additional field at the free cyclotron frequency can be used to couple the cyclotron and magnetron motion to allow simultaneous efficient cooling of both modes. This technique is also called axialisation¹⁷.

CLASSICAL DESCRIPTION

The general solutions for the radial motion of an ion in a Penning trap can be written in the complex form

$$\begin{bmatrix} x \\ y \end{bmatrix} = \frac{1}{2} \left\{ \frac{\rho_+}{\sqrt{2}} \begin{bmatrix} 1 \\ i \end{bmatrix} e^{-i\omega_+ t} + \frac{\rho_+^*}{\sqrt{2}} \begin{bmatrix} 1 \\ -i \end{bmatrix} e^{i\omega_+ t} \right\} + \frac{1}{2} \left\{ \frac{\rho_-}{\sqrt{2}} \begin{bmatrix} 1 \\ i \end{bmatrix} e^{-i\omega_- t} + \frac{\rho_-^*}{\sqrt{2}} \begin{bmatrix} 1 \\ -i \end{bmatrix} e^{i\omega_- t} \right\}, \quad (1.25)$$

where $\rho_+ = r_+ e^{-i\delta_+}$ and $\rho_- = r_- e^{-i\delta_-}$.

With the addition of an oscillating quadrupolar potential

$$V_{\text{RF}} = \phi_{\text{RF}}(x^2 - y^2) \cos(\omega_{\text{RF}} t) \quad (1.26)$$

to the static trapping potential, the axial mode is left unaffected while the two radial modes couple together when the drive frequency is quasi-resonant with the sum frequency of the radial modes[§]. In the weak coupling limit $\phi_{\text{RF}} \ll \phi_0$ we can assume that the complex amplitudes of the cyclotron and magnetron modes vary slowly with time so that $\rho_{\pm} \equiv \rho_{\pm}(t)$.

When the frequency of the axialisation drive is closely detuned to the true cyclotron frequency, the time dependence of the mode amplitudes is captured by the pair of coupled equations

$$\frac{\Omega_{\text{RF}}^2}{4} e^{-i\delta t} \rho_-^*(t) - i\Omega \dot{\rho}_+(t) = 0, \quad (1.27a)$$

$$\frac{\Omega_{\text{RF}}^2}{4} e^{i\delta t} \rho_+(t) - i\Omega \dot{\rho}_-^*(t) = 0, \quad (1.27b)$$

where $\delta \equiv \omega_{\text{RF}} - (\omega_+ + \omega_-) = \omega_{\text{RF}} - \omega_c$ is the detuning, $\Omega = (\omega_+ - \omega_-)/2$, and $\Omega_{\text{RF}} = \sqrt{2e\phi_{\text{RF}}/m}$. With the initial conditions $\rho_+(0) = r_+ e^{-i\delta_+}$ and $\rho_-(0) = r_- e^{-i\delta_-}$, we get the oscillating solutions

$$\begin{aligned} \rho_+(t) = & \left\{ -\frac{\nu_-}{\sqrt{\delta^2 + \Omega_{\text{RF}}^4/(4\Omega^2)}} r_+ e^{-i\delta_+} + \frac{\Omega_{\text{RF}}^2}{4\Omega \sqrt{\delta^2 + \Omega_{\text{RF}}^4/(4\Omega^2)}} r_- e^{i\delta_-} \right\} e^{-i\nu_+ t} \\ & + \left\{ \frac{\nu_+}{\sqrt{\delta^2 + \Omega_{\text{RF}}^4/(4\Omega^2)}} r_+ e^{-i\delta_+} - \frac{\Omega_{\text{RF}}^2}{4\Omega \sqrt{\delta^2 + \Omega_{\text{RF}}^4/(4\Omega^2)}} r_- e^{i\delta_-} \right\} e^{-i\nu_- t}, \end{aligned} \quad (1.28a)$$

[§]For the cylindrically symmetric trap, $\omega_+ + \omega_- = \omega_c$.

$$\begin{aligned} \rho_-(t) = & \left\{ -\frac{\Omega_{\text{RF}}^2}{4\Omega\sqrt{\delta^2 + \Omega_{\text{RF}}^4/(4\Omega^2)}} r_+ e^{i\delta_+} - \frac{\nu_-}{\sqrt{\delta^2 + \Omega_{\text{RF}}^4/(4\Omega^2)}} r_- e^{-i\delta_-} \right\} e^{-i\nu_+ t} \\ & + \left\{ \frac{\Omega_{\text{RF}}^2}{4\Omega\sqrt{\delta^2 + \Omega_{\text{RF}}^4/(4\Omega^2)}} r_+ e^{i\delta_+} + \frac{\nu_+}{\sqrt{\delta^2 + \Omega_{\text{RF}}^4/(4\Omega^2)}} r_- e^{-i\delta_-} \right\} e^{-i\nu_- t}, \end{aligned} \quad (1.28b)$$

where the frequencies ν_{\pm} are defined as

$$\nu_{\pm} = \frac{\delta \pm \sqrt{\delta^2 + \Omega_{\text{RF}}^4/(4\Omega^2)}}{2}. \quad (1.29)$$

The absolute values of the amplitudes are

$$\begin{aligned} |\rho_+(t)|^2 = & r_+^2 \left\{ \frac{\delta^2}{\delta^2 + \Omega_{\text{RF}}^4/(4\Omega^2)} + \frac{\Omega_{\text{RF}}^4/(8\Omega^2)}{\delta^2 + \Omega_{\text{RF}}^4/(4\Omega^2)} (1 + \cos(\sqrt{\delta^2 + \Omega_{\text{RF}}^4/(4\Omega^2)} t)) \right\} \\ & + r_-^2 \left\{ \frac{\Omega_{\text{RF}}^4/(8\Omega^2)}{\delta^2 + \Omega_{\text{RF}}^4/(4\Omega^2)} (1 - \cos(\sqrt{\delta^2 + \Omega_{\text{RF}}^4/(4\Omega^2)} t)) \right\} \\ & - r_+ r_- \left\{ \frac{\delta \Omega_{\text{RF}}^2/(2\Omega)}{\delta^2 + \Omega_{\text{RF}}^4/(4\Omega^2)} \cos(\delta_+ + \delta_-) (1 - \cos(\sqrt{\delta^2 + \Omega_{\text{RF}}^4/(4\Omega^2)} t)) \right\} \\ & + r_+ r_- \left\{ \frac{\sqrt{\delta^2 + \Omega_{\text{RF}}^4/(4\Omega^2)} \Omega_{\text{RF}}^2/(2\Omega)}{\delta^2 + \Omega_{\text{RF}}^4/(4\Omega^2)} \sin(\delta_+ + \delta_-) \sin(\sqrt{\delta^2 + \Omega_{\text{RF}}^4/(4\Omega^2)} t) \right\}, \end{aligned} \quad (1.30a)$$

$$\begin{aligned} |\rho_-(t)|^2 = & r_-^2 \left\{ \frac{\delta^2}{\delta^2 + \Omega_{\text{RF}}^4/(4\Omega^2)} + \frac{\Omega_{\text{RF}}^4/(8\Omega^2)}{\delta^2 + \Omega_{\text{RF}}^4/(4\Omega^2)} (1 + \cos(\sqrt{\delta^2 + \Omega_{\text{RF}}^4/(4\Omega^2)} t)) \right\} \\ & + r_+^2 \left\{ \frac{\Omega_{\text{RF}}^4/(8\Omega^2)}{\delta^2 + \Omega_{\text{RF}}^4/(4\Omega^2)} (1 - \cos(\sqrt{\delta^2 + \Omega_{\text{RF}}^4/(4\Omega^2)} t)) \right\} \\ & + r_+ r_- \left\{ \frac{\delta \Omega_{\text{RF}}^2/(2\Omega)}{\delta^2 + \Omega_{\text{RF}}^4/(4\Omega^2)} \cos(\delta_+ + \delta_-) (1 - \cos(\sqrt{\delta^2 + \Omega_{\text{RF}}^4/(4\Omega^2)} t)) \right\} \\ & - r_+ r_- \left\{ \frac{\sqrt{\delta^2 + \Omega_{\text{RF}}^4/(4\Omega^2)} \Omega_{\text{RF}}^2/(2\Omega)}{\delta^2 + \Omega_{\text{RF}}^4/(4\Omega^2)} \sin(\delta_+ + \delta_-) \sin(\sqrt{\delta^2 + \Omega_{\text{RF}}^4/(4\Omega^2)} t) \right\}. \end{aligned} \quad (1.30b)$$

Since these are representative of the total energy contained in each mode, there is a periodic transfer of energy between the magnetron and cyclotron modes. From the above equations it is clear to see that

$$|\rho_+(t)|^2 + |\rho_-(t)|^2 = r_+^2 + r_-^2 \quad (1.31)$$

is a constant of motion while the time-averaged values are given by

$$\langle |\rho_+(t)|^2 \rangle_t = \frac{\delta^2 + \Omega_{\text{RF}}^4/(8\Omega^2)}{\delta^2 + \Omega_{\text{RF}}^4/(4\Omega^2)} r_+^2 + \frac{\Omega_{\text{RF}}^4/(8\Omega^2)}{\delta^2 + \Omega_{\text{RF}}^4/(4\Omega^2)} r_-^2 - \frac{\delta \Omega_{\text{RF}}^2/(2\Omega)}{\delta^2 + \Omega_{\text{RF}}^4/(4\Omega^2)} r_+ r_- \cos(\delta_+ + \delta_-), \quad (1.32a)$$

$$\langle |\rho_{-}(t)|^2 \rangle_t = \frac{\Omega_{\text{RF}}^4/(8\Omega^2)}{\delta^2 + \Omega_{\text{RF}}^4/(4\Omega^2)} r_+^2 + \frac{\delta^2 + \Omega_{\text{RF}}^4/(8\Omega^2)}{\delta^2 + \Omega_{\text{RF}}^4/(4\Omega^2)} r_-^2 + \frac{\delta \Omega_{\text{RF}}^2/(2\Omega)}{\delta^2 + \Omega_{\text{RF}}^4/(4\Omega^2)} r_+ r_- \cos(\delta_+ + \delta_-). \quad (1.32b)$$

For the resonant case, $\delta = 0$ and we get

$$v_{\pm} = \pm \frac{e\phi_{\text{RF}}}{2m(\omega_+ - \omega_-)} \equiv \pm \omega_B. \quad (1.33)$$

The solutions for the mode amplitudes simplify to

$$\rho_+(t) = \left\{ \frac{1}{2} r_+ e^{-i\delta_+} + \frac{1}{2} r_- e^{i\delta_-} \right\} e^{-i\omega_B t} + \left\{ \frac{1}{2} r_+ e^{-i\delta_+} - \frac{1}{2} r_- e^{i\delta_-} \right\} e^{i\omega_B t}, \quad (1.34a)$$

$$\rho_-(t) = \left\{ -\frac{1}{2} r_+ e^{i\delta_+} + \frac{1}{2} r_- e^{-i\delta_-} \right\} e^{-i\omega_B t} + \left\{ \frac{1}{2} r_+ e^{i\delta_+} + \frac{1}{2} r_- e^{-i\delta_-} \right\} e^{i\omega_B t}, \quad (1.34b)$$

meaning

$$|\rho_+(t)|^2 = r_+^2 \cos^2(\omega_B t) + r_-^2 \sin^2(\omega_B t) + r_+ r_- \sin(\delta_+ + \delta_-) \sin(2\omega_B t), \quad (1.35a)$$

$$|\rho_-(t)|^2 = r_-^2 \cos^2(\omega_B t) + r_+^2 \sin^2(\omega_B t) - r_+ r_- \sin(\delta_+ + \delta_-) \sin(2\omega_B t), \quad (1.35b)$$

and

$$\langle |\rho_+(t)|^2 \rangle_t = \langle |\rho_-(t)|^2 \rangle_t = \frac{r_+^2 + r_-^2}{2}. \quad (1.36)$$

Thus the average amplitudes of the two radial motions equilibrate when the axialisation drive is resonant with the bare cyclotron frequency, ω_c . It can be recognised that this behaviour resembles that of coupled driven mechanical oscillators.

It is also important to note that the breaking of the cylindrical symmetry due to the form of the oscillating quadrupole is necessary for the coupling of the two radial modes. Such an effect can not be achieved by simply modulating the trapping potential at a frequency close to the cyclotron frequency¹⁰. As a result additional electrode structures need to be designed to produce the oscillating field.

QUANTUM DESCRIPTION

With the application of an rf drive, the radial part of the quantum mechanical Hamiltonian for the ion reads

$$H_r = H_0 + H_I(t), \quad (1.37)$$

where

$$H_0 \equiv H_{xy} = \hbar\omega_+ \left(a_+^\dagger a_+ + \frac{1}{2} \right) - \hbar\omega_- \left(a_-^\dagger a_- + \frac{1}{2} \right). \quad (1.38)$$

The additional potential V_{RF} leads to an interaction term

$$H_I(t) \equiv e V_{\text{RF}}(t) = e \phi_{\text{RF}}(x^2 - y^2) \cos(\omega_{\text{RF}} t), \quad (1.39)$$

where x and y are now operators. Writing these in the second quantised form, the interaction term in the interaction picture simplifies to, in the rotating wave approximation,

$$\begin{aligned} V_I(t) &= e^{iH_0 t/\hbar} H_I(t) e^{-iH_0 t/\hbar} \\ &= \hbar g (a_+ a_-^\dagger e^{i\delta t} + a_+^\dagger a_- e^{-i\delta t}), \end{aligned} \quad (1.40)$$

where we have defined the coupling constant

$$g \equiv \frac{2e\phi_{\text{RF}}}{m(\omega_+ - \omega_-)}. \quad (1.41)$$

Transforming back into the original frame,

$$H_I(t) = \hbar g (a_+ a_-^\dagger e^{i\omega_{\text{RF}} t} + a_+^\dagger a_- e^{-i\omega_{\text{RF}} t}) \quad (1.42)$$

and the total radial Hamiltonian is given by

$$H = \hbar \omega_+ \left(a_+^\dagger a_+ + \frac{1}{2} \right) - \hbar \omega_- \left(a_-^\dagger a_- + \frac{1}{2} \right) + \hbar g (a_+ a_-^\dagger e^{i\omega_{\text{RF}} t} + a_+^\dagger a_- e^{-i\omega_{\text{RF}} t}). \quad (1.43)$$

The terms $a_+ a_-^\dagger$ and $a_+^\dagger a_-$ arising due to the axialisation drive effect the coupling between the bare radial modes of the ion, as can be seen in fig. 1.2. Analogous to the treatment of two-level atoms interacting with laser light in quantum optics¹⁸, we can study the modes of the coupled system in the dressed-state formalism.

The explicit time-dependence in the Hamiltonian can be removed by a change of reference frame through the application of the unitary operator

$$U(t) = \exp\left\{i \frac{\omega_{\text{RF}}}{2} (a_+^\dagger a_+ - a_-^\dagger a_-) t\right\} \quad (1.44)$$

so that

$$\begin{aligned} H' &= U(t) H U^\dagger(t) + i \hbar \dot{U}(t) U^\dagger(t) \\ &= \frac{\hbar(\omega_+ - \omega_- - \delta)}{2} a_+^\dagger a_+ + \frac{\hbar(\omega_+ - \omega_- + \delta)}{2} a_-^\dagger a_- + \hbar g (a_+ a_-^\dagger + a_+^\dagger a_-) + \frac{\hbar(\omega_+ - \omega_-)}{2}. \end{aligned} \quad (1.45)$$

Defining the operators corresponding to the dressed modes

$$b_+^\dagger = \cos \frac{\theta}{2} a_+^\dagger - \sin \frac{\theta}{2} a_-^\dagger, \quad (1.46a)$$

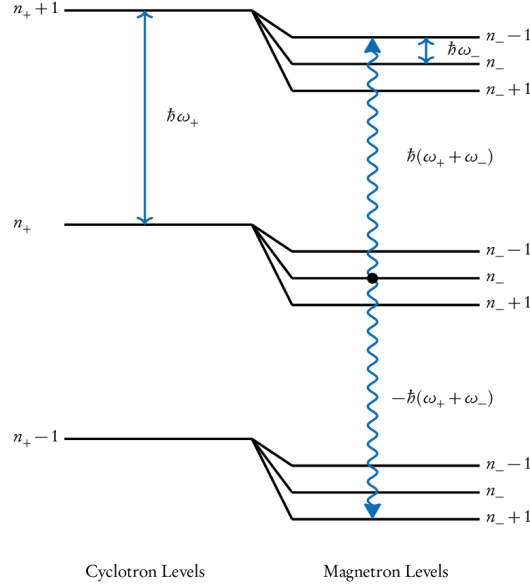


Figure 1.2: Coupling between the different levels of the cyclotron and magnetron modes. The $|n_+, n_- \rangle$ state can be coupled to the $|n_+ + 1, n_- - 1 \rangle$ and $|n_+ - 1, n_- + 1 \rangle$ states.

$$b_+ = \cos \frac{\theta}{2} a_+ - \sin \frac{\theta}{2} a_-, \quad (1.46b)$$

$$b_-^\dagger = \sin \frac{\theta}{2} a_+^\dagger + \cos \frac{\theta}{2} a_-^\dagger, \quad (1.46c)$$

$$b_- = \sin \frac{\theta}{2} a_+ + \cos \frac{\theta}{2} a_-, \quad (1.46d)$$

we can rewrite the Hamiltonian as

$$H' = \hbar \xi_+ \left(b_+^\dagger b_+ + \frac{1}{2} \right) + \hbar \xi_- \left(b_-^\dagger b_- + \frac{1}{2} \right), \quad (1.47)$$

where

$$\theta = \tan^{-1} \left(\frac{2g}{\delta} \right), \quad (1.48a)$$

$$\xi_\pm = \frac{\omega_+ - \omega_- \pm \Delta}{2}, \quad (1.48b)$$

$$\Delta = \sqrt{4g^2 + \delta^2}. \quad (1.48c)$$

The energy levels of the dress modes are thus given by the frequencies ξ_\pm .

2

Arrays of Penning Traps

2.1 CLASSICAL MOTION

We now consider an array of N identical Penning traps each containing a singly charged ion (of the same species) arranged on an arbitrary lattice with lattice constant d . Each lattice site defines the quadrupole centre of the corresponding Penning trap. The Coulomb interaction leads to an additional force on each of the ions and a coupling between their motional states. As a result the system has $3N$ collective normal modes of motion.

In the laboratory frame of reference, with no oscillatory fields present, the Lagrangian of the system is given by

$$L = \sum_{j=1}^N \left\{ \frac{1}{2} m |\dot{\mathbf{R}}_j|^2 + e \mathbf{A}_j \cdot \dot{\mathbf{R}}_j - e \Phi_j \right\}, \quad (2.1)$$

where m is the mass of each ion, $\mathbf{R}_j = X_j \hat{x} + Y_j \hat{y} + Z_j \hat{z}$ denotes the lab coordinates of ion j trapped at the lattice site $\mathbf{D}_j = D_{jx} \hat{x} + D_{jy} \hat{y} + D_{jz} \hat{z}$, $\mathbf{A}_j = \frac{1}{2} (\mathbf{B} \times \mathbf{R}_j)$ is the vector potential in the symmetric gauge due to the magnetic field $\mathbf{B} = B_0 \hat{z}$, and Φ_j is the total scalar quadrupole potential. Φ_j contains contributions from the trapping potential which we assume varies near the trap sites in terms of the local coordinates $\bar{\mathbf{r}}_j = \mathbf{R}_j - \mathbf{D}_j$ as

$$\phi_j = \frac{1}{2} m \omega_z^2 \left\{ \bar{z}_j^2 - \frac{\bar{x}_j^2 + \bar{y}_j^2}{2} \right\} \quad (2.2)$$

and the Coulomb interaction with other ions

$$x_j = \frac{1}{2} \sum_{k \neq j} \frac{e}{4\pi\epsilon_0 |\mathbf{R}_j - \mathbf{R}_k|} = \frac{k_e e}{2} \sum_{k \neq j} \frac{1}{|\mathbf{R}_{jk}|}, \quad (2.3)$$

so that $\Phi_j = \phi_j + \varkappa_j$. Here $k_e = 1/(4\pi\epsilon_0)$ is the Coulomb constant.

The normal mode analysis begins by finding the equilibrium configuration of ions, which is determined by the minimum of the total potential energy. By expanding the system Lagrangian about the equilibrium position of each ion $\mathbf{R}_{j0} = X_{j0}\hat{x} + Y_{j0}\hat{y} + Z_{j0}\hat{z}$ in a Taylor series up to second order, we get a Lagrangian in terms of the generalised position vectors $\mathbf{r}_j = \mathbf{R}_j - \mathbf{R}_{j0}$ which specify the displacement of each ion from its equilibrium point. The second order term in the expansion effectively dictates the normal mode dynamics of the system near the stable spatial configuration.

Finding such a configuration corresponds to an optimisation problem which gets increasingly difficult to solve for the potential minimum as the number of ions increases. However, the Coulomb interaction term in the potential energy can be treated as a perturbation to the much stronger contribution from the trapping potential in the limit where the ions are not too close together*. This approximation leads us to believe that the equilibrium position of each ion does not lie too far away from its associated quadrupole centre. Starting with an initial configuration where each ion is slightly perturbed from its quadrupole centre, we can numerically deduce the (local) minimum of the potential energy through the time evolution of the system.

At this point it becomes more convenient to utilise vector notation and denote the set of all $3N$ generalised position coordinates by a single $3N$ -dimensional vector $q = [x_1 \dots x_N \quad y_1 \dots y_N \quad z_1 \dots z_N]^T$. This allows us to write the effective phonon Lagrangian in the compact form

$$L = \sum_{j=1}^{3N} \left\{ \frac{1}{2} m \dot{q}_j^2 - \frac{1}{2} \sum_{k=1}^{3N} W_{jk} \dot{q}_j q_k - \frac{1}{2} \sum_{k=1}^{3N} \Phi_{jk} q_j q_k \right\}, \quad (2.4)$$

in which

$$W = m\omega_c \begin{bmatrix} \mathbb{O}_N & \mathbb{I}_N & \mathbb{O}_N \\ -\mathbb{I}_N & \mathbb{O}_N & \mathbb{O}_N \\ \mathbb{O}_N & \mathbb{O}_N & \mathbb{O}_N \end{bmatrix}, \quad (2.5a)$$

$$\Phi = \begin{bmatrix} \Phi^{xx} & \Phi^{xy} & \Phi^{xz} \\ \Phi^{yx} & \Phi^{yy} & \Phi^{yz} \\ \Phi^{zx} & \Phi^{zy} & \Phi^{zz} \end{bmatrix} \quad (2.5b)$$

are $3N \times 3N$ block matrices constructed in terms of $N \times N$ sub-matrices, \mathbb{I}_N and \mathbb{O}_N which represent the $N \times N$ identity and zero matrices respectively, and

$$\Phi_{jk}^{xx} = \begin{cases} -\frac{1}{2} m \omega_z^2 - k_e e^2 \sum_{l \neq j} \frac{R_{jl0}^2 - 3R_{jl0}^{x2}}{R_{jl0}^5} & , j = k \\ k_e e^2 \frac{R_{jk0}^2 - 3R_{jk0}^{x2}}{R_{jk0}^5} & , j \neq k \end{cases}, \quad (2.6a)$$

*This limit holds well for ions in quantum simulation experiments

$$\Phi_{jk}^{yy} = \begin{cases} -\frac{1}{2}m\omega_z^2 - k_e e^2 \sum_{l \neq j} \frac{R_{j10}^2 - 3R_{j10}^{y2}}{R_{j10}^5} & , j = k \\ k_e e^2 \frac{R_{jk0}^2 - 3R_{jk0}^{y2}}{R_{jk0}^5} & , j \neq k \end{cases}, \quad (2.6b)$$

$$\Phi_{jk}^{zz} = \begin{cases} m\omega_z^2 - k_e e^2 \sum_{l \neq j} \frac{R_{j10}^2 - 3R_{j10}^{z2}}{R_{j10}^5} & , j = k \\ k_e e^2 \frac{R_{jk0}^2 - 3R_{jk0}^{z2}}{R_{jk0}^5} & , j \neq k \end{cases}, \quad (2.6c)$$

$$\Phi_{jk}^{xy} = \Phi_{jk}^{yx} = \begin{cases} 3k_e e^2 \sum_{l \neq j} \frac{R_{j10}^x R_{j10}^y}{R_{j10}^5} & , j = k \\ -3k_e e^2 \frac{R_{j10}^x R_{j10}^y}{R_{jk0}^5} & , j \neq k \end{cases}, \quad (2.6d)$$

$$\Phi_{jk}^{yz} = \Phi_{jk}^{zy} = \begin{cases} 3k_e e^2 \sum_{l \neq j} \frac{R_{j10}^y R_{j10}^z}{R_{j10}^5} & , j = k \\ -3k_e e^2 \frac{R_{j10}^y R_{j10}^z}{R_{jk0}^5} & , j \neq k \end{cases}, \quad (2.6e)$$

$$\Phi_{jk}^{xz} = \Phi_{jk}^{zx} = \begin{cases} 3k_e e^2 \sum_{l \neq j} \frac{R_{j10}^x R_{j10}^z}{R_{j10}^5} & , j = k \\ -3k_e e^2 \frac{R_{j10}^x R_{j10}^z}{R_{jk0}^5} & , j \neq k \end{cases}, \quad (2.6f)$$

where we define $R_{jk0} = |\mathbf{R}_{j0} - \mathbf{R}_{k0}|$ and the indices j, k and l run from 1 to N .

By construction, W is a real antisymmetric matrix, while Φ is a real symmetric matrix. These properties will be useful in determining the characteristics of the normal mode eigenfrequencies and eigenvectors.

From the Lagrangian, the equation of motion for the coordinate q_j can be derived as

$$m\ddot{q}_j - \sum_{k=1}^{3N} W_{jk} \dot{q}_k + \sum_{k=1}^{3N} \Phi_{jk} q_k = 0 \quad (2.7)$$

and these $3N$ equations can be written collectively in vector form as

$$m\ddot{q} - W\dot{q} + \Phi q = 0, \quad (2.8)$$

To find the normal modes of motion, we substitute the ansatz $q = q_0 e^{-i\omega t}$ which yields a Quadratic Eigenvalue Problem (QEP)

$$[\omega^2(m \cdot \mathbb{I}_{3N} + \omega(-iW) - \Phi)q_0 = 0, \quad (2.9)$$

to be solved for (complex) eigenvectors q_0 and eigenvalues ω . The set of eigenvalues $\{\omega_\lambda\}$ are the normal mode frequencies while the corresponding normalised eigenvectors $\{q_\lambda\}$ give us the normal mode coordinates.

The general solution can be written as

$$q(t) = \sum_{\lambda=1}^{3N} \rho_\lambda q_\lambda e^{-i\omega_\lambda t}, \quad (2.10)$$

where ρ_λ are complex scalars. The motion of the ions in terms of the normal modes can then be retrieved as

$$r(t) = \text{Re}(q(t)) = \frac{1}{2} \sum_{\lambda=1}^{3N} (\rho_\lambda q_\lambda e^{-i\omega_\lambda t} + \rho_\lambda^* q_\lambda^* e^{i\omega_\lambda t}). \quad (2.11)$$

The stability of the system is guaranteed if all frequencies are purely real. The existence of any complex eigenvalues means that the motion is unbounded or non-oscillatory, and the equilibrium configuration used to derive the normal modes is unstable.

The total energy of the system is given by

$$E = \frac{1}{4} \sum_{\lambda=1}^{3N} |\rho_\lambda|^2 (m\omega_\lambda^2 + q_\lambda^H \Phi q_\lambda) \quad (2.12)$$

and is again a constant of motion. The total energy contained in each mode is given by

$$E_\lambda = \frac{1}{4} |\rho_\lambda|^2 (m\omega_\lambda^2 + q_\lambda^H \Phi q_\lambda) \quad (2.13)$$

and its sign is determined by the quantity $(m\omega_\lambda^2 + q_\lambda^H \Phi q_\lambda)$. This quantity is not trivially positive for each mode since Φ is not a positive-definite matrix in the case of Penning traps[†], unlike Paul traps.

Typically we will observe N modes dominated by motion along the axial direction and it is convenient to continue calling these modes axial modes in the context of the N ion array of Penning traps. Each of the axial modes has a positive total mode energy. Similarly there are $2N$ radial modes out of which N have each a positive mode energy and N have each a negative mode energy. We will call the radial modes with positive sign as reduced cyclotron modes and the ones with negative sign as magnetron modes.

By linearising the QEP, we can derive from elementary identities in linear algebra the following relation between the normal mode frequencies of an N -ion system and the strength of the magnetic field

$$\sum_{\lambda=1}^{3N} \omega_\lambda^2 = N\omega_c^2. \quad (2.14)$$

This result holds even when the trap is imperfect. A real trap can suffer from misalignments between the magnetic field and the confining axis of the quadrupole potential. The trapping potential itself may not be of the idealised cylindrically symmetric form and its Hessian matrix could have non-zero off-diagonal terms. The result (2.14) is valid as long as the trap is stable, and can as such be treated as a generalisation of the well known Brown-Gabrielse invariance theorem for a single ion in a Penning trap¹⁰,

$$\omega_+^2 + \omega_-^2 + \omega_z^2 = \omega_c^2. \quad (2.15)$$

[†] Φ can indeed be made positive-definite by moving to a suitable rotating frame. This approach is not considered here due to lack of necessity, but is often used in the case of ion crystals in a single Penning trap where there is a natural bulk rotation of the crystal¹⁹.

and could possibly have a similar significance in experiments. It must be emphasised that this extension to an N -ion system does not follow trivially from the single-ion invariance theorem.

Some interesting behaviour can be observed in the normal modes of honeycomb lattices formed in the plane defined by the confining axis, \hat{z} , and one of the anti-confining axes of the trapping potential, say \hat{x} . Since these two axes are not symmetric the normal mode structure depends on the orientation of the bonds between different ions along the two axes. Two different arrangements for a 54 ion honeycomb lattice with the respective frequency spectra are shown in figure 2.1. The frequency spectrum for the arrangement on the left shows a clear splitting of each of the cyclotron, axial and magnetron mode branches into two sub-branches. This splitting is absent in the arrangement on the right and the modes form a (quasi-)continuum in each branch.

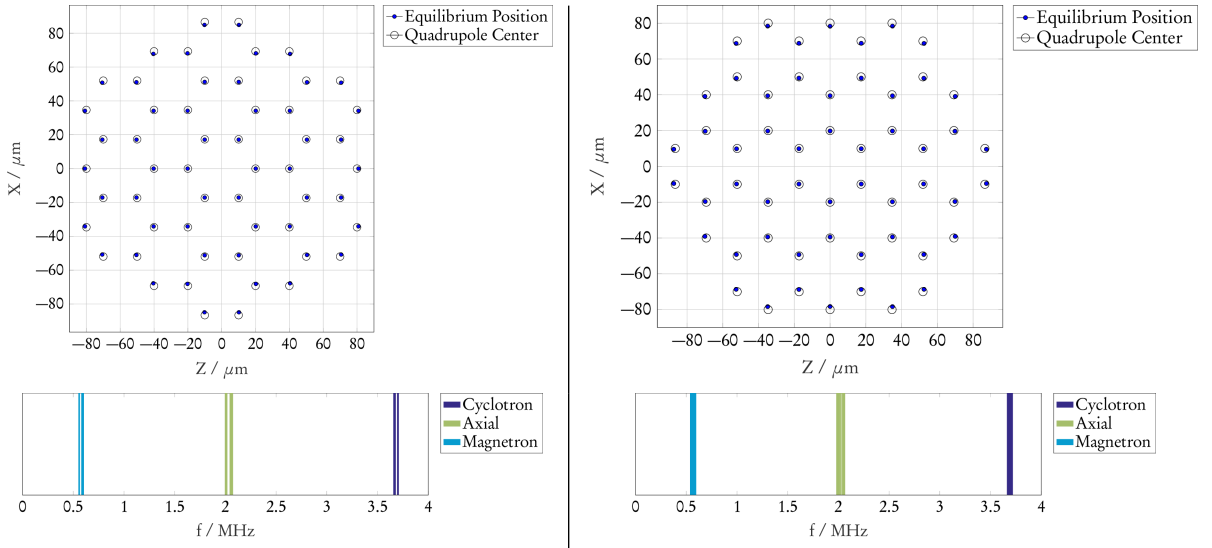


Figure 2.1: Equilibrium positions and frequency spectra for two different orientations of a 54 ion honeycomb lattice

2.2 QUANTUM MOTION

For a system of N oscillating ions coupled together through Coulomb forces, the eigenstates of the motional Hamiltonian become a linear combination of the individual modes of motion of each ion. These eigenstates are the normal modes of the system.

From the Lagrangian derived earlier we can identify the canonical momentum variables p_j conjugate to the canonical position q_j as

$$p_j = m\dot{q}_j - \frac{1}{2} \sum_{k=1}^{3N} W_{jk} q_k. \quad (2.16)$$

The quantum mechanical Hamiltonian of the system then reads as

$$H = \sum_{j=1}^{3N} \left\{ \frac{p_j^2}{2m} + \frac{1}{4m} \sum_{k=1}^{3N} W_{jk} (p_j q_k - q_j p_k) - \frac{1}{8m} \sum_{k=1}^{3N} T_{jk} q_j q_k + \frac{1}{2} \sum_{k=1}^{3N} \Phi_{jk} q_j q_k \right\}, \quad (2.17)$$

where we define the matrix $T = W^2$, and q_j and p_j are now operators satisfying the commutation relations

$$[q_j, q_k] = 0, \quad [p_j, p_k] = 0, \quad [q_j, p_k] = i \hbar \delta_{jk}. \quad (2.18)$$

To diagonalise the Hamiltonian in the second quantised form $H = \sum_{\lambda=1}^{3N} \hbar \omega_{\lambda} (a_{\lambda}^{\dagger} a_{\lambda} + \frac{1}{2})$, we follow the method employed in the case of ion Coulomb crystals in Penning traps¹⁹ and form the phonon creation and annihilation operators, a_{λ}^{\dagger} and a_{λ} , for the mode λ as linear combinations of the generalised position and momentum operators,

$$a_{\lambda}^{\dagger} = \sum_{j=1}^{3N} (\alpha_{\lambda j} p_j + \beta_{\lambda j} q_j), \quad (2.19)$$

$$a_{\lambda} = \sum_{j=1}^{3N} (\alpha_{\lambda j}^* p_j + \beta_{\lambda j}^* q_j), \quad (2.20)$$

where α and β are complex numbers.

For the commutation relation $[a_{\lambda}, a_k^{\dagger}] = \delta_{\lambda k}$ to hold, the Hamiltonian must satisfy the commutation relation

$$[H, a_{\lambda}^{\dagger}] = \hbar \omega_{\lambda} a_{\lambda}^{\dagger}. \quad (2.21)$$

Substituting the phonon operators in terms of the operators p_l and q_l in the Hamiltonian we get a set of coupled equations for each mode λ

$$-\frac{i \hbar}{m} \beta_{\lambda j} + \frac{i \hbar}{2m} \sum_{k=1}^{3N} W_{jk} \alpha_{\lambda k} = \hbar \omega_{\lambda} \alpha_{\lambda j}, \quad (2.22a)$$

$$\frac{i \hbar}{2m} \sum_{k=1}^{3N} W_{jk} \beta_{\lambda k} - \frac{i \hbar}{4m} \sum_{k=1}^{3N} T_{jk} \alpha_{\lambda k} + i \hbar \sum_{k=1}^{3N} \Phi_{jk} \alpha_{\lambda k} = \hbar \omega_{\lambda} \beta_{\lambda k}, \quad (2.22b)$$

which can be written in vector form as

$$-\frac{i \hbar}{m} \beta_{\lambda} + \frac{i \hbar}{2m} W \alpha_{\lambda} = \hbar \omega_{\lambda} \alpha_{\lambda}, \quad (2.23a)$$

$$\frac{i \hbar}{2m} W \beta_{\lambda} - \frac{i \hbar}{4m} T \alpha_{\lambda} + i \hbar \Phi \alpha_{\lambda} = \hbar \omega_{\lambda} \beta_{\lambda}. \quad (2.23b)$$

Eliminating $\beta_\lambda = i\omega_\lambda m\alpha_\lambda + \frac{1}{2}W\alpha_\lambda$, we arrive at

$$[\omega_\lambda^2 m \cdot \mathbb{I}_{3N} + \omega_\lambda(-iW) - \Phi]\alpha_\lambda = 0, \quad (2.24)$$

which is the same quadratic eigenvalue problem we had to solve in the classical treatment.

To fix the normalisation of the eigenvectors α_λ so that $[a_\lambda, a_\lambda^\dagger] = 1$, we make the substitution $\alpha_\lambda = c_\lambda \gamma_\lambda$ and $\beta_\lambda = c_\lambda \zeta_\lambda$, where γ_λ is normalised to one and c_λ is a complex number. Then,

$$|c_\lambda|^2 = \frac{\omega_\lambda}{\hbar} \left\{ \frac{1}{m\omega_\lambda^2 + \gamma_\lambda^H \Phi \gamma_\lambda} \right\} \quad (2.25)$$

is always non-negative and the commutator can be equal to positive unity only when ω_λ and the quantity $(m\omega_\lambda^2 + \gamma_\lambda^H \Phi \gamma_\lambda)$ are of the same sign. We choose ω_λ as positive for the frequencies satisfying $(m\omega_\lambda^2 + \gamma_\lambda^H \Phi \gamma_\lambda) > 0$ and as negative when $(m\omega_\lambda^2 + \gamma_\lambda^H \Phi \gamma_\lambda) < 0$.

The creation and annihilation operators then reduce to

$$a_\lambda^\dagger = c_\lambda \sum_{j=1}^{3N} (\gamma_{\lambda j} p_j + \zeta_{\lambda j} q_j), \quad (2.26a)$$

$$a_\lambda = c_\lambda \sum_{j=1}^{3N} (\gamma_{\lambda j}^* p_j + \zeta_{\lambda j}^* q_j), \quad (2.26b)$$

where

$$c_\lambda = \sqrt{\frac{\omega_\lambda}{\hbar(m\omega_\lambda^2 + \gamma_\lambda^H \Phi \gamma_\lambda)}} \quad (2.27)$$

and the operators follow the standard commutation relations,

$$[a_\lambda^\dagger, a_{\lambda'}^\dagger] = 0, \quad [a_\lambda, a_{\lambda'}] = 0, \quad [a_\lambda, a_{\lambda'}^\dagger] = \delta_{\lambda\lambda'}. \quad (2.28)$$

The position and momentum operators can be written in the second quantised form

$$q_j = -i\hbar \sum_{\lambda=1}^{3N} c_\lambda (\gamma_{\lambda j}^* a_\lambda^\dagger - \gamma_{\lambda j} a_\lambda), \quad (2.29a)$$

$$p_j = i\hbar \sum_{\lambda=1}^{3N} c_\lambda (\zeta_{\lambda j}^* a_\lambda^\dagger - \zeta_{\lambda j} a_\lambda). \quad (2.29b)$$

To make clear the nature of the mode frequencies, we can separate the Hamiltonian into three parts

$$\begin{aligned}
H &\equiv H_z + H_+ + H_- \\
&= \sum_{\lambda=1}^N \hbar |\omega_{z\lambda}| (a_{z\lambda}^\dagger a_{z\lambda} + \frac{1}{2}) + \sum_{\lambda=1}^N \hbar |\omega_{+\lambda}| (a_{+\lambda}^\dagger a_{+\lambda} + \frac{1}{2}) - \sum_{\lambda=1}^N \hbar |\omega_{-\lambda}| (a_{-\lambda}^\dagger a_{-\lambda} + \frac{1}{2}).
\end{aligned} \tag{2.30}$$

Each magnetron mode has a negative total energy and can as such be treated as an inverted harmonic oscillator. The axial and reduced cyclotron modes are simple harmonic oscillators and have a positive total energy. Comparing the Hamiltonian to the classical energy contained in each mode, we get the correspondence between the quantum numbers and classical amplitudes as

$$|\rho_\lambda|^2 \sim 4 \left(n_\lambda + \frac{1}{2} \right) (\hbar c_\lambda)^2. \tag{2.31}$$

2.3 AXIALISATION DRIVE

The coupling of different magnetron and cyclotron modes with each other can be achieved by the application of a weak axialisation potential in addition to the static trapping potential at each trap centre. Such coupling has the same kind of benefits for laser cooling ion arrays as for the single ion in a Penning trap[‡]. A classical analysis of the effects of axialisation on the normal modes of a multiple ion system in the manner of the one made previously for the single ion is more challenging since each magnetron mode could (off-resonantly) couple to various cyclotron modes, especially when the modes are not too far spaced in the frequency spectrum. One possible method to gain solutions of the motion of the ions in the presence of axialisation involves moving to a reference frame rotating at half the drive frequency. In this frame the corresponding effective potential loses its time dependence and a full normal mode analysis is possible. This is effectively the approach used in the mode calculation of ion Coulomb crystals in Penning traps and a detailed description in both the classical and quantum regimes can be found, for instance, in ref.²⁰ and ref.¹⁹.

It is important to note that when the modes are spread wider, for instance when the ions are close together, a single drive frequency could possibly not suffice to couple all radial modes with efficacy. In such a case a superposition of different frequencies would be necessary in the applied voltage signal but this should not be a major experimental issue.

[‡] In ionic Coulomb crystals an additional rotating wall potential oscillating at radio frequencies is applied to lock the bulk rotational angular frequency of the crystal to a set value. When each ion is placed in its own trap the array of ions does not rotate as a whole and thus the need for such a potential is avoided.

3

Laser Cooling of Ions

The thermal motion of ions can be cooled through the average light pressure exerted by a laser. Doppler cooling is a laser cooling technique¹¹ used in the regime where the motional sidebands of the trapped ions are not well resolved with respect to the natural linewidth Γ of the relevant cooling transition so that $\omega_\lambda < \Gamma$. Doppler cooling is more complicated in Penning traps as compared to harmonic traps due to the nature of the magnetron motion. To avoid confusion, the term cooling refers here to reducing the kinetic energy of the ions or equivalently reducing the amplitude of motion.

3.1 DOPPLER COOLING OF A SINGLE ION

A quantitative semi-classical analysis of Doppler cooling in a Penning trap begins by finding the change in amplitude of each mode before and after a photon scattering event due to the laser-ion interaction. By assuming that the scattering event leaves the position of the ion unaltered but causes an instantaneous change in velocity due to the momentum kick* we arrive at

$$\Delta r_z^2 = \left(\frac{\Delta v_z}{.png\ meg a_z} \right)^2 - \frac{2\Delta v_z r_z}{\omega_z} \sin(\omega_z t + \delta_z), \quad (3.1a)$$

$$\Delta r_+^2 = \frac{\Delta v_x^2 + \Delta v_y^2}{4\Omega^2} - \frac{r_+}{\Omega} \left[\Delta v_x \sin(\omega_+ t + \delta_+) + \Delta v_y \cos(\omega_+ t + \delta_+) \right], \quad (3.1b)$$

$$\Delta r_-^2 = \frac{\Delta v_x^2 + \Delta v_y^2}{4\Omega^2} + \frac{r_-}{\Omega} \left[\Delta v_x \sin(\omega_- t + \delta_-) + \Delta v_y \cos(\omega_- t + \delta_-) \right]. \quad (3.1c)$$

*This assumption is valid when timescale of the motion is much longer than the timescale of light-ion interaction and holds for the typical values of frequencies in trapped ion experiments

The changes in velocity can be found through conservation of momentum

$$\Delta \mathbf{v} = \frac{\hbar(\mathbf{k} - \mathbf{k}_s)}{m} \quad (3.2)$$

due to the absorption of a photon with momentum $\hbar \mathbf{k}$ and spontaneous emission of a photon with momentum $\hbar \mathbf{k}_s$. In the low intensity limit, the average rate of change in the mode amplitudes can be found by multiplying the change in amplitude with each scattering event by the photon incidence rate and the scattering cross section and then averaging over the mode amplitudes, phases and scattering directions.

For a laser with uniform intensity I the number of photons per unit time per unit area is $I/\hbar\omega$ and the cross-section takes the velocity dependent form

$$\sigma(\omega, \mathbf{v}) = \frac{\sigma_0(\Gamma/2)^2}{(\omega_0 + \mathbf{k} \cdot \mathbf{v} + R/\hbar - \omega)^2 + (\Gamma/2)^2}, \quad (3.3)$$

where σ_0 is a constant particular to the cooling transition and $R = \hbar^2 k^2/2m$.

Ignoring the small R/\hbar term and defining the detuning $\delta = \omega - \omega_0$, we can make the following approximation for small velocities

$$\sigma(\omega, \mathbf{v}) \approx \frac{\sigma_0(\Gamma/2)^2}{\delta^2 + (\Gamma/2)^2} \left\{ 1 + \frac{2\delta \mathbf{k} \cdot \mathbf{v}}{\delta^2 + (\Gamma/2)^2} \right\}. \quad (3.4)$$

If the laser wave vector $\mathbf{k} = k(e_x \hat{x} + e_y \hat{y} + e_z \hat{z})$ is oriented along any general direction we arrive at the equations dictating the rate of change of the amplitudes,

$$\frac{d\langle r_z^2 \rangle}{dt} = \gamma_s \left\{ \frac{2R}{m\omega_z^2} (f_z + f_{sz}) + \frac{2\delta \hbar k^2 f_z}{m(\delta^2 + (\Gamma/2)^2)} \langle r_z^2 \rangle \right\}, \quad (3.5a)$$

$$\frac{d\langle r_+^2 \rangle}{dt} = \gamma_s \left\{ \frac{R}{4m\Omega^2} (f_x + f_y + f_{sx} + f_{sy}) + \frac{\delta \omega_+ \hbar k^2 (f_x + f_y)}{m\Omega(\delta^2 + (\Gamma/2)^2)} \langle r_+^2 \rangle \right\}, \quad (3.5b)$$

$$\frac{d\langle r_-^2 \rangle}{dt} = \gamma_s \left\{ \frac{R}{4m\Omega^2} (f_x + f_y + f_{sx} + f_{sy}) - \frac{\delta \omega_- \hbar k^2 (f_x + f_y)}{m\Omega(\delta^2 + (\Gamma/2)^2)} \langle r_-^2 \rangle \right\}, \quad (3.5c)$$

where $f_\mu = e_\mu^2$, $f_{s\mu} = \langle e_{s\mu}^2 \rangle_{\mathbf{k}}$, and $\gamma_s \equiv \frac{I}{\hbar\omega} \cdot \frac{\sigma_0(\Gamma/2)^2}{(\Gamma/2)^2 + \delta^2}$.

The first term on the right hand side of each equation is positive and refers to the heating rate due to spontaneous emission. The second term could be positive or negative depending on the detuning of the laser. For a negative detuning $\delta < 0$, the amplitude of both the axial and cyclotron modes decreases while that of the magnetron mode increases. A positive detuning on the other hand leads to a shrinking magnetron radius while the other two modes get heated. This problem was anticipated, of course, from the negative total energy of the magnetron mode. One could cool the axial motion separately with a red-detuned laser along the \hat{z} -axis but any uniform laser beam along the radial plane will be of no use given the fact that the cooling requirements of the cyclotron and magnetron modes are incompatible. Thus no combination of uniform beams can cool all three

modes simultaneously.

One way to resolve this issue is the use of an inhomogeneous beam with a positive intensity gradient on the half of the radial plane where the direction of photon propagation coincides with the magnetron motion¹¹. The intensity gradient imparts energy to the magnetron mode and reduces its amplitude and if the detuning is set as negative such a beam can simultaneously cool the cyclotron mode as well. The axial motion can be cooled by tilting the non-uniform beam so that there is a component along the \hat{z} -axis or by using a separate red-detuned uniform beam.

While this can be easily achieved using standard Doppler cooling lasers, the final temperatures reached for both radial modes are greater than one would expect from the standard Doppler cooling limit¹¹, meaning that nonuniform beams are not a very efficient way of cooling in a Penning trap. For higher axial frequencies a higher intensity gradient is required to cool the radial modes and with a laser beam having a fixed gradient, the final temperatures reached increase. This effectively restricts the range of motional frequencies that allow for cooling all three modes.

An alternative solution is to couple the cyclotron and magnetron modes by applying a weak quadrupolar electric field oscillating at the bare cyclotron frequency¹⁷. As discussed before, this coupling technique is called axialisation[†] and leads to a periodic exchange of energy between the two radial modes. From the rate equations it is clear that for a given red-detuned laser, the rate of cooling of the higher frequency cyclotron mode is much greater than the rate of heating of the magnetron mode. By transferring energy from the magnetron to the cyclotron mode and cooling the cyclotron by the usual Doppler cooling method, the amplitudes of both modes can be reduced on average. It needs to be emphasised that a simple modulation of the trapping potential at the true cyclotron frequency provides no benefit with respect to cooling the magnetron motion and the additional driving force results in heating alone.

With the axialisation drive the system no longer consists of just electrostatic fields but since the amplitude of such a drive is much lower than the amplitude of the rf drive required in Paul traps, the deleterious effects of micromotion are accordingly much smaller. Moreover, axialisation works efficiently at all trap frequencies, allowing trapping in regimes not accessible through the use of just inhomogeneous beams.

The derivation of the rate equations of the mode amplitudes is much more algebraically involved in the presence of axialisation. A simple description of laser cooling an ion with the axialisation technique has been made previously²¹. This model takes into account the position and time dependent forces due to the total electric potential and the velocity dependent forces due to the magnetic field and the laser light. By switching to the frame rotating at half the true cyclotron frequency one effectively solves for the normal modes of the system with the complex frequencies reflecting the damping of the mode amplitudes over time. This however yields only the cooling rate of each mode and no cooling limits since diffusive heating is not considered in the model. Nevertheless it should be sufficient to numerically integrate the equations of motion of the trapped ion while including the additional force due to axialisation and a stochastic process to simulate the photon scattering events

[†] Axialisation is sometimes referred to as, in the context of precision measurement experiments, as sideband cooling. This should not be confused with the resolved sideband cooling technique. The same effect can also be achieved by coupling the magnetron mode with the axial mode through the application of an axialising field $V_{\text{RF}} = \phi_{\text{RF}} x z \cos(\omega_{\text{RF}} t)$ at the frequency $\omega_{\text{RF}} \approx \omega_z + \omega_-$.

due to light-ion interaction. By running the simulation a large number of times, the average amplitudes of each mode can be found. Figure 3.1 shows the variation of the average amplitudes and phonon numbers during the Doppler cooling process for a single ${}^9\text{Be}^+$ ion.

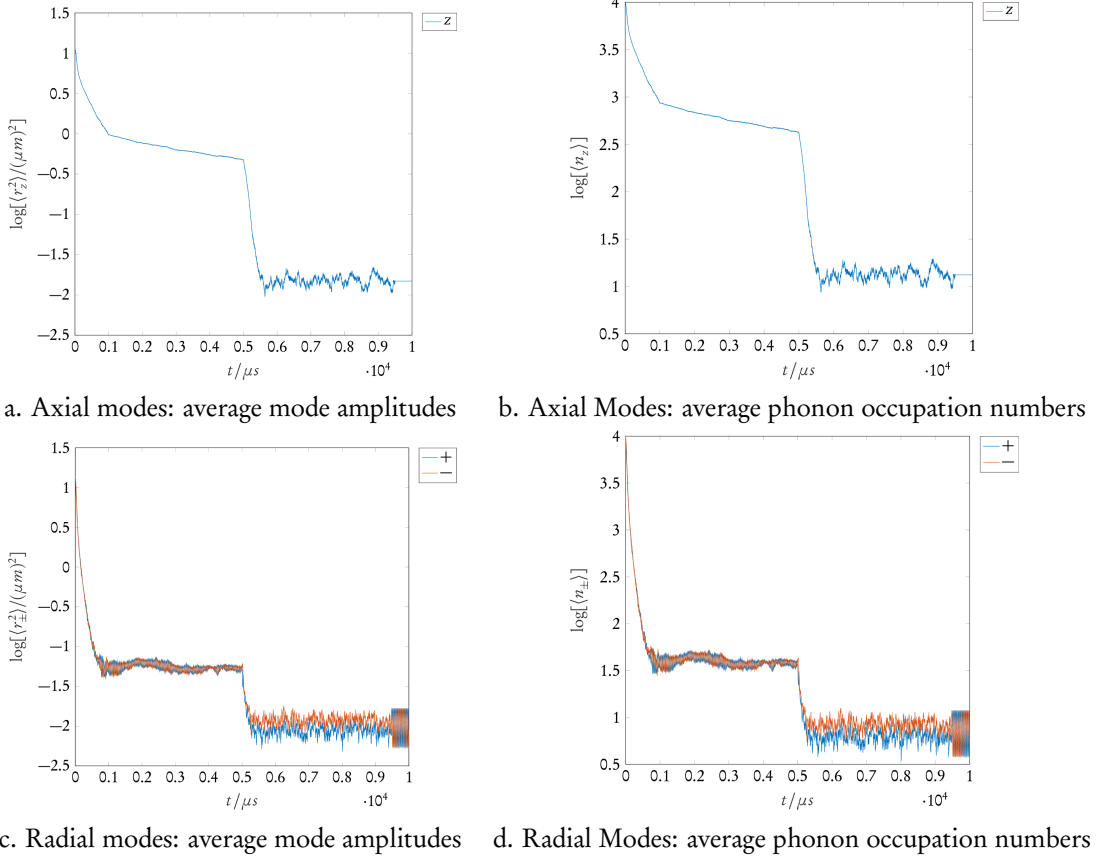


Figure 3.1: Laser cooling of a single Be^+ ion in a Penning trap. For $B_0 = 2.5$ T and $\omega_z = 2\pi \cdot 2$ MHz, $\omega_+ = 2\pi \cdot 3.723$ MHz and $\omega_- = 2\pi \cdot 0.537$ MHz. The uniform laser beam is oriented at an angle of 20° to the radial plane. The axialisation voltage is chosen to be $\phi_{\text{RF}} = 0.02\phi_0$. The initial quantum numbers for each mode are chosen as $10^4 \pm 5\%$. The final quantum numbers achieved are $\langle n_+ \rangle = 7.47$, $\langle n_z \rangle = 12.75$ and $\langle n_- \rangle = 7.20$, which means the motion is close to the ground state for each mode

3.2 ARRAYS OF TRAPS

The semi-classical analysis of Doppler cooling ions in an array of Penning traps can be carried out in a similar manner. The collective motion of the N ions is composed of the $3N$ normal modes of vibration. The change in the amplitude of mode λ due to a single interaction event between a uniform laser beam and the ion j can be

derived from the equations of motion as

$$\begin{aligned}\Delta r_\lambda^2 &\equiv r_\lambda'^2 - r_\lambda^2 \\ &= \frac{1}{\epsilon_\lambda^2} \left\{ (m\bar{q}_\lambda^T \Delta v)^2 + (m\tilde{q}_\lambda^T \Delta v)^2 - 2(m\bar{q}_\lambda^T \Delta v)\epsilon_\lambda r_\lambda \sin(\omega_\lambda t + \delta_\lambda) + 2(m\tilde{q}_\lambda^T \Delta v)\epsilon_\lambda r_\lambda \cos(\omega_\lambda t + \delta_\lambda) \right\},\end{aligned}\quad (3.6)$$

where $\epsilon_\lambda = (m\omega_\lambda^2 + q_\lambda^H \Phi q_\lambda)/2\omega_\lambda$, \bar{q}_λ and \tilde{q}_λ are respectively the real and imaginary parts of the eigenvector q_λ , and $\Delta v \equiv \Delta v_j$ is the change in velocity vector as a result of the absorption-emission process.

Defining the quantities

$$F_{\lambda j} = (\hbar \sum_\mu \bar{q}_{\lambda j}^\mu k^\mu)^2 + (\hbar \sum_\mu \tilde{q}_{\lambda j}^\mu k^\mu)^2, \quad (3.7)$$

$$F_{\lambda s j} = \hbar^2 \sum_\mu \{(\bar{q}_{\lambda j}^\mu)^2 + (\tilde{q}_{\lambda j}^\mu)^2\} k^2 f_{s\mu} \quad (3.8)$$

in terms of the Cartesian components $\mu = x, y, z$ of the mode eigenvector and the laser, and using other quantities defined in the previous section, we can write the rate equation as

$$\frac{d}{dt} \langle r_\lambda^2 \rangle = \frac{\gamma_s}{\epsilon_\lambda^2} \left\{ F_{\lambda j} + F_{\lambda s j} + \frac{\delta(m\omega_\lambda^2 + q_\lambda^H \Phi q_\lambda) F_{\lambda j} / \hbar}{(\gamma/2)^2 + \delta^2} \langle r_\lambda^2 \rangle \right\}. \quad (3.9)$$

If the laser beam is uniformly incident on all ions, the total rate of cooling can be found by simply summing the above expression over all ions so that

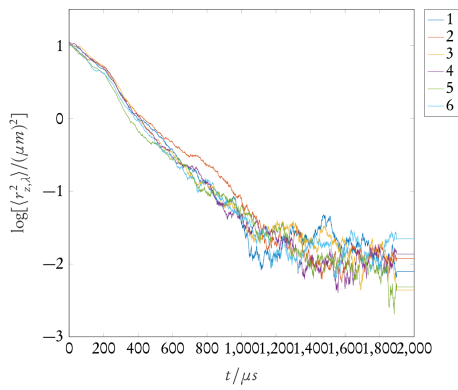
$$\frac{d}{dt} \langle r_\lambda^2 \rangle = \sum_{j=1}^N \frac{\gamma_s}{\epsilon_\lambda^2} \left\{ F_{\lambda j} + F_{\lambda s j} + \frac{\delta(m\omega_\lambda^2 + q_\lambda^H \Phi q_\lambda) F_{\lambda j} / \hbar}{(\gamma/2)^2 + \delta^2} \langle r_\lambda^2 \rangle \right\}. \quad (3.10)$$

The first two terms on the right hand side of this equation are positive and denote the heating rate of the mode. The second term is independent of the laser direction, meaning some form of heating is always present due to spontaneous emission. The sign of the third term is determined by the detuning and the mode dependent measure $(m\omega_\lambda^2 + q_\lambda^H \Phi q_\lambda)$. The magnitude depends on both the participation of each ion in the mode as well as the direction of the laser beam. For instance, this would be zero for the axial centre of mass mode if the laser is directed along the radial plane.

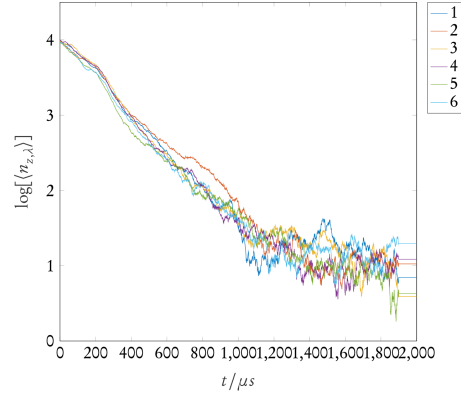
It is clear that the mode will be cooled if δ and $(m\omega_\lambda^2 + q_\lambda^H \Phi q_\lambda)$ are of different signs. Thus, not surprisingly, the same complications arise for cooling the modes of an array of ions since $(m\omega_\lambda^2 + q_\lambda^H \Phi q_\lambda)$ is positive for the N axial and N cyclotron modes but negative for the N magnetron modes. A laser of negative detuning cools the axial and cyclotron modes but heats the magnetron modes while the reverse is true for a positive detuning. A suitably oriented inhomogeneous beam could allow for the simultaneous cooling of all modes of the system. However with the limited range of allowed frequencies and the additional issue of maintaining a steep intensity gradient over the entire array of ions makes this an even more inefficient technique to cool the motion of an array of ions as compared to a single ion. Once again, a more viable solution would be the application of a radio

frequency potential in addition to the static trapping potential at each trap site such that the radial modes are coupled. Axialisation in conjunction with a red-detuned uniform-intensity laser beam would efficiently cool all modes without considerable micromotion.

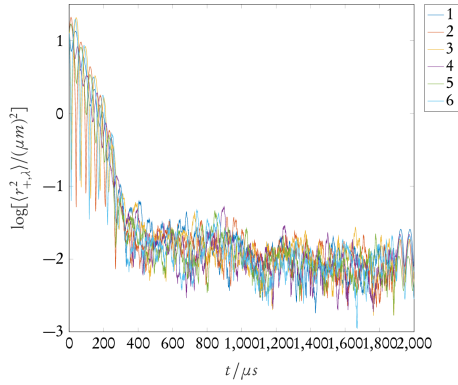
Like for the case of the single ion, it is straightforward to find the average amplitudes of each mode due to the cooling process through numerical simulation. Fig. 3.2 and fig. 3.3 show the results for Doppler cooling a small honeycomb lattice consisting of six ${}^9\text{Be}^+$ ions arranged with their confining quadrupole axes tilted at angle of 20° with respect to the normal of the electrode plane. Such an orientation allows simultaneous cooling of all modes with laser beams parallel to the electrode surface.



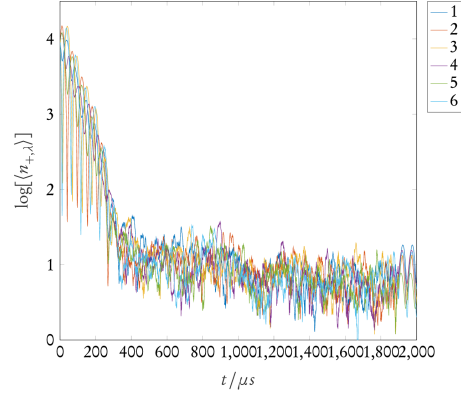
a. Axial modes - average amplitudes



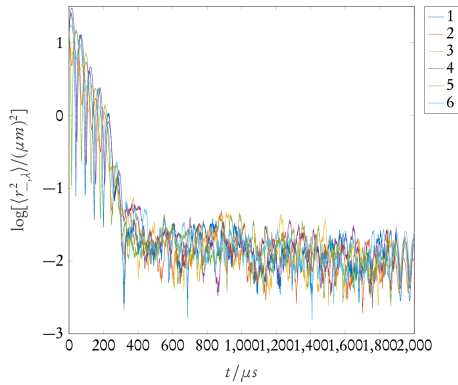
b. Axial modes - average mode occupation numbers



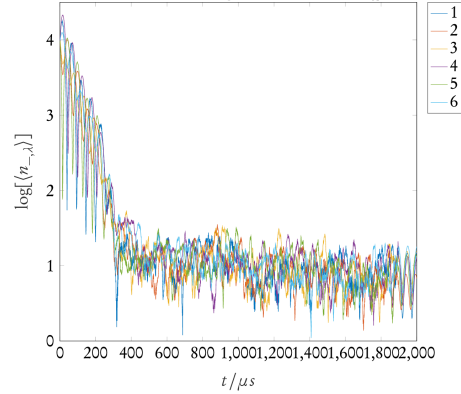
b. Cyclotron modes - average amplitudes



b. Cyclotron modes - average mode occupation numbers



c. Magnetron modes - average amplitudes



b. Magnetron modes - average mode occupation numbers

Figure 3.2: Laser cooling of a six ${}^9\text{Be}^+$ ion honeycomb lattice with lattice constant $30 \mu\text{m}$ with the confining axes tilted at $\theta = 20^\circ$ with respect to the radial plane. Here $B_0 = 2.5 \text{ T}$ and $\omega_z = 2\pi \cdot 2 \text{ MHz}$. The uniform laser beam is oriented along the electrode plane so that $\mathbf{k} = \cos\theta\hat{x} + \sin\theta\hat{z}$. The axialisation voltage is chosen to be $\phi_{\text{RF}} = 0.02\phi_0$. The initial quantum numbers for each mode are chosen as $10^4 \pm 5\%$

λ	$\omega_+/(2\pi)$	$\omega_z/(2\pi)$	$\omega_-/(2\pi)$
1	3.732	2	0.53709
2	3.7312	1.9951	0.53397
3	3.7301	1.9937	0.53308
4	3.7277	1.9898	0.53072
5	3.7268	1.9881	0.52959
6	3.7238	1.9868	0.52881

a. Mode frequencies

λ	$\langle r_{+, \lambda}^2 \rangle / (\mu m)^2$	$\langle n_{+, \lambda} \rangle$	$\langle r_{z, \lambda}^2 \rangle / (\mu m)^2$	$\langle n_{z, \lambda} \rangle$	$\langle r_{-, \lambda}^2 \rangle / (\mu m)^2$	$\langle n_{-, \lambda} \rangle$
1	0.016521	11.2934	0.0078963	6.53881	0.011279	7.51005
2	0.011764	7.89309	0.011894	10.0755	0.0071947	4.6184
3	0.012028	8.07607	0.0043885	3.39967	0.014532	9.84396
4	0.015182	10.3081	0.013715	11.6618	0.010876	7.25306
5	0.0073386	4.72168	0.0048467	3.79457	0.011566	7.7503
6	0.012268	8.21238	0.022199	19.1554	0.015232	10.3708

b. Final average amplitudes and phonon numbers achieved

Figure 3.3: Normal mode frequencies of the six ${}^9\text{Be}^+$ ion honeycomb lattice considered along with results for laser cooling of each mode

4

Spin-Spin Coupling

By isolating two suitable energy levels of an ion and controlling them with high fidelity, the internal structure of the ion can be effectively reduced to a spin-1/2 system, $\{|\uparrow\rangle, |\downarrow\rangle\}$. Such level of control is possible to achieve with the help of well developed techniques in atomic physics. Then through the application of state-dependent forces the total energy of the system of ions can be modified in a manner that depends on the internal (pseudo)spin-state of the ions, thus generating an effective spin-spin interaction.¹⁶

One possibility to engineer such interactions comes through spin-dependent optical dipole forces (ODF) obtained from bichromatic laser radiation off-resonant with respect to the internal transition. The two laser beams can be labeled as U and L , so that their frequencies and wavevectors are ω_U, ω_L and $\mathbf{k}_U, \mathbf{k}_L$ respectively. The interference of the two beams at the ion crystal results in a one-dimensional optical lattice or intensity standing-wave if the beams have the same frequency. If the beams have a frequency difference $\mu_R \equiv \omega_U - \omega_L$ between them, a traveling-wave interference pattern is produced instead and the ions experience an ODF oscillating at the frequency μ_R . The ODF is directed either towards or away from regions of high laser intensity, depending on the AC Stark shift from the lasers. By appropriately tuning the frequency and polarisations of the laser beams, it is possible to generate forces that are equal in magnitude but opposite in sign on the $|\uparrow\rangle$ and $|\downarrow\rangle$ spin states, resulting in the ODF interaction

$$H_{\text{ODF}} = - \sum_{j=1}^N E_O \cos(\mathbf{k}_R \cdot \mathbf{R}_j - \mu_R t) \sigma_j^z, \quad (4.1)$$

where E_O is the magnitude of the AC Stark shift, $\mathbf{k}_R \equiv \mathbf{k}_U - \mathbf{k}_L$ is the wavevector difference between the two beams and $\mathbf{R}_j = \mathbf{R}_{j0} + \mathbf{r}_j$ is the position of ion j in the lab frame. For small coherent displacements \mathbf{r}_j of the ions from their equilibrium positions \mathbf{R}_{j0} , we can assume that each ion is in the Lamb-Dicke regime based on the ‘wavelength’ of the optical dipole force such that $|\mathbf{k}_r \cdot \mathbf{r}_j| \ll 1$. The ODF interaction can then be approximated

as

$$H_{\text{ODF}} \approx \sum_{j=1}^N E_O \mathbf{k}_R \cdot \mathbf{r}_j \sin(\mathbf{k}_R \cdot \mathbf{R}_{j0} - \mu_R t) \sigma_j^z. \quad (4.2)$$

Quantum mechanically, one solves for the evolution operator associated with the Hamiltonian H_{ODF} . This can be done by carrying out a Magnus expansion in the Interaction Picture²². The explicit time dependence of the interaction term means that the expansion could involve an infinite sequence of commutators of the interaction term with itself at different times. This sequence truncates, however, after two terms²³.

The first term, $V_I(t)$, involves a product of the position operators (or equivalently the creation and annihilation operators corresponding to the normal modes of oscillation) and the Pauli spin operators σ_z .

$$\begin{aligned} V_I(t) &\equiv e^{iH_{\text{PH}}t/\hbar} H_{\text{ODF}}(t) e^{-iH_{\text{PH}}t/\hbar} \\ &= -i \hbar E_O \sum_{j=1}^N \sin(\mathbf{k}_R \cdot \mathbf{R}_{j0} - \mu_R t) \sum_{\nu} k_R^{\nu} \sum_{\lambda=1}^{3N} (\alpha_{\lambda j \nu}^* e^{i\omega_{\lambda} t} a_{\lambda}^{\dagger} \sigma_j^z - \alpha_{\lambda j \nu} e^{-i\omega_{\lambda} t} a_{\lambda} \sigma_j^z), \end{aligned} \quad (4.3)$$

where

$$H_{\text{PH}} = \sum_{\lambda=1}^{3N} \hbar \omega_{\lambda} \left(a_{\lambda}^{\dagger} a_{\lambda} + \frac{1}{2} \right) \quad (4.4)$$

and $\nu = x, y, z$. This term describes spin-motion entanglement generated by the optical dipole force and can be minimised by adiabatically turning on and off the interaction²⁴, or by tuning away from the motional frequencies.

The second term, $H_{\text{SPIN}}(t)$, involves the product of different spin operators and describes the effective spin-spin interaction

$$H_{\text{SPIN}}(t) = \frac{i}{2\hbar} [W_I(t), V_I(t)], \quad (4.5)$$

where

$$W_I(t) = \int_0^t V_I(t') dt'. \quad (4.6)$$

By explicitly calculating the commutator, we arrive at the expression for an Ising-like spin Hamiltonian

$$H_{\text{SPIN}} = \sum_{jj'} J_{jj'}(t) \sigma_j^z \sigma_{j'}^z, \quad (4.7)$$

with the static part of the spin-spin interactions $J_{jj'}(t)$ given by

$$\begin{aligned} J_{jj'}^0 &= \frac{E_O^2}{2} \sum_{\nu, \nu'} \sum_{\lambda} \frac{\omega_{\lambda}^2}{m\omega_{\lambda}^2 + \gamma_{\lambda}^H \Phi \gamma_{\lambda}} \frac{k_R^{\nu} k_R^{\nu'}}{\mu_R^2 - \omega_{\lambda}^2} \cos(\phi_j - \phi_{j'}) \text{Re}(\gamma_{\lambda j \nu}^* \gamma_{\lambda j' \nu'}) \\ &\quad - \frac{E_O^2}{2} \sum_{\nu, \nu'} \sum_{\lambda} \frac{\omega_{\lambda} \mu_R}{m\omega_{\lambda}^2 + \gamma_{\lambda}^H \Phi \gamma_{\lambda}} \frac{k_R^{\nu} k_R^{\nu'}}{\mu_R^2 - \omega_{\lambda}^2} \sin(\phi_j - \phi_{j'}) \text{Im}(\gamma_{\lambda j \nu}^* \gamma_{\lambda j' \nu'}). \end{aligned} \quad (4.8)$$

Here γ_λ is the normalised normal mode eigenvector corresponding to the frequency ω_λ , the indices ν, ν' run over x, y, z and the ion-specific phases are defined as $\phi_j = \mathbf{k}_R \cdot \mathbf{R}_{j0}$. This expression together with a calculation of the normal modes, can be used to determine the effective spin-spin interactions for the given frequency difference and geometric arrangement of the ODF generating laser beams.

It is thus evident that the structure of the normal modes of the trapped ions is essential to the discussion of the resulting interactions. The coupling terms have a dependence on the equilibrium configuration but this dependence can be removed completely in certain conditions. For instance, if the ion system equilibrates in the radial plane, the axial and radial modes decouple and the centre-of-mass (COM) mode is the highest frequency mode among the axial modes with $\omega_{z,COM} = \omega_z$. Now if the wave vector is made to align precisely in the axial direction so that $\mathbf{k}_R = k_R \hat{z}$, the coupling terms simplify to

$$J_{jj'}^0 = \frac{F_O^2}{4m} \sum_\lambda \frac{\gamma_{\lambda jz} \gamma_{\lambda j'z}}{\mu_R^2 - \omega_\lambda^2}, \quad (4.9)$$

where $F_O = E_0 k_R$ and the index λ effectively runs only over the axial modes. Experiments carried so far using both Paul traps (for eg. ref.⁸) and Penning traps (for eg. ref.¹³) are based on this simplification. As the detuning of the bichromatic radiation from the spin-motional sidebands is varied, the couplings follow an approximate power-law like decay $J_{jj'}^0 \propto d_{jj'}^{-a}$ with the inter-ion distance $d_{jj'} \equiv R_{jj'0}$. This behaviour is evident from fig. 4.1. When μ_R is tuned just above ω_z , the contribution of all other modes in the spin-spin coupling terms can be neglected and hence all terms are equal and positive, thus allowing to simulate infinitely-long-ranged interactions ($a = 0$). As μ_R is increasingly tuned away from ω_z , the range of interactions accordingly shortens and Coulomb interactions ($a = 1$), monopole-dipole interactions ($a = 2$) and dipole-dipole interactions ($a = 3$) can be simulated by choosing μ_R appropriately. Since all coupling terms are positive, the effective spin Hamiltonian corresponds to an antiferromagnetic Ising model.

It is worth reemphasising the relevance of the COM mode of a particular branch of modes lying on one extreme

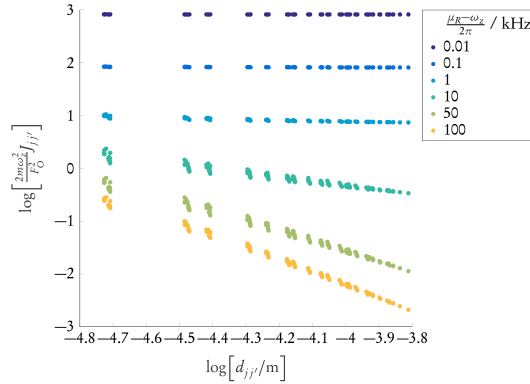


Figure 4.1: Tuneable Antiferromagnetic Couplings produced with increasing $\mu_R - \omega_z$ (in kHz) for a 61 ion $20 \mu\text{m}$ triangular lattice

of the branch. When the COM mode lies within the branch detuning μ_R in either direction from ω_z does not reveal a well-defined power law decay and the coupling terms are frustrated with different signs. A histogram plot in fig. 4.2 shows this behaviour. This behaviour is in general expected whenever μ_R lies in the middle of the branch of modes used.

The modulation of the terms due to phases originating from the static equilibrium configuration can also be

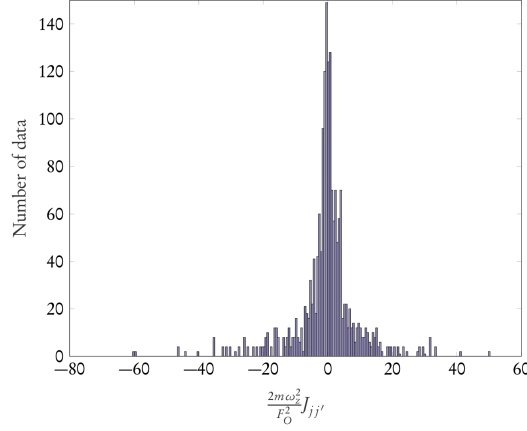


Figure 4.2: Histogram for couplings obtained when μ_R is close to the COM axial mode but the COM mode lies within the axial branch for a 61 ion 20μ m triangular lattice arranged in the \hat{x} - \hat{z} plane.

suppressed by appropriately choosing the wave vector difference \mathbf{k}_R . This is because for an array of Penning traps, the equilibrium positions of the ions are also arranged (almost perfectly) in a periodic fashion. Take for instance a simple triangular lattice with lattice constant d in the radial plane. The equilibrium configuration of the ions is as shown in figure 4.3, with $R_{j0}^x - R_{j'0}^x \approx md/2$ for an integer m . If $\mathbf{k}_U = (k \sin(\theta_R/2), k \cos(\theta_R/2), 0)$ and $\mathbf{k}_L = (-k \sin(\theta_R/2), k \cos(\theta_R/2), 0)$, the wave vector difference $\mathbf{k}_R = 2k \sin(\theta_R/2)\hat{x}$ lies along the \hat{x} -axis alone and can be tuned by changing the angle of the two beams with respect to each other. If the condition $kd \sin(\theta_R/2) = n\pi, n \in \mathbb{Z}$ is met then for all pairs j, j' , $\cos(\phi_j - \phi_{j'}) \approx 1$ and $\sin(\phi_j - \phi_{j'}) \approx 0$ and the coupling terms

$$J_{jj'}^0 \approx \frac{F_0^2}{2} \sum_{\lambda} \frac{\omega_{\lambda}^2}{m\omega_{\lambda}^2 + \gamma_{\lambda}^H \Phi \gamma_{\lambda}} \frac{\text{Re}(\gamma_{\lambda jx}^* \gamma_{\lambda j'x})}{\mu_R^2 - \omega_{\lambda}^2} \quad (4.10)$$

are approximately independent of the phases. Similar expressions for matching the phases can be derived in the case of other lattices. Since the COM cyclotron mode with $\omega_{+,COM} = \omega_+$ has the lowest frequency in its branch, increasingly tuning the difference frequency μ_R below ω_+ can produce a range of ferromagnetic couplings, as depicted in fig. 4.4.

The above approximation fails quickly as the angle is varied to match a higher value of n since the equilibrium positions are not exactly periodic. Thus k_R and, in turn, the strength of couplings that can be achieved are limited but this approach does illustrate the possibility of generating both ferromagnetic and antiferromagnetic

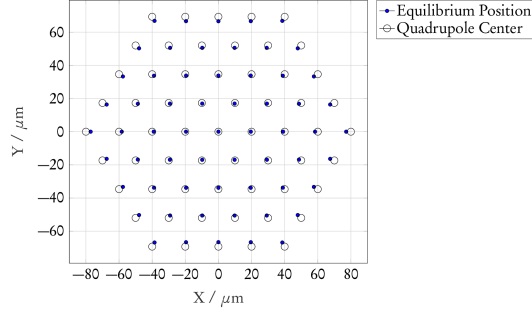


Figure 4.3: Equilibrium configuration of 61 ion 20 μ m triangular lattice with B-field out of plane

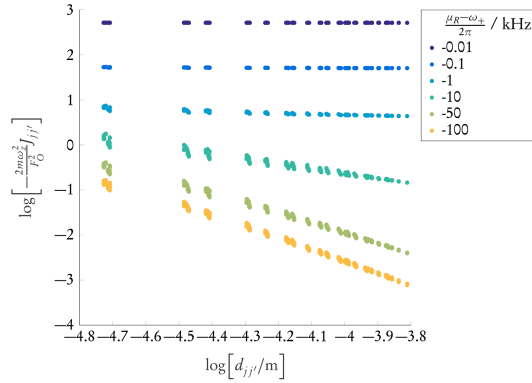


Figure 4.4: Tuneable Ferromagnetic Couplings produced with increasing $\omega_+ - \mu_R$ (in kHz) for a 61 ion 20 μ m triangular lattice

couplings using the same configuration of ions by changing the relative orientation and frequencies of the lasers. More optimistically, by choosing a slightly irregular lattice so that the ions equilibrate exactly as the desired regular lattice, the phase dependence could be removed entirely. Such manipulation of the configuration is indeed possible in microfabricated arrays and not possible to achieve in single traps since equilibrium positions in single traps are naturally determined by the competition between the trapping potential and Coulomb repulsion. The same effect could also be achieved using at each trap additional compensation electrodes, which in practice would be required anyway for the desired level of control over individual ions.

These complications aside, the analysis in this chapter demonstrates a major qualitative difference between quantum simulation experiments using ion crystals in a single Penning trap and arrays of ions in separate traps. Due to the bulk rotation of the crystal, the equilibrium positions of the ions in the radial plane vary sinusoidally as a function of time with the bulk rotational frequency. This prohibits the use of radial modes for emulating Ising-like interactions since there are no static terms, except for the approximate case when the simulation time is very small.

The strategy for generating spin-spin interactions discussed in this thesis is based on the $\sigma_z \sigma_z$ geometric phase

gate where the spin-dependent force acts on the σ_z logical basis. Gates in the $\sigma_\phi = \cos(\phi)\sigma_x + \sin(\phi)\sigma_y$ basis can be implemented, for example, using the Mølmer-Sørensen protocol²⁵ or the Bermúdez protocol²⁶. There exist ways alternative to optical dipole forces in order to generate interactions between ions. State-dependent forces could be achieved through the application of microwave or radio frequency fields without the use of any laser beams²⁷. Such laserless interaction minimises the errors caused due to light scattering and two qubit gates based on this architecture have been demonstrated²⁸.

5

Surface Electrode Traps

Surface electrode structures provide a logical means to create two-dimensional arrays of individually controllable Penning traps. As opposed to crystals of ions in large single traps where the arrangement of ions is determined naturally by the trapping potential and the inter-ion Coulomb forces an array of traps containing a single ion each provides much greater flexibility over the spatial configuration²⁹.

The optimisation of the electrode structure to achieve the desired trapping potential at a set of points in space without the generation of any spurious traps is a non-trivial problem. Apart from producing a harmonic potential with identical spatial variance in the vicinity of the lattice sites, there are other constraints that the electrode geometry must satisfy.

Ions in surface traps suffer from motional heating in the proximity of the electrodes due to electric-field noise and the heating rate scales rapidly with decreasing ion-electrode distance³⁰. While recent studies suggest that these effects can be significantly suppressed through techniques such as electrode-surface treatment³¹ and cryogenic cooling³², the control of ion systems invariably requires laser beams and it is desirable to avoid scattering of light from the surface. As such the trap centres where the ions sit must be kept as far as possible from the electrodes. This task becomes more difficult if the ions are to be trapped closer together to ensure stronger motional coupling³³.

For the ions to be confined in the stiff regime such that laser cooling is more efficient, the motional frequencies obtained due to the trapping electrodes, and in turn the applied voltages, must be high enough. Any material used for electrode fabrication has an intrinsic electric field breakdown limit and this makes it challenging to achieve tight confinement of the ions at larger ion-electrode distances without surpassing this limit.

Two basic choices exist for the geometric layout of surface traps. One involves a single plane on which the electrodes are arranged while the alternative consists of a bilayer configuration with the ions trapped in the region between the two electrode planes. Theoretical studies suggest that ions can be brought much closer together

for a given ion-electrode distance using bilayer traps and the mirror symmetry leads to lower anharmonicities in the trapping potential³³. Single layer traps on the other hand have an open planar structure which allows easier access to lasers thereby reducing light scattering and its associated deleterious effects. Optical access in Penning traps, in any case, can be quite restricted due to the trap chip being placed inside the bore of a superconducting magnet. We focus our attention, therefore, on single layer surface electrode traps.

A method for obtaining optimal electrode geometries has been suggested originally for arrays of rf traps by Roman Schmied et al.¹⁵ but applies equally well in the case of electrostatic potentials. This approach can thus be used for micro-fabricated Penning trap arrays without the need for any pseudopotential approximation. The results in this thesis are based on the associated Mathematica Package, SurfacePattern, developed by Roman Schmied*.

The package pixellates the plane of electrodes at the desired resolution and then returns the optimal pixel distribution of voltages by solving a linear optimisation problem such that certain constraints on the trapping potential are met. These constraints include a specification of the derivatives of the potential at different points in space. Given a lattice with a certain inter-ion separation and a height above the electrode plane where the ions should be trapped, it is typically sufficient to specify a potential minimum at the lattice sites, along with the required curvatures in the form of a Hessian matrix. The voltages required to reach the desired trapping frequencies at a given height allow us to analyse the maximal ion-electrode distances that can be achieved.

In the case of infinite arrays of Penning traps, it suffices to specify these constraints for each point forming the basis in a unit cell of the underlying Bravais lattice. Optimisation of finite arrays, on the other hand, requires every single lattice point to be specified. While this makes it a considerably more intensive computational task, the obtained curvatures are much higher than for infinite arrays³⁴ meaning for the same trapping frequencies and electrode voltages the traps can be placed further away from the surface. With larger finite arrays, the size of the linear programming problem to be solved ultimately causes failure of the interior solving routine in Mathematica to converge, limiting both the size of the system that can be simulated and the resolution of the resulting electrode pattern. Moreover the inherent binary nature of the solutions returned suggests that the results presented in this thesis should as such be treated as preliminary optimisations which can most likely be improved upon through much more flexible approaches that allow for a larger set of voltage values.

*This software package can be found [here](#)

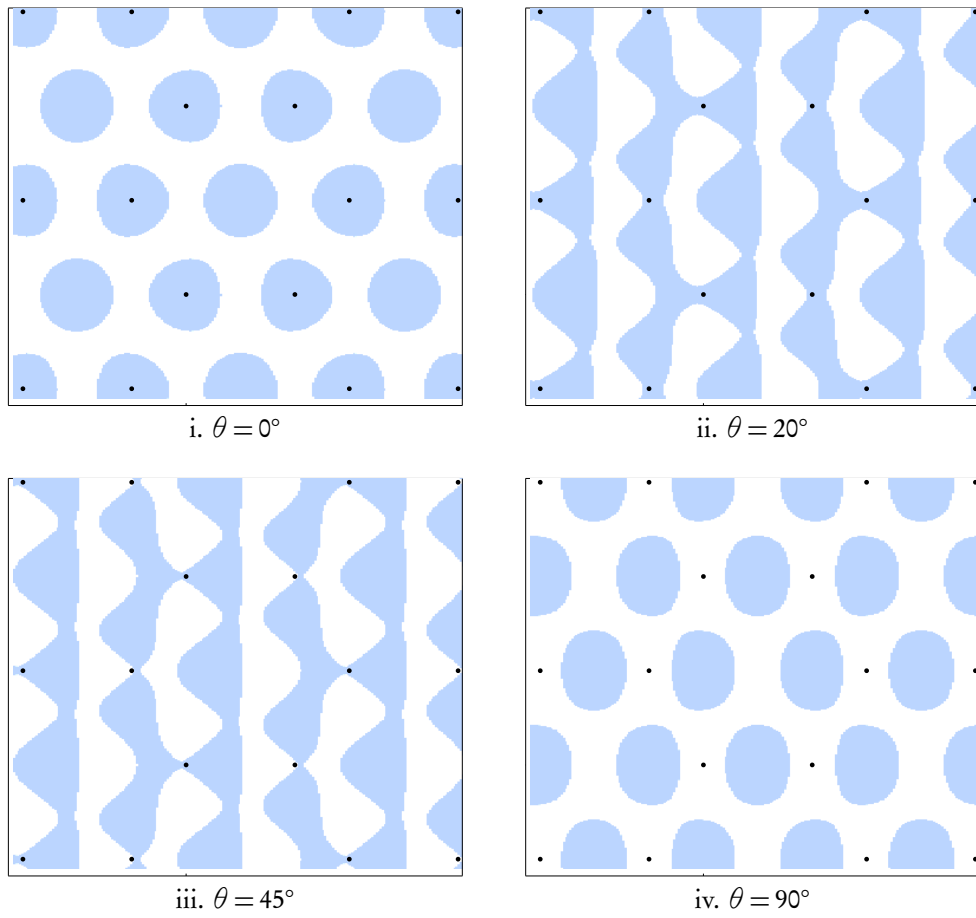


Figure 5.1: Optimal patterns for infinite honeycomb lattices for different angles of tilt. Here $b/d = 5/3$

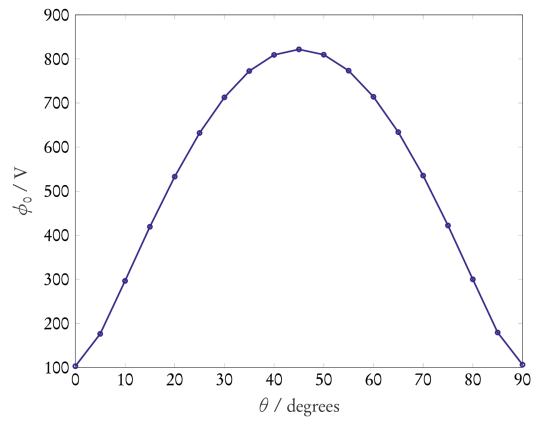


Figure 5.2: Variation of voltage required to achieve an axial frequency of $\omega_z = 2\pi \cdot 2\text{MHz}$ with increasing angle of tilt. Here nearest neighbour distance $d = 30\mu\text{m}$ and ion-electrode distance $h = 50\mu\text{m}$

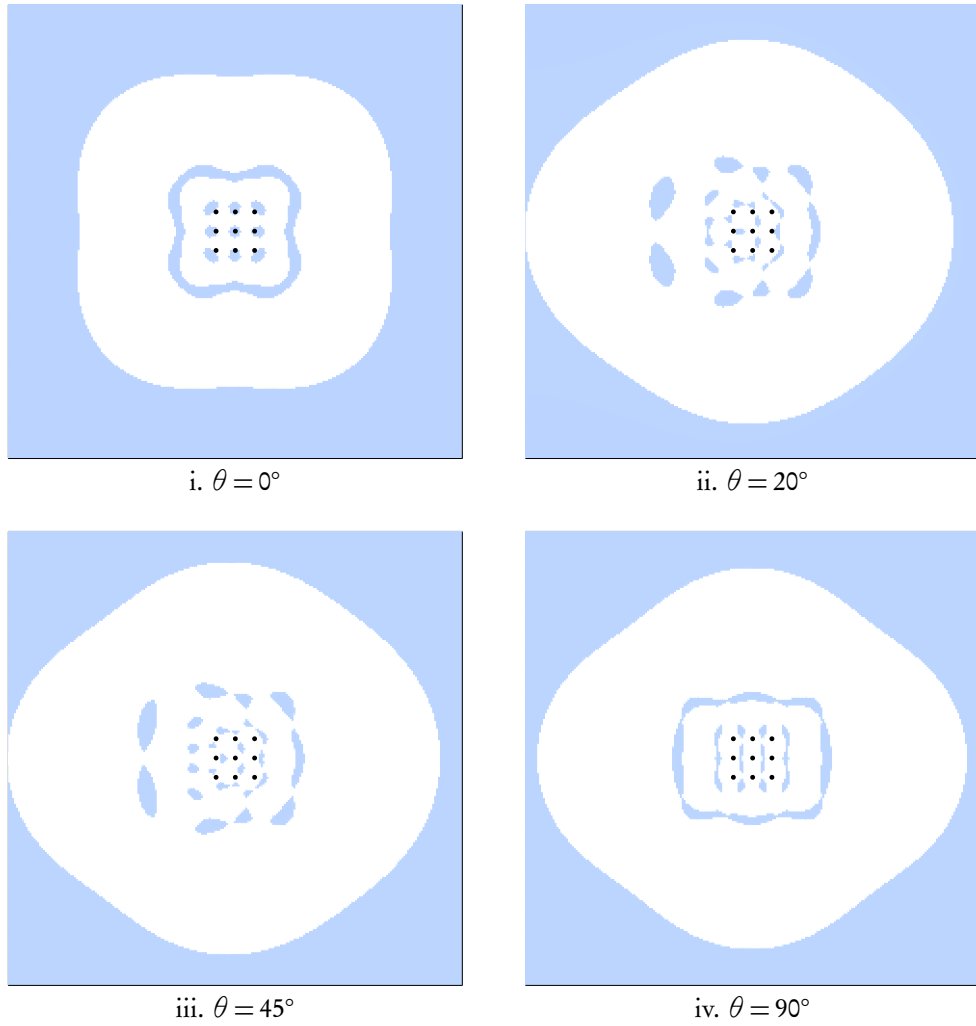


Figure 5.3: Optimal patterns for finite (9 ion) square lattices for different angles of tilt. Here $b/d = 2$

6

Benchmarking Results

Since the use of surface electrode traps allows a multitude of possible lattice formations it becomes important to compare the advantages and disadvantages of employing the different available geometries to realise a quantum spin simulator. Here 3 broad categories of the possible geometries are considered. For the sake of brevity these will be called Geometry A, B and C and are illustrated with the help of a six ion honeycomb lattice in figure 6.1. The largest quantum-spin simulator so far has been built in the NIST Boulder group of J. Bollinger and is based on a centimeter sized three-dimensional Penning trap in which a crystal of around 200 ${}^9\text{Be}^+$ ions arranges naturally in a triangular lattice in the radial plane. For a more faithful qualitative and quantitative comparison of different possible geometric implementations of two-dimensional micro-Penning trap arrays between themselves and with the NIST simulator, the results in this section are based on a 217 ${}^9\text{Be}^+$ ion triangular lattice with nearest neighbour separation of $20\ \mu\text{m}$. For identical traps with a bare axial frequency of $\omega_z = 2\ \text{MHz}$ and a magnetic field $B_0 = 2.5\ \text{T}$, all collective modes of motion can be Doppler cooled to low occupation numbers. This means the effects of spin-phonon entanglement can be suppressed more easily and the beat-note frequency of the ODF can be tuned closer to the mode frequency of choice.

GEOMETRY A

This is the geometric arrangement of two-dimensional ion arrays studied most often and closely resembles the natural formation of planar ion Coulomb crystals in large single Penning traps, such as the NIST trap. With such an arrangement, the axial and radial motion is decoupled and the resulting normal mode calculation is quite simplified. The frequency spectrum is shown in fig. 6.2 and clearly, the centre of mass mode in each of the mode branches is of either the highest or lowest frequency. This allows for the simulation of both ferromagnetic and antiferromagnetic Ising-type Hamiltonians with variable range couplings, using appropriately oriented and detuned ODF lasers (or other methods). This is depicted in fig. 6.3.

The creation of an ODF along the axial direction requires the lasers to be tilted with respect to the electrode plane. Even if the spin-spin interactions are effected through laserless methods, the cooling of the axial modes would invariably require a component of the laser beam along the confining axis. Since laser cooling of all modes of motion cannot be achieved through laser beams parallel to the surface, light scattering and its associated problems would be hard to avoid in such an arrangement.

GEOMETRY B

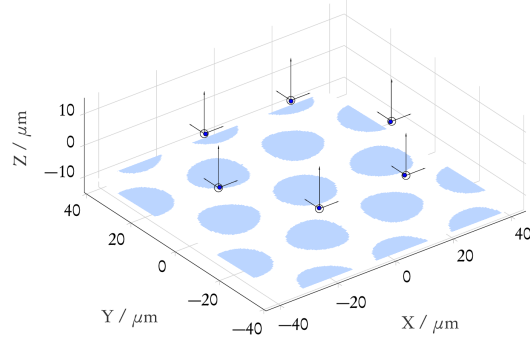
By tilting quadrupole potential produced by each trap with respect to the normal of the electrode plane, the resulting axial and radial modes are no longer decoupled. Such a geometric arrangement, however, allows for laser cooling all modes with the help beams parallel to the electrodes, thus eliminating possible scattering of light from the surface. When the angle of tilt is not too large ($\theta \lesssim 35^\circ$ for the given lattice and trap parameters), the centre of mass modes lie on either extrema of their respective branch. This is evident from fig. 6.4. Thus again both ferromagnetic and antiferromagnetic type couplings can be achieved, as shown in fig. 6.5. With certain orientations of the ODF generating laser beams it could be possible to attain this by changing a single experimental parameter, the relative frequency μ_R . Due to the time dependence of the radial components of the equilibrium positions in ion Coulomb crystals such interactions can fundamentally not be engineered in the NIST simulator.

The electrode structure required becomes more complex, with higher voltages required to trap ions, and the magnetic field also needs to be applied at angle with respect to the electrode plane. This complication in the arrangement of the superconducting magnet, however, is much less significant in comparison to the advantages gained from employing this geometry.

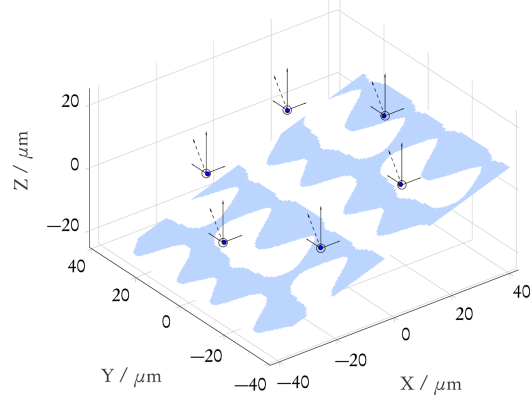
GEOMETRY C

With a lattice of ions along the confining axis and one of the anti-confining axes of the traps efficient cooling is possible with an appropriately oriented laser beam along the electrode plane. The optimal surface electrode patterns are not too complicated and the trap can be realised with the magnetic field pointing in the direction of the confining axis. The COM modes lie away from the extrema of their respective branches, as is clear from fig. 6.6. As a result, variable range couplings cannot be achieved by tuning the difference frequency of the ODF lasers alone. Fig. 6.7 and fig. 6.8 show the behaviour of the spin-spin couplings for different detunings.

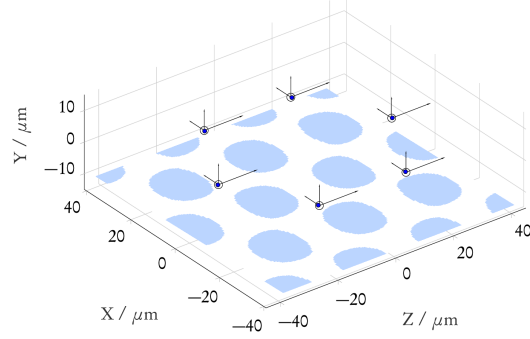
For Geometry C, more complicated ways to engineer such interactions would need to be employed, for instance the method suggested by Korenblit et al.³⁵. It could be possible however to use such an arrangement for the study of spin disorder dynamics, for example, in quantum spin glasses¹⁹. Since the defining axes of the lattice are not symmetric, the Coulomb interaction between the ions also leads to the emergence of interesting phenomena in the normal modes of certain lattices, for example, the honeycomb lattice. This was discussed before in Chapter 2.



i. Geometry A



ii. Geometry B



iii. Geometry C

Figure 6.1: Illustration of different geometries studied using a 6 ion honeycomb lattice trapped above the electrode plane (voltage is applied to the shaded regions while the unshaded regions are grounded). The empty circles represent the quadrupole centres while the filled circles represent the equilibrium positions of the ions. The three arrows at each quadrupole centre denote the quadrupole axes. The magnetic field is always aligned along the \hat{z} -axis, represented by the long axis of the quadrupole.

i. Geometry A: Lattice in the radial plane with the magnetic field perpendicular to this plane

ii. Geometry B: Each quadrupole is tilted about the \hat{y} -axis through the angle θ . In the figure show, $\theta = 20^\circ$. The dashed arrows depict the normal of the electrode plane or equivalently the plane formed by the lattice of quadrupole centres. The magnetic field is also aligned at the same angle with respect to this plane

iii. Geometry C: Lattice formed in the $\hat{x} - \hat{z}$ plane so that the magnetic field points along the plane

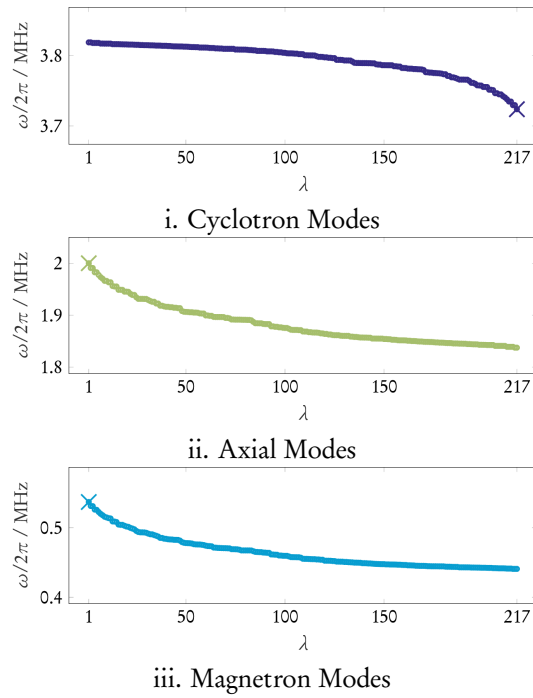


Figure 6.2: Frequency spectrum of a 217 ion triangular lattice ($d = 20 \mu\text{m}$) arranged with Geometry A. Shown here are the cyclotron, axial and magnetron branches of the normal modes. The centre of mass frequency in each mode branch is marked with a cross.

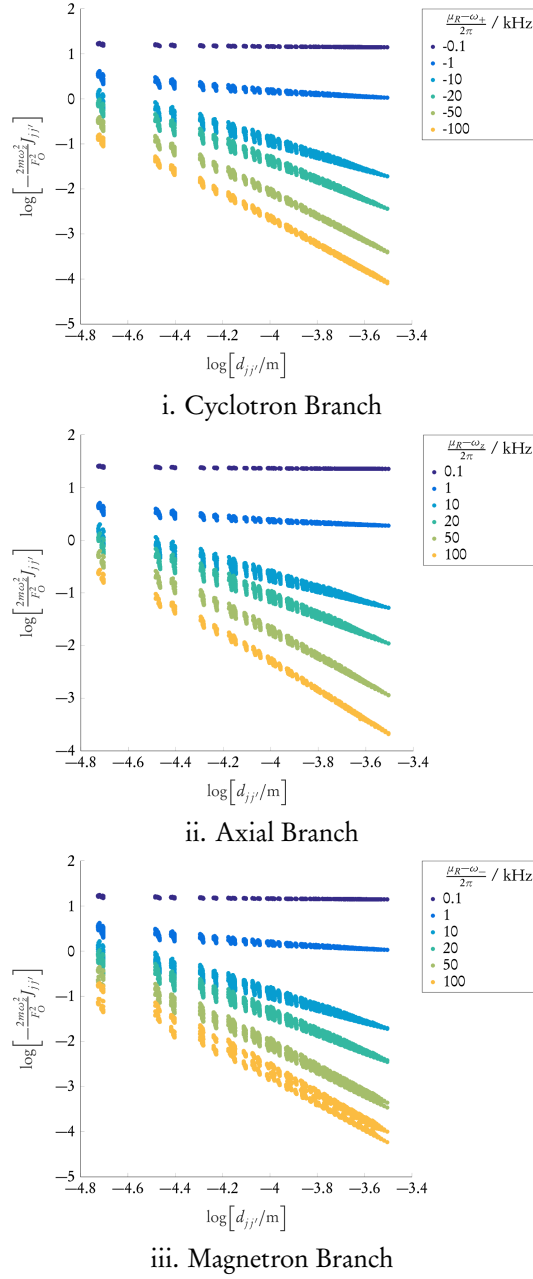


Figure 6.3: Spin-spin coupling terms generated with an optical dipole force for a 217 ion triangular lattice ($d = 20 \mu\text{m}$) arranged with Geometry A. For exciting the radial modes, the ODF can be created by two laser beams so that the difference wave vector \mathbf{k}_R lies along the \hat{x} -axis. When the beatnote frequency μ_R lies to the red of the cyclotron branch, all couplings $J_{jj'}$ are negative and a ferromagnetic Ising interaction can be engineered. These couplings follow an approximate power law decay $J_{jj'} \propto d_{jj'}^a$ and the exponent a increases with increasing $|\mu_R - \omega_+|$. Similar tuneable ferromagnetic couplings can be achieved by tuning to the blue of the magnetron COM mode. When the difference wave vector lies along the \hat{z} -axis and μ_R is to the blue of ω_z , all couplings are positive and hence variable range antiferromagnetic Ising like interactions can be generated by increasingly tuning away from the axial branch. The coupling strengths can be increased by using more powerful lasers or by increasing the angle between the two beams.

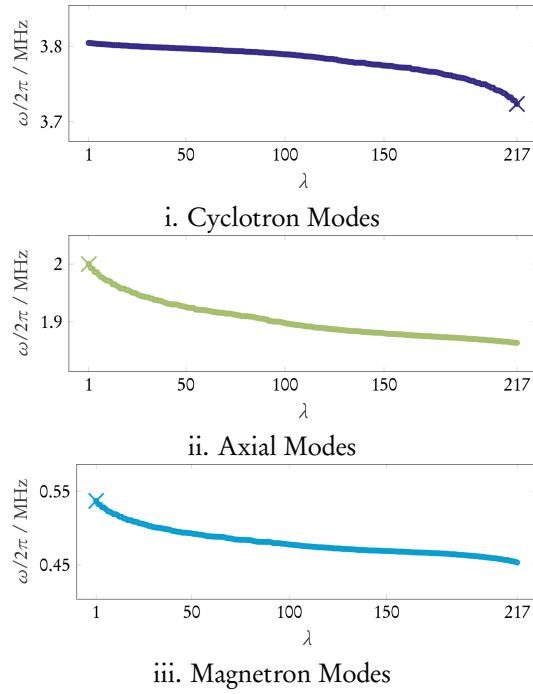


Figure 6.4: Frequency spectrum of a 217 ion triangular lattice ($d = 20 \mu\text{m}$) arranged with Geometry B ($\theta = 20^\circ$). Shown here are the cyclotron, axial and magnetron branches of the normal modes. The centre of mass frequency in each mode branch is marked with a cross

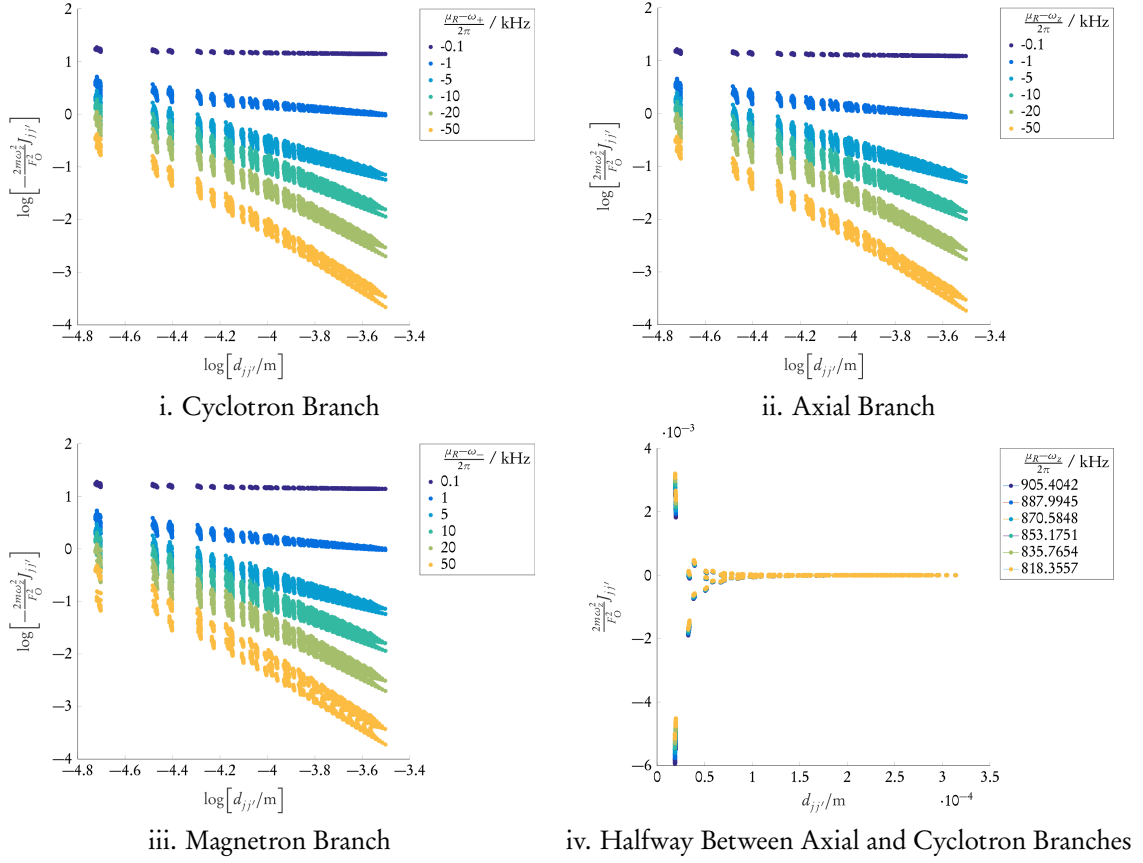


Figure 6.5: Spin-spin coupling terms generated with an optical dipole force for a 217 ion triangular lattice ($d = 20\mu\text{m}$) arranged with Geometry B ($\theta = 20^\circ$). The ODF can be created by two laser beams along the plane of the electrodes so that the difference wave vector is given by $\mathbf{k}_R = k_R \cos(\theta)\hat{x} + k_R \sin(\theta)\hat{z}$. When the beatnote frequency μ_R lies to the red of the cyclotron branch, all couplings are negative and a ferromagnetic Ising interaction can be engineered. These couplings follow an approximate power law decay $J_{ij'} \propto d_{ij'}^a$, and the exponent a increases with increasing $|\mu_R - \omega_+|$. Similar tuneable ferromagnetic couplings can be achieved by tuning to the blue of the magnetron COM mode. For the radial modes, lasers parallel to the electrode plane can also be used to create a wavevector difference along the \hat{y} -axis. When μ_R is increasingly tuned away from the axial branch, all couplings are positive and hence variable range antiferromagnetic Ising like interactions can be generated. The strength of these couplings is limited by the angle of tilt θ .

This behaviour is similar to the one observed in Geometry A but for larger detunings from the desired COM mode, the coupling terms vary over a greater range of magnitude for a given inter-ion distance. This is because the axial and radial modes are not decoupled and the difference wave vector chosen also results in participation of all modes. The contribution of the radial modes outweighs that of the axial modes when μ_R lies close to the cyclotron or magnetron modes and all couplings are negative. When μ_R is closer to the axial branch the contribution from the axial modes dominates in the coupling terms and hence these are all positive. Between the axial and cyclotron branches when the competition between these contributions is more even, roughly half the couplings are positive with the other half negative. An approximate dipole-dipole like behaviour is still evident in the magnitudes of the coupling strengths. Here $\omega_+ - \omega_z \approx 2\pi \cdot 1.72$ MHz.

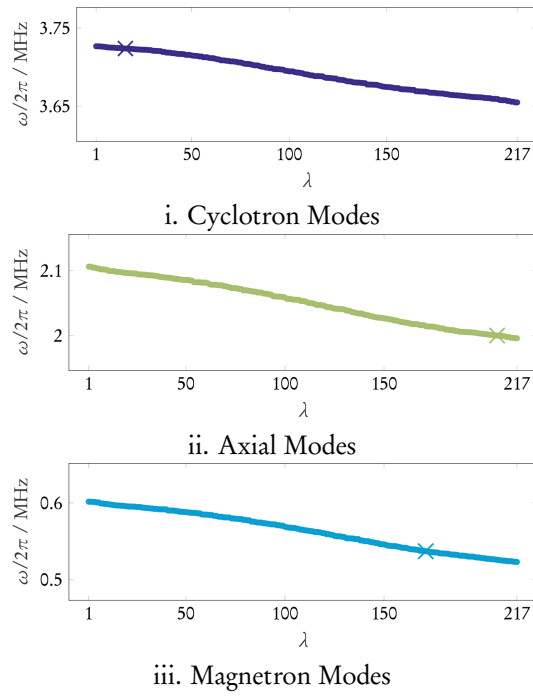


Figure 6.6: Frequency spectrum of a 217 ion triangular lattice ($d = 20 \mu\text{m}$) arranged with Geometry C. Shown here are the cyclotron, axial and magnetron branches of the normal modes. The centre of mass frequency in each mode branch is marked with a cross

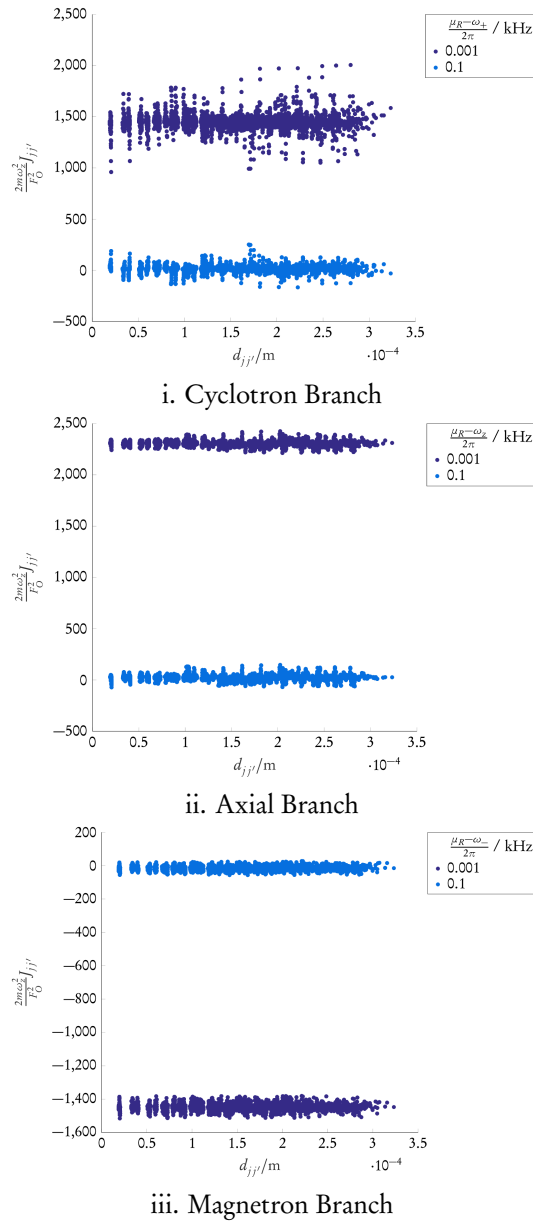
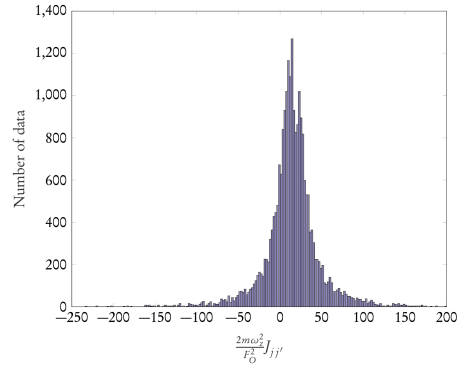
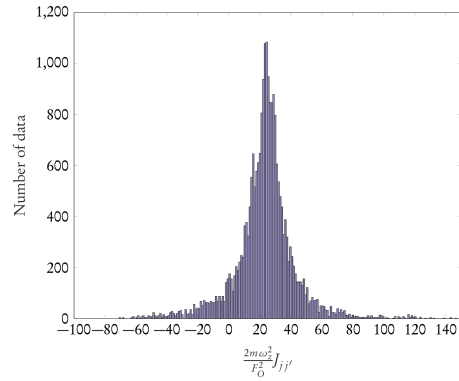


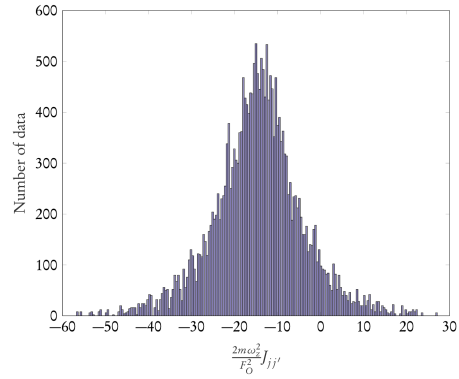
Figure 6.7: Spin-spin coupling terms generated with an optical dipole force for a 217 ion triangular lattice ($d = 20\mu\text{m}$) arranged with Geometry C. The ODF exciting either the radial or axial modes can be generated with laser beams parallel to the electrode plane. For the beatnote frequency really close to the desired COM mode only that mode is principally excited and all couplings are of the same sign and order of magnitude. Increasing $|\mu_R - \omega_{\text{COM}}|$ to $2\pi \cdot 0.1$ kHz leads to a frustration in the signs of different couplings, meaning only long range couplings can be achieved.



i. Cyclotron Branch



ii. Axial Branch



iii. Magneton Branch

Figure 6.8: Histogram plots for spin-spin coupling terms for a 217 ion triangular lattice ($d = 20 \mu\text{m}$) arranged with Geometry C when the beat note frequency μ_R is tuned slightly away from the COM frequency of each branch. Here $|\mu_R - \omega_{\text{COM}}| = 2\pi \cdot 0.1 \text{ kHz}$

7

Conclusions and Outlook

In this thesis, a thorough theoretical treatment of quantum spin simulators based on arrays of micro-fabricated Penning traps is presented. This includes the analysis of the normal modes of motion in the classical regime, a prescription to quantise the motion, and a method for generating spin-spin interactions by coupling the phonon motion and state-dependent forces. In addition, a semi-classical study of Doppler cooling of a system of ions in Penning traps is carried out. Different geometries for ion lattices are considered and an overview of methods to optimally generate them using surface electrode structures is offered. Although the results presented are based on ${}^9\text{Be}^+$ ions, the theoretical analysis can be applied to other ions as well. In fact an even more generalised treatment can be found in the appendices and used in the study of mixed-species ion arrays.

Numerical results included here indicate the possibility of simulating variable range Ising Hamiltonians of both the ferromagnetic and antiferromagnetic type using suitably arranged arrays of Penning traps. On the other hand, only the latter kind of couplings can be achieved with ion Coulomb crystals in single Penning traps. This qualitative advantage along with the much greater level of control over the configurations of ions manageable through surface electrode traps makes micro-fabricated trap arrays a more viable prospect for experimental quantum simulations of two-dimensional models.

This thesis represents the first step towards an experimental implementation of such a simulator. On the theoretical side, further work needs to be done on the optimisation of surface electrode patterns for realising the traps. It would be also interesting to examine the addition of a transverse field to the Ising model and the quantum phase transitions that could be achieved. Many more issues would invariably arise during the process of designing the actual experiment and these would have to be accordingly resolved.



Quadratic Eigenvalue Problem

The Quadratic Eigenvalue Problem (QEP) is a kind of non-linear eigenvalue problem where the aim is to find set of scalars λ and non-zero eigenvectors u and v that satisfy the equations

$$(\lambda^2 M + \lambda C + K)u = 0 \quad (\text{A.1a})$$

$$v^H (\lambda^2 M + \lambda C + K) = 0 \quad (\text{A.1b})$$

where M , C and K are $n \times n$ complex matrices and u and v are respectively the right and left eigenvectors corresponding to the eigenvalue λ . The QEP has $2n$ eigenvalues with upto $2n$ right and $2n$ left eigenvectors. Although QEPs have found widespread application in certain fields of physics such as the dynamic analysis of structural mechanical, and acoustic systems, they are much less frequently encountered or solved in comparison to the standard eigenvalue problem (SEP),

$$Au = \lambda u \quad (\text{A.2})$$

and the generalised eigenvalue problem (GEP)

$$Au = \lambda B u \quad (\text{A.3})$$

This section summarises some useful properties relevant to the type of QEPs encountered while studying the normal mode dynamics of trapped ions in the stable regime. Here, stability means that the eigenvalues are all finite, real, and non-zero, and hence the motion of the ions is bounded. If the solution of the QEP yields any imaginary or infinite eigenvalues the ions can not be confined with the given combination of electric and magnetic fields in the trap.

Noting the symmetries present in the matrices in our equations of motion we additionally restrict our discussion

to a class of the standard QEP $[\lambda^2 M + \lambda C + K]u = 0$ where the matrices M , C and K are Hermitian, M and K are non-singular and real, and $C^* = -C$. For typical physical systems, including ours, M refers to the mass matrix, K is the stiffness matrix while C is the damping matrix that captures the effect of velocity dependent forces.

A more general and thorough treatment of QEPs, their applications, and techniques for numerical solution can be found in the review paper by Tisseur et al.³⁶.

SOME PROPERTIES

1. Unlike SEPs and GEPs, the eigenvectors of the QEP in general do not form a linearly independent set since there can be more than n eigenvectors. We can rewrite the QEP as $Q(\lambda)u = 0$, where the λ -matrix $Q(\lambda) = \lambda^2 M + \lambda C + K$ is called regular if $\det Q(\lambda)$ is not identically zero for any arbitrary value of λ . Since K is non-singular, it is easy to see that $\det Q(\lambda) \neq 0$ for $\lambda = 0$. Hence for the class of QEPs studied here, $Q(\lambda)$ is regular and there exists a set of n linearly independent eigenvectors if $Q(\lambda)$ has $2n$ distinct eigenvalues³⁷. This is a non-trivial generalisation of standard results for the SEP and the GEP. For simplicity we will assume the lack of any degenerate eigenvalues and with this we are guaranteed a subset of eigenvectors that can form a basis in the n -dimensional vector space. Additionally, in general the eigenvectors of the QEP are not orthogonal in the conventional linear-algebraic sense i.e. $u_j^H u_k \neq \delta_{jk}$. Nevertheless we can derive some generalised orthogonality and normalisation conditions by employing the symmetry properties of our matrices.

2. For an eigenvector u with eigenvalue λ , we have

$$\lambda^2 M u + \lambda C u + K u = 0 \quad (\text{A.4})$$

Since eigenvalues are all real and M , C and K are Hermitian it is easy to see by taking the conjugate transpose of the QEP that

$$\lambda^2 u^H M + \lambda u^H C + u^H K = 0 \quad (\text{A.5})$$

Thus if u is a right eigenvector of the QEP with eigenvalue λ then it is also a left eigenvector with the same eigenvalue.

3. Taking just the complex conjugate on the other hand yields

$$\lambda^2 M u^* - \lambda C u^* + K u^* = 0 \quad (\text{A.6})$$

where we have used the fact that M and K are real and $C^* = -C$. Thus if u is an eigenvector with eigenvalue λ then so is u^* with eigenvalue $-\lambda$. Thus eigenvectors and their corresponding eigenvalues come in pairs $\{u, u^*\}$ and $\{\lambda, -\lambda\}$ respectively.

4. Combining the above equations, we get

$$\lambda^2 u^H M u^* + \lambda u^H C u^* + u^H K u^* = 0 \quad (\text{A.7a})$$

$$\lambda^2 u^H M u^* - \lambda u^H C u^* + u^H K u^* = 0 \quad (\text{A.7b})$$

which means

$$u^H C u^* = 0 \quad (\text{A.8})$$

5. For two distinct eigenvalues λ_j and λ_k corresponding to the eigenvectors u_j and u_k respectively,

$$\lambda_j^2 M u_j + \lambda_j C u_j + K u_j = 0 \quad (\text{A.9a})$$

$$\lambda_k^2 M u_k + \lambda_k C u_k + K u_k = 0 \quad (\text{A.9b})$$

Then

$$\lambda_k^2 u_k^H M u_j + \lambda_k u_k^H C u_j + u_k^H K u_j = 0 \quad (\text{A.10a})$$

$$\lambda_j^2 u_k^H M u_j + \lambda_j u_k^H C u_j + u_k^H K u_j = 0 \quad (\text{A.10b})$$

and hence

$$(\lambda_k^2 - \lambda_j^2) u_k^H M u_j + (\lambda_k - \lambda_j) u_k^H C u_j = 0 \quad (\text{A.11})$$

Since $\lambda_j \neq \lambda_k$, the eigenvectors u_j and u_k satisfy the following generalised condition for orthogonality:

$$(\lambda_k + \lambda_j) u_k^H M u_j + u_k^H C u_j = 0 \quad (\text{A.12})$$

6. For two distinct eigenvalues λ_j and λ_k corresponding to the same eigenvector u ,

$$\lambda_j^2 M u + \lambda_j C u + K u = 0 \quad (\text{A.13a})$$

$$\lambda_k^2 M u + \lambda_k C u + K u = 0 \quad (\text{A.13b})$$

Then

$$(\lambda_j^2 - \lambda_k^2) M u + (\lambda_j - \lambda_k) C u = 0 \quad (\text{A.14})$$

$$M^{-1} C u = -(\lambda_j + \lambda_k) u \quad (\text{A.15})$$

Thus u is an eigenvector of $M^{-1}C$ with eigenvalue $-(\lambda_j + \lambda_k)$.

LINEARISATION OF THE QEP

One technique to solve a QEP is to map it onto a GEP with the same eigenvalues and twice the dimension of the original problem, and then utilising the known methods for solution of GEPs. This linearisation process can be easily carried out by using the substitution $v = \lambda u$ in $\lambda^2 M u + \lambda C u + K u = 0$ and rewriting the equation as

$$\lambda M v + \lambda C u + K u = 0, \quad (\text{A.16})$$

yielding the GEP corresponding to the so-called first companion form

$$\begin{bmatrix} \mathbb{O}_n & \mathbb{I}_n \\ -K & -C \end{bmatrix} \begin{bmatrix} u \\ v \end{bmatrix} = \lambda \begin{bmatrix} \mathbb{I}_n & \mathbb{O}_n \\ \mathbb{O}_n & M \end{bmatrix} \begin{bmatrix} u \\ v \end{bmatrix} \quad (\text{A.17})$$

where \mathbb{O}_n and \mathbb{I}_n are respectively $n \times n$ zero and identity matrices. This procedure is analogous to the reduction of a second-order differential equation to a first-order equation.

B

Normal Mode Analysis: Classical Description

We consider a system of N Penning traps containing a single ion each (with charge $+e$) arranged arbitrarily in space. The Coulomb interaction between ions leads to a coupling between their motional states, resulting in $3N$ collective normal modes of motion.

LAGRANGIAN FORMULATION

We begin by defining the different sets of coordinates we will use in the course of the normal mode analysis. In the laboratory frame of reference, it is convenient to use a coordinate system with axes parallel to the axes defined by the form of each quadrupole potential. Equivalently the local coordinates of each ion with respect to its trap centre can be expressed in a coordinate system aligned with the lab frame axes.

Let the quadrupole center j and the position of the ion j in the reference frame of the lab be defined by the coordinates $\mathbf{D}_j = D_{jx}\hat{x} + D_{jy}\hat{y} + D_{jz}\hat{z}$ and $\mathbf{R}_j = X_j\hat{x} + Y_j\hat{y} + Z_j\hat{z}$ respectively. Then the local coordinates of the ion j with respect to this quadrupole center are given by the vector $\bar{\mathbf{r}}_j = \bar{x}_j\hat{x} + \bar{y}_j\hat{y} + \bar{z}_j\hat{z} = \mathbf{R}_j - \mathbf{D}_j$. Because of the Coulomb repulsion the equilibrium position of the ion $\mathbf{R}_{j0} = X_{j0}\hat{x} + Y_{j0}\hat{y} + Z_{j0}\hat{z}$ in the lab frame does not coincide with its corresponding quadrupole center.

The trapping electrodes create a static quadrupole electric potential centered at each site j . This potential satisfies the Laplace equation and can be written as $\phi_j = \sum_{\mu\nu} \phi_{j0}^{\mu\nu} \bar{r}_j^\mu \bar{r}_j^\nu$, where the indices μ and ν run over the Cartesian components, x , y and z .

The electrostatic potential acting on the ion j due to the Coulomb interaction with other ions is

$$\chi_j = \sum_{k \neq j} \frac{e}{4\pi\epsilon_0 |\mathbf{R}_j - \mathbf{R}_k|} = k_e e \sum_{k \neq j} \frac{1}{|\mathbf{R}_{jk}|}, \quad (\text{B.1})$$

where $k_e = 1/(4\pi\epsilon_0)$ is the Coulomb constant.

The total electric potential, in the absence of any oscillating fields, is thus given by $\Phi_j = \phi_j + \chi_j$.

A static homogeneous magnetic field $\mathbf{B} = B_0 \sin \theta \cos \psi \hat{x} + B_0 \sin \theta \sin \psi \hat{y} + B_0 \cos \theta \hat{z}$ creates the vector potential \mathbf{A}_j at the site j . In the symmetric gauge, $\mathbf{A}_j = \frac{1}{2}(\mathbf{B} \times \mathbf{R}_j)$.

In the laboratory frame of reference, the Lagrangian of the system is then given by

$$L = \sum_{j=1}^N \left\{ \frac{1}{2} m_j |\dot{\mathbf{R}}_j|^2 + e \mathbf{A}_j \cdot \dot{\mathbf{R}}_j - e \Phi_j \right\} \quad (\text{B.2})$$

where m_j is the mass of the j th ion.

The normal mode analysis begins by finding the equilibrium configuration of ions, which is determined by the minimum of the total potential energy. By expanding the system Lagrangian about the equilibrium position of each ion in a Taylor series up to second order, we get a Lagrangian in terms of the generalised position vectors $\mathbf{r}_j = \mathbf{R}_j - \mathbf{R}_{j0}$ which specify the displacement of each ion from its equilibrium point. The second order term in the expansion effectively dictates the normal mode dynamics of the system near the stable spatial configuration and is given by

$$L = \sum_{j=1}^N \left\{ \frac{1}{2} m_j |\dot{\mathbf{r}}_j|^2 + \frac{e}{2} (\mathbf{B} \times \mathbf{r}_j) \cdot \dot{\mathbf{r}}_j - e \sum_{\mu\nu} \phi_{j0}^{\mu\nu} r_j^\mu r_j^\nu \right\} \\ - \frac{k_e e^2}{2} \sum_{j=1}^N \sum_{k \neq j}^N \left\{ \sum_{\mu} \frac{3R_{jk0}^{\mu 2} - R_{jk0}^2}{R_{jk0}^5} (r_j^\mu - r_k^\mu)^2 + \sum_{\mu \neq \nu} \frac{3R_{jk0}^\mu R_{jk0}^\nu}{R_{jk0}^5} (r_j^\mu - r_k^\mu)(r_j^\nu - r_k^\nu) \right\}, \quad (\text{B.3})$$

Putting together all generalised position coordinates into a single $3N$ -dimensional vector $q = [x_1 \dots x_N \quad y_1 \dots y_N \quad z_1 \dots z_N]^T$ we can express the Lagrangian in a more compact form,

$$L = \sum_{j=1}^{3N} \left\{ \frac{1}{2} M_{jj} \dot{q}_j^2 - \frac{1}{2} \sum_{k=1}^{3N} W_{jk} \dot{q}_j q_k - \frac{1}{2} \sum_{k=1}^{3N} V_{jk} q_j q_k - \frac{1}{2} \sum_{k=1}^{3N} K_{jk} q_j q_k \right\} \quad (\text{B.4})$$

in which M , W , V and K are $3N \times 3N$ block matrices constructed in terms of $N \times N$ sub-matrices

$$M = \begin{bmatrix} M^{xx} & \mathbb{O}_N & \mathbb{O}_N \\ \mathbb{O}_N & M^{yy} & \mathbb{O}_N \\ \mathbb{O}_N & \mathbb{O}_N & M^{zz} \end{bmatrix} \quad (\text{B.5a})$$

$$W = eB_0 \begin{bmatrix} \mathbb{O}_N & \cos \theta \cdot \mathbb{I}_N & -\sin \theta \sin \varphi \cdot \mathbb{I}_N \\ -\cos \theta \cdot \mathbb{I}_N & \mathbb{O}_N & \sin \theta \cos \varphi \cdot \mathbb{I}_N \\ \sin \theta \sin \varphi \cdot \mathbb{I}_N & -\sin \theta \cos \varphi \cdot \mathbb{I}_N & \mathbb{O}_N \end{bmatrix} \quad (\text{B.5b})$$

$$V = \begin{bmatrix} V^{xx} & V^{xy} & V^{xz} \\ V^{yx} & V^{yy} & V^{yz} \\ V^{zx} & V^{zy} & V^{zz} \end{bmatrix} \quad (\text{B.5c})$$

$$K = \begin{bmatrix} K^{xx} & K^{xy} & K^{xz} \\ K^{yx} & K^{yy} & K^{yz} \\ K^{zx} & K^{zy} & K^{zz} \end{bmatrix} \quad (\text{B.5d})$$

Here \mathbb{I}_N and \mathbb{O}_N represent the $N \times N$ identity and zero matrices respectively and the components of other sub-matrices are defined as

$$M_{jk}^{\mu\mu} = m_j \delta_{jk} \quad (\text{B.6})$$

$$V_{jk}^{\mu\nu} = 2e\phi_{j0}^{\mu\nu} \delta_{jk}, \quad (\text{B.7})$$

$$K_{jk}^{\mu\mu} = \begin{cases} -k_e e^2 \sum_{l \neq j} \frac{R_{jl0}^2 - 3R_{jl0}^{\mu 2}}{R_{jl0}^5}, & j = k \\ k_e e^2 \frac{R_{jko}^2 - 3R_{jko}^{\mu 2}}{R_{jko}^5}, & j \neq k \end{cases}, \quad (\text{B.8a})$$

$$K_{jk}^{\mu\nu} = K_{jk}^{\nu\mu} = \begin{cases} 3k_e e^2 \sum_{l \neq j} \frac{R_{jl0}^{\mu} R_{jl0}^{\nu}}{R_{jl0}^5}, & j = k \\ -3k_e e^2 \frac{R_{jlo}^{\mu} R_{jlo}^{\nu}}{R_{jko}^5}, & j \neq k \end{cases}, \quad \mu \neq \nu, \quad (\text{B.8b})$$

where indices j and k run from 1 to N while again the indices μ and ν refer to the components x, y and z .

With $\Phi = V + K$, the effective phonon Lagrangian can be written as

$$L = \sum_{j=1}^{3N} \left\{ \frac{1}{2} M_{jj} \dot{q}_j^2 - \frac{1}{2} \sum_{k=1}^{3N} W_{jk} \dot{q}_j q_k - \frac{1}{2} \sum_{k=1}^{3N} \Phi_{jk} q_j q_k \right\}, \quad (\text{B.9})$$

By construction, M is a real diagonal matrix, W is a real antisymmetric matrix, while Φ is a real symmetric matrix. These properties will be useful in determining the characteristics of the normal mode eigenfrequencies and eigenvectors.

EQUATIONS OF MOTION

Through the Euler-Lagrange equations

$$\frac{d}{dt} \left\{ \frac{\partial L}{\partial \dot{q}_j} \right\} = \frac{\partial L}{\partial q_j} \quad (\text{B.10})$$

we can derive from the Lagrangian the equations of motion of our system.

Noting that

$$\frac{\partial L}{\partial \dot{q}_j} = M_{jj} \dot{q}_j - \frac{1}{2} \sum_{k=1}^{3N} W_{jk} q_k \quad (\text{B.11})$$

and

$$\frac{\partial L}{\partial q_j} = \frac{1}{2} \sum_{k=1}^{3N} W_{jk} \dot{q}_k - \sum_{k=1}^{3N} \Phi_{jk} q_k \quad (\text{B.12})$$

we get

$$M_{jj} \ddot{q}_j - \frac{1}{2} \sum_{k=1}^{3N} W_{jk} \dot{q}_k = \frac{1}{2} \sum_{k=1}^{3N} W_{jk} \dot{q}_k - \sum_{k=1}^{3N} \Phi_{jk} q_k \quad (\text{B.13})$$

or

$$M_{jj} \ddot{q}_j - \sum_{k=1}^{3N} W_{jk} \dot{q}_k + \sum_{k=1}^{3N} \Phi_{jk} q_k = 0 \quad (\text{B.14})$$

Thus the equations of motion reduce to, in vector form,

$$M \ddot{q} - W \dot{q} + \Phi q = 0, \quad (\text{B.15})$$

To find the normal modes of motion, we substitute the oscillating trial solution $q = q_0 e^{-i\omega t}$ which yields the QEP

$$[\omega^2(M + \omega(-iW) - \Phi)]q_0 = 0, \quad (\text{B.16})$$

that can be solved for complex eigenvectors q_0 and eigenvalues ω , which in general can be complex. The set of eigenvalues $\{\omega_\lambda\}$ are the normal mode frequencies while the corresponding normalised eigenvectors $\{q_\lambda\}$ give us the normal mode coordinates.

The general solution can be written as

$$q(t) = \sum_{\lambda=1}^{3N} \rho_\lambda q_\lambda e^{-i\omega_\lambda t} \quad (\text{B.17})$$

where ρ_λ are complex scalars. The motion of the ions in terms of the normal modes can then be retrieved as

$$r(t) = \text{Re}(q(t)) = \frac{1}{2} \sum_{\lambda=1}^{3N} (\rho_\lambda q_\lambda e^{-i\omega_\lambda t} + \rho_\lambda^* q_\lambda^* e^{i\omega_\lambda t}) \quad (\text{B.18})$$

For real frequencies, the collective motion is bounded and hence all ions are confined.

MODE ENERGIES

With the general solution for $r(t)$

$$r(t) = \frac{1}{2} \sum_{\lambda=1}^{3N} \left\{ \rho_{\lambda} q_{\lambda} e^{-i\omega_{\lambda} t} + \rho_{\lambda}^* q_{\lambda}^* e^{i\omega_{\lambda} t} \right\} \quad (\text{B.19})$$

the velocity vector can be written as

$$\dot{r}(t) = \frac{1}{2} \left\{ \sum_{\lambda=1}^{3N} -i\omega_{\lambda} \rho_{\lambda} q_{\lambda} e^{-i\omega_{\lambda} t} + i\omega_{\lambda} \rho_{\lambda}^* q_{\lambda}^* e^{i\omega_{\lambda} t} \right\} \quad (\text{B.20})$$

Taking the transpose on both sides,

$$r^T(t) = \frac{1}{2} \sum_{\lambda=1}^{3N} \left\{ \rho_{\lambda} q_{\lambda}^T e^{-i\omega_{\lambda} t} + \rho_{\lambda}^* q_{\lambda}^H e^{i\omega_{\lambda} t} \right\} \quad (\text{B.21})$$

$$\dot{r}^T(t) = \frac{1}{2} \sum_{\lambda=1}^{3N} \left\{ -i\omega_{\lambda} \rho_{\lambda} q_{\lambda}^T e^{-i\omega_{\lambda} t} + i\omega_{\lambda} \rho_{\lambda}^* q_{\lambda}^H e^{i\omega_{\lambda} t} \right\} \quad (\text{B.22})$$

The total energy of the system is given by

$$\begin{aligned} E &= \sum_{j=1}^{3N} \left\{ \frac{1}{2} M_{jj} \dot{r}_j^2 + \frac{1}{2} \sum_{k=1}^{3N} \Phi_{jk} r_j r_k \right\} \\ &= \frac{1}{2} \dot{r}^T M \dot{r} + \frac{1}{2} r^T \Phi r \end{aligned} \quad (\text{B.23})$$

Substituting equations B.21 and B.22,

$$\begin{aligned} E &= \frac{1}{4} \sum_{\lambda'=1}^{3N} \left\{ -i\omega_{\lambda'} \rho_{\lambda'} q_{\lambda'}^T e^{-i\omega_{\lambda'} t} + i\omega_{\lambda'} \rho_{\lambda'}^* q_{\lambda'}^H e^{i\omega_{\lambda'} t} \right\} M \dot{r} \\ &\quad + \frac{1}{4} \sum_{\lambda'=1}^{3N} \left\{ \rho_{\lambda'} q_{\lambda'}^T e^{-i\omega_{\lambda'} t} + \rho_{\lambda'}^* q_{\lambda'}^H e^{i\omega_{\lambda'} t} \right\} \Phi r \end{aligned} \quad (\text{B.24})$$

Using $q_{\lambda'}^T \Phi = \omega_{\lambda'}^2 q_{\lambda'}^T M + i\omega_{\lambda'} q_{\lambda'}^T W$ and $q_{\lambda'}^H \Phi = \omega_{\lambda'}^2 q_{\lambda'}^H M - i\omega_{\lambda'} q_{\lambda'}^H W$

$$\begin{aligned}
E &= \frac{1}{4} \sum_{\lambda'=1}^{3N} \left\{ -i\omega_{\lambda'} \rho_{\lambda'} q_{\lambda'}^T e^{-i\omega_{\lambda'} t} + i\omega_{\lambda'} \rho_{\lambda'}^* q_{\lambda'}^H e^{i\omega_{\lambda'} t} \right\} M \dot{r} \\
&+ \frac{1}{4} \sum_{\lambda'=1}^{3N} \left\{ \rho_{\lambda'} e^{-i\omega_{\lambda'} t} (\omega_{\lambda'}^2 q_{\lambda'}^T M + i\omega_{\lambda'} q_{\lambda'}^T W) + \rho_{\lambda'}^* e^{i\omega_{\lambda'} t} (\omega_{\lambda'}^2 q_{\lambda'}^H M - i\omega_{\lambda'} q_{\lambda'}^H W) \right\} r \\
&= \frac{1}{4} \sum_{\lambda'=1}^{3N} \left\{ \omega_{\lambda'} \rho_{\lambda'} e^{-i\omega_{\lambda'} t} (-i q_{\lambda'}^T M \dot{r} + \omega_{\lambda'} q_{\lambda'}^T M r + q_{\lambda'}^T (iW) r) \right\} \\
&+ \frac{1}{4} \sum_{\lambda'=1}^{3N} \left\{ \omega_{\lambda'} \rho_{\lambda'} e^{i\omega_{\lambda'} t} (i q_{\lambda'}^H M \dot{r} + \omega_{\lambda'} q_{\lambda'}^H M r + q_{\lambda'}^H (-iW) r) \right\}
\end{aligned} \tag{B.25}$$

We can calculate the first of these sums as

$$\begin{aligned}
E_1 &= \frac{1}{4} \sum_{\lambda'=1}^{3N} \omega_{\lambda'} \rho_{\lambda'} e^{-i\omega_{\lambda'} t} \left\{ -i q_{\lambda'}^T M \dot{r} + \omega_{\lambda'} q_{\lambda'}^T M r + q_{\lambda'}^T (iW) r \right\} \\
&= \frac{1}{8} \sum_{\lambda'=1}^{3N} \omega_{\lambda'} \rho_{\lambda'} e^{-i\omega_{\lambda'} t} \sum_{\lambda=1}^{3N} \left\{ -i q_{\lambda'}^T M (-i\omega_{\lambda} \rho_{\lambda} q_{\lambda} e^{-i\omega_{\lambda} t} + i\omega_{\lambda} \rho_{\lambda}^* q_{\lambda}^* e^{i\omega_{\lambda} t}) + (\omega_{\lambda} q_{\lambda'}^T M + q_{\lambda'}^T (iW)) (\rho_{\lambda} q_{\lambda} e^{-i\omega_{\lambda} t} + \rho_{\lambda}^* q_{\lambda}^* e^{i\omega_{\lambda} t}) \right\} \\
&= \frac{1}{8} \sum_{\lambda'=1}^{3N} \omega_{\lambda'} \rho_{\lambda'} e^{-i\omega_{\lambda'} t} \sum_{\lambda=1}^{3N} \rho_{\lambda} e^{-i\omega_{\lambda} t} \left\{ -\omega_{\lambda} q_{\lambda'}^T M q_{\lambda} + \omega_{\lambda} q_{\lambda'}^T M q_{\lambda} + q_{\lambda'}^T (iW) q_{\lambda} \right\} \\
&+ \frac{1}{8} \sum_{\lambda'=1}^{3N} \omega_{\lambda'} \rho_{\lambda'}^* e^{i\omega_{\lambda'} t} \sum_{\lambda=1}^{3N} \rho_{\lambda}^* e^{i\omega_{\lambda} t} \left\{ -\omega_{\lambda} q_{\lambda'}^T M q_{\lambda}^* + \omega_{\lambda} q_{\lambda'}^T M q_{\lambda}^* + q_{\lambda'}^T (iW) q_{\lambda}^* \right\} \\
&= \frac{1}{8} \sum_{\lambda'=1}^{3N} \omega_{\lambda'} \rho_{\lambda'} e^{-i\omega_{\lambda'} t} \sum_{\lambda=1}^{3N} \rho_{\lambda} e^{-i\omega_{\lambda} t} \left\{ \cdot 0 \right\} \\
&+ \frac{1}{8} \sum_{\lambda'=1}^{3N} \omega_{\lambda'} \rho_{\lambda'}^* e^{i\omega_{\lambda'} t} \sum_{\lambda=1}^{3N} \rho_{\lambda}^* e^{i\omega_{\lambda} t} \left\{ \frac{1}{\omega_{\lambda}} (\omega_{\lambda}^2 q_{\lambda}^T M q_{\lambda}^* + q_{\lambda}^T \Phi q_{\lambda}^*) \delta_{\lambda\lambda'} \right\} \\
&= \frac{1}{8} \sum_{\lambda=1}^{3N} |\rho_{\lambda}|^2 (\omega_{\lambda}^2 q_{\lambda}^T M q_{\lambda}^* + q_{\lambda}^T \Phi q_{\lambda}^*)
\end{aligned} \tag{B.26}$$

and the second of these sums as

$$\begin{aligned}
E_2 &= \frac{1}{4} \sum_{\lambda'=1}^{3N} \omega_{\lambda'} \rho_{\lambda'}^* e^{i\omega_{\lambda'} t} \left\{ i q_{\lambda'}^H M \dot{r} + \omega_{\lambda'} q_{\lambda'}^H M r + q_{\lambda'}^H (-iW) r \right\} \\
&= \frac{1}{8} \sum_{\lambda'=1}^{3N} \omega_{\lambda'} \rho_{\lambda'}^* e^{i\omega_{\lambda'} t} \sum_{\lambda=1}^{3N} \left\{ i q_{\lambda'}^H M (-i\omega_{\lambda} \rho_{\lambda} q_{\lambda} e^{-i\omega_{\lambda} t} + i\omega_{\lambda} \rho_{\lambda}^* q_{\lambda}^* e^{i\omega_{\lambda} t}) + (\omega_{\lambda} q_{\lambda'}^H M + q_{\lambda'}^H (-iW)) (\rho_{\lambda} q_{\lambda} e^{-i\omega_{\lambda} t} + \rho_{\lambda}^* q_{\lambda}^* e^{i\omega_{\lambda} t}) \right\} \\
&= \frac{1}{8} \sum_{\lambda'=1}^{3N} \omega_{\lambda'} \rho_{\lambda'}^* e^{i\omega_{\lambda'} t} \sum_{\lambda=1}^{3N} \rho_{\lambda} e^{-i\omega_{\lambda} t} \left\{ \omega_{\lambda} q_{\lambda'}^H M q_{\lambda} + \omega_{\lambda'} q_{\lambda'}^H M q_{\lambda} + q_{\lambda'}^H (-iW) q_{\lambda} \right\} \\
&\quad + \frac{1}{8} \sum_{\lambda'=1}^{3N} \omega_{\lambda'} \rho_{\lambda'}^* e^{i\omega_{\lambda'} t} \sum_{\lambda=1}^{3N} \rho_{\lambda}^* e^{i\omega_{\lambda} t} \left\{ -\omega_{\lambda} q_{\lambda'}^H M q_{\lambda}^* + \omega_{\lambda'} q_{\lambda'}^H M q_{\lambda}^* + q_{\lambda'}^H (iW) q_{\lambda}^* \right\} \\
&= \frac{1}{8} \sum_{\lambda'=1}^{3N} \omega_{\lambda'} \rho_{\lambda'}^* e^{i\omega_{\lambda'} t} \sum_{\lambda=1}^{3N} \rho_{\lambda} e^{-i\omega_{\lambda} t} \left\{ \frac{1}{\omega_{\lambda}} (\omega_{\lambda}^2 q_{\lambda}^H M q_{\lambda} + q_{\lambda}^H \Phi q_{\lambda}) \delta_{\lambda\lambda'} \right\} \\
&\quad + \frac{1}{8} \sum_{\lambda'=1}^{3N} \omega_{\lambda'} \rho_{\lambda'}^* e^{i\omega_{\lambda'} t} \sum_{\lambda=1}^{3N} \rho_{\lambda}^* e^{i\omega_{\lambda} t} \left\{ \cdot 0 \right\} \\
&= \frac{1}{8} \sum_{\lambda=1}^{3N} |\rho_{\lambda}|^2 (\omega_{\lambda}^2 q_{\lambda}^H M q_{\lambda} + q_{\lambda}^H \Phi q_{\lambda})
\end{aligned} \tag{B.27}$$

Thus the total energy is given by

$$\begin{aligned}
E &= E_1 + E_2 \\
&= \frac{1}{8} \sum_{\lambda=1}^{3N} |\rho_{\lambda}|^2 (\omega_{\lambda}^2 q_{\lambda}^T M q_{\lambda}^* + q_{\lambda}^T \Phi q_{\lambda}^*) + \frac{1}{8} \sum_{\lambda=1}^{3N} |\rho_{\lambda}|^2 (\omega_{\lambda}^2 q_{\lambda}^H M q_{\lambda} + q_{\lambda}^H \Phi q_{\lambda}) \\
&= \frac{1}{4} \sum_{\lambda=1}^{3N} |\rho_{\lambda}|^2 (\omega_{\lambda}^2 q_{\lambda}^H M q_{\lambda} + q_{\lambda}^H \Phi q_{\lambda})
\end{aligned} \tag{B.28}$$

where the last simplification follows from the Hermiticity of matrices M and Φ . Thus the total energy of the system as well as the energy contained in each mode,

$$E_{\lambda} = \frac{1}{4} |\rho_{\lambda}|^2 (\omega_{\lambda}^2 q_{\lambda}^H M q_{\lambda} + q_{\lambda}^H \Phi q_{\lambda}) \tag{B.29}$$

is constant.



Normal Mode Analysis: Quantum Description

From the Lagrangian of the system we can identify canonical conjugate variables to formulate our Hamiltonian. The generalised momentum corresponding to the generalised position q_j is given by

$$p_j = \frac{\partial L}{\partial \dot{q}_j} = M_{jj} \dot{q}_j - \frac{1}{2} \sum_{k=1}^{3N} W_{jk} q_k \quad (\text{C.1})$$

These variables satisfy the standard commutation relations

$$[q_j, q_k] = 0, \quad [p_j, p_k] = 0, \quad [q_j, p_k] = i \hbar \delta_{jk} \quad (\text{C.2})$$

The Hamiltonian of the system is then

$$\begin{aligned} H &= \sum_{j=1}^{3N} \dot{q}_j p_j - L \\ &= \sum_{j=1}^{3N} \left\{ M_{jj} \dot{q}_j^2 - \frac{1}{2} \sum_{k=1}^{3N} W_{jk} \dot{q}_j q_k \right\} - \sum_{j=1}^{3N} \left\{ \frac{1}{2} M_{jj} \dot{q}_j^2 - \frac{1}{2} \sum_{k=1}^{3N} \Phi_{jk} q_j q_k - \frac{1}{2} \sum_{k=1}^{3N} W_{jk} \dot{q}_j q_k \right\} \\ &= \sum_{j=1}^{3N} \left\{ \frac{1}{2} M_{jj} \dot{q}_j^2 + \frac{1}{2} \sum_{k=1}^{3N} \Phi_{jk} q_j q_k \right\}, \end{aligned} \quad (\text{C.3})$$

or in terms of the canonical variables,

$$H = \sum_{j=1}^{3N} \left\{ \frac{p_j^2}{2M_{jj}} + \frac{1}{4M_{jj}} \sum_{k=1}^{3N} W_{jk} p_j q_k - \sum_{k=1}^{3N} \frac{W_{jk}}{4M_{kk}} q_j p_k - \frac{1}{8} \sum_{k=1}^{3N} T_{jk} q_j q_k + \frac{1}{2} \sum_{k=1}^{3N} \Phi_{jk} q_j q_k \right\}, \quad (\text{C.4})$$

where $T = WM^{-1}W$ is a real symmetric matrix.

To diagonalise the Hamiltonian in the second quantised form $H = \sum_{\lambda=1}^{3N} \hbar\omega_{\lambda}(a_{\lambda}^{\dagger}a_{\lambda} + \frac{1}{2})$, we form the phonon creation and annihilation operators, a_{λ}^{\dagger} and a_{λ} , for the mode λ as linear combinations of the generalised position and momentum operators.

$$a_{\lambda}^{\dagger} = \sum_{k=1}^{3N} (\alpha_{\lambda k} p_k + \beta_{\lambda k} q_k) \quad (\text{C.5})$$

$$a_{\lambda} = \sum_{k=1}^{3N} (\alpha_{\lambda k}^* p_k + \beta_{\lambda k}^* q_k) \quad (\text{C.6})$$

where $\alpha_{\lambda k}$ and $\beta_{\lambda k}$ are complex numbers. For the commutation relation $[a_{\lambda}, a_{\lambda'}^{\dagger}] = \delta_{\lambda\lambda'}$ to hold, the Hamiltonian must satisfy the commutation relation

$$[H, a_{\lambda}^{\dagger}] = \hbar\omega_{\lambda} a_{\lambda}^{\dagger} \quad (\text{C.7})$$

This commutator can be calculated by substituting H and a_{λ}^{\dagger} in terms of the canonical variables and involves the following sub-components

$$\begin{aligned} [p_l^2, a_{\lambda}^{\dagger}] &= [p_l^2, \sum_{k=1}^{3N} (\alpha_{\lambda k} p_k + \beta_{\lambda k} q_k)] \\ &= \sum_{k=1}^{3N} [p_l^2, (\alpha_{\lambda k} p_k + \beta_{\lambda k} q_k)] \\ &= \sum_{k=1}^{3N} (\alpha_{\lambda k} [p_l^2, p_k] + \beta_{\lambda k} [p_l^2, q_k]) \\ &= \sum_{k=1}^{3N} (\alpha_{\lambda k} \cdot 0 + \beta_{\lambda k} \cdot (-2i\hbar\delta_{lk} p_l)) \\ &= -2i\hbar\beta_{\lambda l} p_l \end{aligned} \quad (\text{C.8a})$$

$$\begin{aligned} [p_l q_m, a_{\lambda}^{\dagger}] &= [p_l q_m, \sum_{k=1}^{3N} (\alpha_{\lambda k} p_k + \beta_{\lambda k} q_k)] \\ &= \sum_{k=1}^{3N} [p_l q_m, (\alpha_{\lambda k} p_k + \beta_{\lambda k} q_k)] \\ &= \sum_{k=1}^{3N} (\alpha_{\lambda k} [p_l q_m, p_k] + \beta_{\lambda k} [p_l q_m, q_k]) \\ &= \sum_{k=1}^{3N} (\alpha_{\lambda k} \cdot (i\hbar\delta_{mk} p_l) + \beta_{\lambda k} \cdot (-i\hbar\delta_{lk} q_m)) \\ &= i\hbar\alpha_{\lambda m} p_l - i\hbar\beta_{\lambda l} q_m \end{aligned} \quad (\text{C.8b})$$

$$\begin{aligned}
[q_l p_m, a_\lambda^\dagger] &= [q_l p_m, \sum_{k=1}^{3N} (\alpha_{\lambda k} p_k + \beta_{\lambda k} q_k)] \\
&= \sum_{k=1}^{3N} [q_l p_m, (\alpha_{\lambda k} p_k + \beta_{\lambda k} q_k)] \\
&= \sum_{k=1}^{3N} (\alpha_{\lambda k} [q_l p_m, p_k] + \beta_{\lambda k} [q_l p_m, q_k]) \\
&= \sum_{k=1}^{3N} (\alpha_{\lambda k} \cdot (i \hbar \delta_{lk} p_m) + \beta_{\lambda k} \cdot (-i \hbar \delta_{mk} q_l)) \\
&= i \hbar \alpha_{\lambda l} p_m - i \hbar \beta_{\lambda m} q_l
\end{aligned} \tag{C.8c}$$

$$\begin{aligned}
[q_l q_m, a_\lambda^\dagger] &= [q_l q_m, \sum_{k=1}^{3N} (\alpha_{\lambda k} p_k + \beta_{\lambda k} q_k)] \\
&= \sum_{k=1}^{3N} [q_l q_m, (\alpha_{\lambda k} p_k + \beta_{\lambda k} q_k)] \\
&= \sum_{k=1}^{3N} (\alpha_{\lambda k} [q_l q_m, p_k] + \beta_{\lambda k} [q_l q_m, q_k]) \\
&= \sum_{k=1}^{3N} (\alpha_{\lambda k} (i \hbar \delta_{mk} q_l + i \hbar \delta_{lk} q_m) + \beta_{\lambda k} \cdot 0) \\
&= i \hbar \alpha_{\lambda m} q_l + i \hbar \alpha_{\lambda l} q_m
\end{aligned} \tag{C.8d}$$

Then,

$$\begin{aligned}
[H, a_\lambda^\dagger] &= \sum_{l=1}^N \frac{-2i \hbar \beta_{\lambda l} p_l}{2M_{ll}} + \sum_{l=1}^N \sum_{m=1}^N \frac{W_{lm}}{4M_{ll}} (i \hbar \alpha_{\lambda m} p_l - i \hbar \beta_{\lambda l} q_m) - \sum_{l=1}^N \sum_{m=1}^N \frac{W_{lm}}{4M_{mm}} (i \hbar \alpha_{\lambda l} p_m - i \hbar \beta_{\lambda m} q_l) \\
&\quad - \frac{1}{8} \sum_{l=1}^N \sum_{m=1}^N T_{lm} (i \hbar \alpha_{\lambda m} q_l + i \hbar \alpha_{\lambda l} q_m) + \frac{1}{2} \sum_{l=1}^N \sum_{m=1}^N \Phi_{lm} (i \hbar \alpha_{\lambda m} q_l + i \hbar \alpha_{\lambda l} q_m) \\
&= \sum_{l=1}^N \frac{-2i \hbar \beta_{\lambda l} p_l}{2M_{ll}} + \sum_{l=1}^N \sum_{m=1}^N \frac{W_{lm}}{4M_{ll}} (i \hbar \alpha_{\lambda m} p_l) - \sum_{l=1}^N \sum_{m=1}^N \frac{W_{lm}}{4M_{ll}} (i \hbar \beta_{\lambda l} q_m) \\
&\quad - \sum_{l=1}^N \sum_{m=1}^N \frac{W_{lm}}{4M_{mm}} (i \hbar \alpha_{\lambda l} p_m) + \sum_{l=1}^N \sum_{m=1}^N \frac{W_{lm}}{4M_{mm}} (i \hbar \beta_{\lambda m} q_l) - \frac{1}{8} \sum_{l=1}^N \sum_{m=1}^N T_{lm} (i \hbar \alpha_{\lambda m} q_l) \\
&\quad - \frac{1}{8} \sum_{l=1}^N \sum_{m=1}^N T_{lm} (i \hbar \alpha_{\lambda l} q_m) + \frac{1}{2} \sum_{l=1}^N \sum_{m=1}^N \Phi_{lm} (i \hbar \alpha_{\lambda m} q_l) + \frac{1}{2} \sum_{l=1}^N \sum_{m=1}^N \Phi_{lm} (i \hbar \alpha_{\lambda l} q_m)
\end{aligned} \tag{C.9}$$

Using $W_{lm} = -W_{ml}$, $T_{lm} = T_{ml}$ and $\Phi_{lm} = \Phi_{ml}$ and switching indices

$$\begin{aligned}
[H, a_\lambda^\dagger] &= \sum_{l=1}^N \frac{-2i\hbar\beta_{\lambda l} p_l}{2M_{ll}} + \sum_{l=1}^N \sum_{m=1}^N \frac{W_{lm}}{4M_{ll}} (i\hbar\alpha_{\lambda m} p_l) + \sum_{l=1}^N \sum_{m=1}^N \frac{W_{lm}}{4M_{mm}} (i\hbar\beta_{\lambda m} q_l) \\
&+ \sum_{l=1}^N \sum_{m=1}^N \frac{W_{lm}}{4M_{ll}} (i\hbar\alpha_{\lambda m} p_l) + \sum_{l=1}^N \sum_{m=1}^N \frac{W_{lm}}{4M_{mm}} (i\hbar\beta_{\lambda m} q_l) - \frac{1}{8} \sum_{l=1}^N \sum_{m=1}^N T_{lm} (i\hbar\alpha_{\lambda m} q_l) \quad (\text{C.10}) \\
&- \frac{1}{8} \sum_{l=1}^N \sum_{m=1}^N T_{lm} (i\hbar\alpha_{\lambda m} q_l) + \frac{1}{2} \sum_{l=1}^N \sum_{m=1}^N \Phi_{lm} (i\hbar\alpha_{\lambda m} q_l) + \frac{1}{2} \sum_{l=1}^N \sum_{m=1}^N \Phi_{lm} (i\hbar\alpha_{\lambda m} q_l)
\end{aligned}$$

Comparing the coefficients of p_l and q_l with $[H, a_\lambda^\dagger] = \hbar\omega_\lambda \sum_{l=1}^{3N} (\alpha_{\lambda l} p_l + \beta_{\lambda l} q_l)$,

$$-i\hbar \frac{\beta_{\lambda l}}{M_{ll}} + \frac{i\hbar}{2} \sum_{m=1}^N \frac{W_{lm}}{M_{ll}} \alpha_{\lambda m} = \hbar\omega_\lambda \alpha_{\lambda l} \quad (\text{C.11a})$$

$$\frac{i\hbar}{2} \sum_{m=1}^N \frac{W_{lm}}{M_{mm}} \beta_{\lambda m} - \frac{i\hbar}{4} \sum_{m=1}^N T_{lm} \alpha_{\lambda m} + i\hbar \sum_{m=1}^N \Phi_{lm} \alpha_{\lambda m} = \hbar\omega_\lambda \beta_{\lambda l} \quad (\text{C.11b})$$

These can be written in vector form as

$$-i\hbar M^{-1} \beta_\lambda + \frac{i\hbar}{2} M^{-1} W \alpha_\lambda = \hbar\omega_\lambda \alpha_\lambda \quad (\text{C.12a})$$

$$\frac{i\hbar}{2} W M^{-1} \beta_\lambda - \frac{i\hbar}{4} T \alpha_\lambda + i\hbar \Phi \alpha_\lambda = \hbar\omega_\lambda \beta_\lambda \quad (\text{C.12b})$$

Eliminating $\beta_\lambda = i\omega_\lambda M \alpha_\lambda + \frac{1}{2} W \alpha_\lambda$,

$$\frac{i\hbar}{2} W M^{-1} (i\omega_\lambda M \alpha_\lambda + \frac{1}{2} W \alpha_\lambda) - \frac{i\hbar}{4} T \alpha_\lambda + i\hbar \Phi \alpha_\lambda = \hbar\omega_\lambda (i\omega_\lambda M \alpha_\lambda + \frac{1}{2} W \alpha_\lambda), \quad (\text{C.13})$$

or

$$\frac{i\hbar}{4} T \alpha_\lambda - \frac{\hbar}{2} \omega_\lambda W \alpha_\lambda - \frac{i\hbar}{4} T \alpha_\lambda + i\hbar \Phi \alpha_\lambda = i\hbar \omega_\lambda^2 M \alpha_\lambda + \frac{\hbar}{2} \omega_\lambda W \alpha_\lambda, \quad (\text{C.14})$$

or

$$\omega_\lambda^2 M \alpha_\lambda - i\omega_\lambda W \alpha_\lambda - \Phi \alpha_\lambda = 0, \quad (\text{C.15})$$

which is the same QEP encountered in the classical analysis in Appendix B.

The QEP yields $6N$ eigenvectors and $6N$ eigenvalues. $3N$ eigenvectors will be used to form the creation operators while the other $3N$ eigenvectors to form the annihilation operators. We note that if the pair (v_λ, u_λ) satisfies the QEP then the pair $(-v_\lambda, u_\lambda^*)$ also satisfies the QEP. Thus the total set of $6N$ eigenpairs

$$S = \{(v_\lambda, u_\lambda), \quad | \quad v_\lambda^2 M u_\lambda - i v_\lambda W u_\lambda - \Phi u_\lambda = 0\} \quad (\text{C.16})$$

for λ running over 1 to $6N$ can be divided into two equally sized subsets depending on the sign of the frequency:

$$\begin{aligned} S_+ &:= \{(\nu_\lambda, u_\lambda), \quad | \quad \nu_\lambda^2 M u_\lambda - i \nu_\lambda W u_\lambda - \Phi u_\lambda = 0 \quad \nu > 0\} \\ S_- &:= \{(-\nu_\lambda, u_\lambda^*), \quad | \quad \nu_\lambda^2 M u_\lambda - i \nu_\lambda W u_\lambda - \Phi u_\lambda = 0, \quad \nu > 0\} \end{aligned} \quad (\text{C.17})$$

where the index λ now runs from 1 to $3N$. Selecting the $3N$ eigenpairs which form the creation operators can be done by checking the commutation relations

$$[a_\lambda, a_{\lambda'}] = 0, [a_\lambda^\dagger, a_{\lambda'}^\dagger] = 0, [a_\lambda, a_{\lambda'}^\dagger] = 1 \quad (\text{C.18})$$

1.

$$\begin{aligned} [a_\lambda, a_{\lambda'}] &= \sum_{jk} [(\alpha_{\lambda_j}^* p_j + \beta_{\lambda_j}^* q_j), (\alpha_{\lambda'_k} p_k + \beta_{\lambda'_k} q_k)] \\ &= \sum_{jk} \{ \alpha_{\lambda_j}^* \alpha_{\lambda'_k} [p_j, p_k] + \alpha_{\lambda_j}^* \beta_{\lambda'_k} [p_j, q_k] + \beta_{\lambda_j}^* \alpha_{\lambda'_k} [q_j, p_k] + \beta_{\lambda_j}^* \beta_{\lambda'_k} [q_j, q_k] \} \\ &= \sum_{jk} \{ \alpha_{\lambda_j}^* \beta_{\lambda'_k} (-i \hbar \delta_{jk}) + \beta_{\lambda_j}^* \alpha_{\lambda'_k} (i \hbar \delta_{jk}) \} \\ &= i \hbar \sum_j \{ \beta_{\lambda_j}^* \alpha_{\lambda'_j} - \alpha_{\lambda_j}^* \beta_{\lambda'_j} \} \end{aligned} \quad (\text{C.19})$$

This equates to zero when $\lambda = \lambda'$. For $\lambda \neq \lambda'$,

$$\begin{aligned} [a_\lambda, a_{\lambda'}] &= i \hbar (\beta_{\lambda'}^H \alpha_{\lambda'}^* - \alpha_{\lambda'}^H \beta_{\lambda'}^*) \\ &= i \hbar \left\{ (-i \omega_{\lambda'} \alpha_{\lambda'}^H M - \frac{1}{2} \alpha_{\lambda'}^H W) \alpha_{\lambda'}^* - \alpha_{\lambda'}^H (-i \omega_{\lambda'} M \alpha_{\lambda'}^* + \frac{1}{2} W \alpha_{\lambda'}^*) \right\} \\ &= \hbar \{ (\omega_{\lambda'} - \omega_{\lambda'}) \alpha_{\lambda'}^H M \alpha_{\lambda'}^* + \alpha_{\lambda'}^H (-i W) \alpha_{\lambda'}^* \} \\ &= 0 \end{aligned} \quad (\text{C.20})$$

2.

$$\begin{aligned} [a_\lambda^\dagger, a_{\lambda'}^\dagger] &= \sum_{jk} [(\alpha_{\lambda_j} p_j + \beta_{\lambda_j} q_j), (\alpha_{\lambda'_k} p_k + \beta_{\lambda'_k} q_k)] \\ &= \sum_{jk} \{ \alpha_{\lambda_j} \alpha_{\lambda'_k} [p_j, p_k] + \alpha_{\lambda_j} \beta_{\lambda'_k} [p_j, q_k] + \beta_{\lambda_j} \alpha_{\lambda'_k} [q_j, p_k] + \beta_{\lambda_j} \beta_{\lambda'_k} [q_j, q_k] \} \\ &= \sum_{jk} \{ \alpha_{\lambda_j} \beta_{\lambda'_k} (-i \hbar \delta_{jk}) + \beta_{\lambda_j} \alpha_{\lambda'_k} (i \hbar \delta_{jk}) \} \\ &= i \hbar \sum_j \{ \beta_{\lambda_j} \alpha_{\lambda'_j} - \alpha_{\lambda_j} \beta_{\lambda'_j} \} \end{aligned} \quad (\text{C.21})$$

Again this equates to zero when $\lambda = \lambda'$. For $\lambda \neq \lambda'$,

$$\begin{aligned} [a_\lambda^\dagger, a_{\lambda'}^\dagger] &= i\hbar \left\{ \sum_j \{ \beta_{\lambda_j}^* \alpha_{\lambda_j}^* - \alpha_{\lambda_j}^* \beta_{\lambda_j}^* \} \right\}^* \\ &= i\hbar \cdot 0 \\ &= 0 \end{aligned} \tag{C.22}$$

3.

$$\begin{aligned} [a_\lambda, a_{\lambda'}^\dagger] &= \sum_{jk} [(\alpha_{\lambda_j}^* p_j + \beta_{\lambda_j}^* q_j), (\alpha_{\lambda'_k} p_k + \beta_{\lambda'_k} q_k)] \\ &= \sum_{jk} \{ \alpha_{\lambda_j}^* \alpha_{\lambda'_k} [p_j, p_k] + \alpha_{\lambda_j}^* \beta_{\lambda'_k} [p_j, q_k] + \beta_{\lambda_j}^* \alpha_{\lambda'_k} [q_j, p_k] + \beta_{\lambda_j}^* \beta_{\lambda'_k} [q_j, q_k] \} \\ &= \sum_{jk} \{ \alpha_{\lambda_j}^* \beta_{\lambda'_k} (-i\hbar \delta_{jk}) + \beta_{\lambda_j}^* \alpha_{\lambda'_k} (i\hbar \delta_{jk}) \} \\ &= i\hbar \sum_j \{ \beta_{\lambda_j}^* \alpha_{\lambda_j} - \alpha_{\lambda_j}^* \beta_{\lambda_j} \} \end{aligned} \tag{C.23}$$

For $\lambda \neq \lambda'$,

$$\begin{aligned} [a_\lambda, a_{\lambda'}^\dagger] &= i\hbar (\beta_\lambda^H \alpha_{\lambda'} - \alpha_\lambda^H \beta_{\lambda'}) \\ &= i\hbar \left\{ (-i\omega_\lambda \alpha_\lambda^H M - \frac{1}{2} \alpha_\lambda^H W) \alpha_{\lambda'} - \alpha_\lambda^H (i\omega_{\lambda'} M \alpha_{\lambda'} + \frac{1}{2} W \alpha_{\lambda'}) \right\} \\ &= \hbar \{ (\omega_\lambda + \omega_{\lambda'}) \alpha_\lambda^H M \alpha_{\lambda'} + \alpha_\lambda^H (-iW) \alpha_{\lambda'} \} \\ &= 0 \end{aligned} \tag{C.24}$$

For $\lambda = \lambda'$,

$$\begin{aligned} [a_\lambda, a_\lambda^\dagger] &= i\hbar (\beta_\lambda^H \alpha_\lambda - \alpha_\lambda^H \beta_\lambda) \\ &= i\hbar \left\{ (-i\omega_\lambda \alpha_\lambda^H M - \frac{1}{2} \alpha_\lambda^H W) \alpha_\lambda - \alpha_\lambda^H (i\omega_\lambda M \alpha_\lambda + \frac{1}{2} W \alpha_\lambda) \right\} \\ &= \hbar \{ \omega_\lambda \alpha_\lambda^H M \alpha_\lambda + \omega_\lambda \alpha_\lambda^H M \alpha_\lambda + \alpha_\lambda^H (-iW) \alpha_\lambda \} \\ &= \frac{\hbar}{\omega_\lambda} \{ \omega_\lambda^2 \alpha_\lambda^H M \alpha_\lambda + \omega_\lambda^2 \alpha_\lambda^H M \alpha_\lambda + \omega_\lambda \alpha_\lambda^H (-iW) \alpha_\lambda \} \\ &= \frac{\hbar}{\omega_\lambda} \{ \omega_\lambda^2 \alpha_\lambda^H M \alpha_\lambda + \alpha_\lambda^H \Phi \alpha_\lambda \} \end{aligned} \tag{C.25}$$

To fix the normalisation of the eigenvectors α_λ so that $[a_\lambda, a_\lambda^\dagger] = 1$, we make the substitution $\alpha_\lambda = c_\lambda \gamma_\lambda$,

where γ_λ is normalised to one. Then,

$$\begin{aligned} [a_\lambda, a_\lambda^\dagger] &= \frac{\hbar |c_\lambda|^2}{\omega_\lambda} \{ \omega_\lambda^2 \gamma_\lambda^H M \gamma_\lambda + \gamma_\lambda^H \Phi \gamma_\lambda \} \\ &= 1 \end{aligned} \quad (\text{C.26})$$

Then

$$|c_\lambda|^2 = \frac{\omega_\lambda}{\hbar} \left\{ \frac{1}{\omega_\lambda^2 \gamma_\lambda^H M \gamma_\lambda + \gamma_\lambda^H \Phi \gamma_\lambda} \right\} \quad (\text{C.27})$$

Noting that since $|c_\lambda|^2$ is non-negative, $[a_\lambda, a_\lambda^\dagger] = 1$ only when the quantity $\omega_\lambda / (\omega_\lambda^2 \gamma_\lambda^H M \gamma_\lambda + \gamma_\lambda^H \Phi \gamma_\lambda)$ is positive. This expression helps us pick out the $3N$ eigenpairs to form the creation operators

$$(\omega_\lambda, \alpha_\lambda) = \begin{cases} (v_\lambda, u_\lambda) & , v_\lambda^2 u_\lambda^H M u_\lambda + u_\lambda^H \Phi u_\lambda > 0 \\ (-v_\lambda, u_\lambda^*) & , v_\lambda^2 u_\lambda^H M u_\lambda + u_\lambda^H \Phi u_\lambda < 0 \end{cases} \quad (\text{C.28})$$

SECOND-QUANTISATION OF CANONICAL OPERATORS

SOME IDENTITIES

Without proof we have the following identities for our system:

1.
$$\sum_{\lambda=1}^{6N} \frac{\gamma_\lambda \gamma_\lambda^H}{\omega_\lambda^2 \gamma_\lambda^H M \gamma_\lambda + \gamma_\lambda^H \Phi \gamma_\lambda} = \Phi^{-1} \quad (\text{C.29})$$

2.
$$\sum_{\lambda=1}^{6N} \frac{\omega_\lambda \gamma_\lambda \gamma_\lambda^H}{\omega_\lambda^2 \gamma_\lambda^H M \gamma_\lambda + \gamma_\lambda^H \Phi \gamma_\lambda} = \mathbb{O}_{3N} \quad (\text{C.30})$$

3.
$$\sum_{\lambda=1}^{6N} \frac{\omega_\lambda^2 \gamma_\lambda \gamma_\lambda^H}{\omega_\lambda^2 \gamma_\lambda^H M \gamma_\lambda + \gamma_\lambda^H \Phi \gamma_\lambda} = M^{-1} \quad (\text{C.31})$$

4.
$$\sum_{\lambda=1}^{6N} \frac{\omega_\lambda^3 \gamma_\lambda \gamma_\lambda^H}{\omega_\lambda^2 \gamma_\lambda^H M \gamma_\lambda + \gamma_\lambda^H \Phi \gamma_\lambda} = i M^{-1} W M^{-1} \quad (\text{C.32})$$

5.
$$\sum_{\lambda=1}^{6N} \frac{\omega_\lambda^4 \gamma_\lambda \gamma_\lambda^H}{\omega_\lambda^2 \gamma_\lambda^H M \gamma_\lambda + \gamma_\lambda^H \Phi \gamma_\lambda} = -M^{-1} W M^{-1} W M^{-1} + M^{-1} \Phi M^{-1} \quad (\text{C.33})$$

We have our creation and annihilation operators as

$$a_\lambda^\dagger = \sum_{k=1}^{3N} (\alpha_{\lambda k} p_k + \beta_{\lambda k} q_k) \quad (\text{C.34})$$

$$a_\lambda = \sum_{k=1}^{3N} (\alpha_{\lambda k}^* p_k + \beta_{\lambda k}^* q_k) \quad (\text{C.35})$$

In vector form $a^\dagger = [a_1^\dagger \ \dots \ a_{3N}^\dagger]^T$ and $a = [a_1 \ \dots \ a_{3N}]^T$; $p = [p_1 \ \dots \ p_{3N}]^T$ and $q = [q_1 \ \dots \ q_{3N}]^T$; matrices $\alpha = [\alpha_1 \ \dots \ \alpha_{3N}]^T$ and $\beta = [\beta_1 \ \dots \ \beta_{3N}]^T$

$$a^\dagger = \alpha^T p + \beta^T q \quad (\text{C.36})$$

$$a = \alpha^H p + \beta^H q \quad (\text{C.37})$$

With the matrix $\Lambda = \text{diag}(\omega_1, \dots, \omega_{3N})$ consisting of all corresponding eigenvalues

$$\beta = iM\alpha\Lambda + \frac{1}{2}W\alpha \quad (\text{C.38})$$

Then

$$\alpha^* a^\dagger - \alpha a = (\alpha^* \alpha^{*H} - \alpha \alpha^H) p + (\alpha^* \beta^{*H} - \alpha \beta^H) q \quad (\text{C.39})$$

$$\begin{aligned} (\alpha^* \alpha^{*H} - \alpha \alpha^H) p &= \left\{ \sum_{\lambda=1}^{6N} \frac{\omega_\lambda \gamma_\lambda \gamma_\lambda^H}{\hbar(\omega_\lambda^2 \gamma_\lambda^H M \gamma_\lambda + \gamma_\lambda^H \Phi \gamma_\lambda)} \right\} p \\ &= \frac{1}{\hbar} \mathbb{O}_{3N} p \\ &= 0 \end{aligned} \quad (\text{C.40})$$

$$\begin{aligned} (\alpha^* \beta^{*H} - \alpha \beta^H) q &= (\alpha^* (i\Lambda \alpha^{*H} M - \frac{1}{2} \alpha^{*H} W) - \alpha (-i\Lambda \alpha^H M - \frac{1}{2} \alpha^H W)) q \\ &= \left\{ i(\alpha^* \Lambda \alpha^{*H} + \alpha \Lambda \alpha^H) M - \frac{1}{2} (\alpha^* \alpha^{*H} - \alpha \alpha^H) W \right\} q \\ &= \left\{ i \sum_{\lambda=1}^{6N} \frac{\omega_\lambda^2 \gamma_\lambda \gamma_\lambda^H}{\hbar(\omega_\lambda^2 \gamma_\lambda^H M \gamma_\lambda + \gamma_\lambda^H \Phi \gamma_\lambda)} M + \frac{1}{2} \sum_{\lambda=1}^{6N} \frac{\omega_\lambda \gamma_\lambda \gamma_\lambda^H}{\hbar(\omega_\lambda^2 \gamma_\lambda^H M \gamma_\lambda + \gamma_\lambda^H \Phi \gamma_\lambda)} W \right\} q \quad (\text{C.41}) \\ &= \left\{ \frac{i}{\hbar} M^{-1} M + \frac{1}{2\hbar} \mathbb{O}_{3N} W \right\} q \\ &= \frac{i}{\hbar} q \end{aligned}$$

Thus

$$\alpha^* a^\dagger - \alpha a = \frac{i}{\hbar} q \quad (\text{C.42})$$

$$q = -i\hbar(\alpha^* a^\dagger - \alpha a) \quad (\text{C.43})$$

And

$$\begin{aligned} q_j &= -i\hbar \sum_{\lambda=1}^{3N} (\alpha_{\lambda j}^* a_\lambda^\dagger - \alpha_{\lambda j} a_\lambda) \\ &= -i\hbar \sum_{\lambda=1}^{3N} c_\lambda (\gamma_{\lambda j}^* a_\lambda^\dagger - \gamma_{\lambda j} a_\lambda) \end{aligned} \quad (\text{C.44})$$

where

$$c_\lambda = \sqrt{\frac{|\omega_\lambda|}{\hbar|\omega_\lambda^2 \gamma_\lambda^H M \gamma_\lambda + \gamma_\lambda^H \Phi \gamma_\lambda|}} \quad (\text{C.45})$$

Similarly

$$\beta^* a^\dagger - \beta a = (\beta^* \alpha^{*H} - \beta \alpha^H) p + (\beta^* \beta^{*H} - \beta \beta^H) q \quad (\text{C.46})$$

$$\begin{aligned} (\beta^* \alpha^{*H} - \beta \alpha^H) p &= -(\alpha^* \beta^{*H} - \alpha \beta^H)^T p \\ &= -\frac{i}{\hbar} p \end{aligned} \quad (\text{C.47})$$

$$\begin{aligned} (\beta^* \beta^{*H} - \beta \beta^H) q &= \left\{ (-iM\alpha^* \Lambda + \frac{1}{2} W \alpha^*) (i\Lambda \alpha^{*H} M - \frac{1}{2} \alpha^{*H} W) \right. \\ &\quad \left. - (iM\alpha \Lambda + \frac{1}{2} W \alpha) (-i\Lambda \alpha^H M - \frac{1}{2} \alpha^H W) \right\} q \\ &= \left\{ M(\alpha^* \Lambda^2 \alpha^{*H} - \alpha \Lambda^2 \alpha^H) M + \frac{i}{2} W(\alpha^* \Lambda \alpha^{*H} + \alpha \Lambda \alpha^H) M \right. \\ &\quad \left. + \frac{i}{2} M(\alpha^* \Lambda \alpha^{*H} + \alpha \Lambda \alpha^H) W - \frac{1}{4} W(\alpha^* \alpha^{*H} - \alpha \alpha^H) W \right\} q \\ &= \left\{ M \sum_{\lambda=1}^{6N} \frac{\omega_\lambda^3 \gamma_\lambda \gamma_\lambda^H}{\hbar(\omega_\lambda^2 \gamma_\lambda^H M \gamma_\lambda + \gamma_\lambda^H \Phi \gamma_\lambda)} M + \frac{i}{2} W \sum_{\lambda=1}^{6N} \frac{\omega_\lambda^2 \gamma_\lambda \gamma_\lambda^H}{\hbar(\omega_\lambda^2 \gamma_\lambda^H M \gamma_\lambda + \gamma_\lambda^H \Phi \gamma_\lambda)} M \right. \\ &\quad \left. + \frac{i}{2} M \sum_{\lambda=1}^{6N} \frac{\omega_\lambda^2 \gamma_\lambda \gamma_\lambda^H}{\hbar(\omega_\lambda^2 \gamma_\lambda^H M \gamma_\lambda + \gamma_\lambda^H \Phi \gamma_\lambda)} W + \frac{1}{4} W \sum_{\lambda=1}^{6N} \frac{\omega_\lambda \gamma_\lambda \gamma_\lambda^H}{\hbar(\omega_\lambda^2 \gamma_\lambda^H M \gamma_\lambda + \gamma_\lambda^H \Phi \gamma_\lambda)} W \right\} q \\ &= \left\{ M \left(\frac{-iM^{-1} W M^{-1}}{\hbar} \right) M + \frac{i}{2} W \left(\frac{M^{-1}}{\hbar} \right) M + \frac{i}{2} M \left(\frac{M^{-1}}{\hbar} \right) W + \frac{1}{4} W \left(\frac{\mathbb{O}_{3N}}{\hbar} \right) W \right\} q \\ &= \left\{ \frac{-iW}{\hbar} + \frac{iW}{2\hbar} + \frac{iW}{2\hbar} \right\} q \\ &= 0 \end{aligned} \quad (\text{C.48})$$

Thus

$$\beta^* a^\dagger - \beta a = -\frac{i}{\hbar} p \quad (\text{C.49})$$

$$p = i\hbar(\beta^* a^\dagger - \beta a) \quad (\text{C.50})$$

And

$$p_j = i \hbar \sum_{\lambda=1}^{3N} (\beta_{\lambda_j}^* a_{\lambda}^{\dagger} - \beta_{\lambda_j} a_{\lambda}) \quad (\text{C.51})$$

D

Trap Imperfections

Consider an arbitrary spatial configuration of N Penning traps, each containing a singly charged ion of the same species. In a real experimental setup, the trapping potential may not be of the idealised form expected from the optimisation of the electrode structures, and may also vary from one lattice site to the other. Similarly the magnetic field could be misaligned with the confining direction of the potential. If no defects due to impurities are present in the system * so that $m_j = m$, the mass matrix M simplifies to

$$M = m \cdot \mathbb{I}_{3N} \quad (\text{D.1})$$

Defining \hat{z} as the common confining direction of the traps and with the polar angle θ and azimuthal angle φ representing the misalignment of the static homogeneous magnetic field with respect to \hat{z} axis, $\mathbf{B} = B_0 \sin \theta \cos \varphi \hat{x} + B_0 \sin \theta \sin \varphi \hat{y} + B_0 \cos \theta \hat{z}$ so that

$$W = m\omega_c \begin{bmatrix} \mathbb{O}_N & \cos \theta \cdot \mathbb{I}_N & -\sin \theta \sin \varphi \cdot \mathbb{I}_N \\ -\cos \theta \cdot \mathbb{I}_N & \mathbb{O}_N & \sin \theta \cos \varphi \cdot \mathbb{I}_N \\ \sin \theta \sin \varphi \cdot \mathbb{I}_N & -\sin \theta \cos \varphi \cdot \mathbb{I}_N & \mathbb{O}_N \end{bmatrix} \quad (\text{D.2})$$

where $\omega_c = eB_0/m$ is the true cyclotron frequency.

The (harmonic) imperfections in the trapping potential are captured by the block matrix V in the general form

$$V = \begin{bmatrix} V^{xx} & V^{xy} & V^{xz} \\ V^{yx} & V^{yy} & V^{yz} \\ V^{zx} & V^{zy} & V^{zz} \end{bmatrix} \quad (\text{D.3})$$

*In the presence of impurity defects, the normal mode analysis of the imperfect trap is equivalent to the more general analysis presented in Appendix B

with the component matrices defined as

$$V_{jk}^{\mu\nu} = 2e\phi_{j0}^{\mu\nu}\delta_{jk}, \quad (\text{D.4})$$

The Coulomb repulsion can again be expressed through the matrix

$$K = \begin{bmatrix} K^{xx} & K^{xy} & K^{xz} \\ K^{yx} & K^{yy} & K^{yz} \\ K^{zx} & K^{zy} & K^{zz} \end{bmatrix} \quad (\text{D.5})$$

with

$$K_{jk}^{\mu\mu} = \begin{cases} -k_e e^2 \sum_{l \neq j} \frac{R_{jl0}^2 - 3R_{jl0}^{\mu 2}}{R_{jl0}^5} & , j = k \\ k_e e^2 \frac{R_{jk0}^2 - 3R_{jk0}^{\mu 2}}{R_{jk0}^5} & , j \neq k \end{cases}, \quad (\text{D.6a})$$

$$K_{jk}^{\mu\nu} = K_{jk}^{\nu\mu} = \begin{cases} 3k_e e^2 \sum_{l \neq j} \frac{R_{jl0}^{\mu} R_{jl0}^{\nu}}{R_{jl0}^5} & , j = k \\ -3k_e e^2 \frac{R_{jk0}^{\mu} R_{jk0}^{\nu}}{R_{jk0}^5} & , j \neq k \end{cases}, \quad \mu \neq \nu, \quad (\text{D.6b})$$

Here indices j and k run from 1 to N while the indices μ and ν refer to the Cartesian components x , y and z . The equilibrium positions in an imperfect trap will, of course, differ from those in a perfectly designed trap. The matrix V is traceless as a direct consequence of Laplace's equation, while the matrix K is traceless because the Coulomb forces being internal forces in the system of ions pairwise cancel each other and the total sum equates to zero. V and K are also both real and symmetric. As a result the stiffness matrix $\Phi = V + K$ is a real symmetric traceless matrix.

Following the procedure outlined in Appendix B, the normal modes of the system can be obtained by solving the QEP

$$[\omega^2 m \cdot \mathbb{I}_{3N} + \omega(-iW) - \Phi]q_0 = 0, \quad (\text{D.7})$$

or dividing by m ,

$$[\omega^2 \cdot \mathbb{I}_{3N} + \omega(-iW') - \Phi']q_0 = 0, \quad (\text{D.8})$$

where we define the matrices $W' = W/m$ and $\Phi' = \Phi/m$. The stability of an imperfect trap setup can be determined by checking if all eigenvalues are real.

Linearisation of the QEP in the first-companion form yields the GEP

$$\begin{bmatrix} \mathbb{O}_{3N} & \mathbb{I}_{3N} \\ \Phi' & iW' \end{bmatrix} \begin{bmatrix} q_0 \\ \omega q_0 \end{bmatrix} - \omega \begin{bmatrix} \mathbb{I}_{3N} & \mathbb{O}_{3N} \\ \mathbb{O}_{3N} & \mathbb{I}_{3N} \end{bmatrix} \begin{bmatrix} q_0 \\ \omega q_0 \end{bmatrix} = 0 \quad (\text{D.9})$$

which is actually just the SEP

$$Av = \omega v \quad (\text{D.10})$$

with $6N$ -dimensional eigenvectors $v = [q_0 \quad \omega q_0]^T$ and $6N$ eigenvalues ω belonging to the $6N \times 6N$ matrix A

$$A = \begin{bmatrix} \mathbb{O}_{3N} & \mathbb{I}_{3N} \\ \Phi' & iW' \end{bmatrix} \quad (\text{D.11})$$

Then

$$A^2 v = \omega^2 v \quad (\text{D.12})$$

where

$$A^2 = \begin{bmatrix} \Phi' & iW' \\ iW'\Phi' & \Phi' - W'^2 \end{bmatrix} \quad (\text{D.13})$$

Since the sum of eigenvalues of a matrix is equal to its trace,

$$\sum_{\lambda=1}^{6N} \omega_\lambda^2 = \text{tr}(A^2) = \text{tr}(2\Phi' - W'^2) = -\text{tr}(W'^2) \quad (\text{D.14})$$

Noting that the frequencies come in pairs of positive-negative values in the stable regime we can express this sum in terms of the $3N$ positive frequencies,

$$\sum_{\lambda=1}^{3N} \omega_\lambda^2 = -\frac{1}{2} \text{tr}(W'^2) \quad (\text{D.15})$$

Since

$$W'^2 = \omega_c^2 \begin{bmatrix} (-\cos^2 \theta - \sin^2 \theta \sin^2 \varphi) \cdot \mathbb{I}_N & \sin^2 \theta \sin \varphi \cos \varphi \cdot \mathbb{I}_N & \sin \theta \cos \theta \cos \varphi \cdot \mathbb{I}_N \\ \sin^2 \theta \sin \varphi \cos \varphi \cdot \mathbb{I}_N & (-\cos^2 \theta - \sin^2 \theta \cos^2 \varphi) \mathbb{I}_N & \sin \theta \cos \theta \sin \varphi \cdot \mathbb{I}_N \\ \sin \theta \cos \theta \cos \varphi \cdot \mathbb{I}_N & \sin \theta \cos \theta \sin \varphi \cdot \mathbb{I}_N & (-\sin^2 \theta \sin^2 \varphi - \sin^2 \theta \cos^2 \varphi) \mathbb{I}_N \end{bmatrix} \quad (\text{D.16})$$

we can explicitly calculate its trace as

$$\begin{aligned} \text{tr}(W'^2) &= N\omega_c^2 \{-2\cos^2 \theta - 2\sin^2 \theta \sin^2 \varphi - 2\sin^2 \theta \cos^2 \varphi\} \\ &= -2N\omega_c^2 \end{aligned} \quad (\text{D.17})$$

Thus

$$\sum_{\lambda=1}^{3N} \omega_\lambda^2 = N\omega_c^2 \quad (\text{D.18})$$

This result can be treated as a non-trivial generalisation of the well known Brown-Gabrielse invariance theorem for a single ion in an imperfect Penning trap,

$$\omega_+^2 + \omega_-^2 + \omega_z^2 = \omega_c^2 \quad (\text{D.19})$$

E

Normal Modes of a Single Ion

CLASSICAL REGIME

From the normal mode analysis of Penning trap arrays it is straightforward to deduce the equation of motion for a single ion in a Penning trap consisting of the radially symmetric quadrupole potential $V(x, y, z) = \phi_0(z^2 - (x^2 + y^2)/2)$ and a uniform magnetic field $\mathbf{B} = B_0 \hat{z}$. Since no other ions are present in the system the Coulomb terms can be omitted and the local coordinates are equivalent to the equilibrium position of the ion $r(t) = [x \ y \ z]^T$.

For an ion of mass m and charge $+e$, the matrices M , W and Φ in the QEP $[\omega^2 M + \omega(-iW) - \Phi]q_0 = 0$ reduce to

$$M = m \begin{bmatrix} 1 & 0 & 0 \\ 0 & 1 & 0 \\ 0 & 0 & 1 \end{bmatrix} \quad (\text{E.1a})$$

$$W = m\omega_c \begin{bmatrix} 0 & 1 & 0 \\ -1 & 0 & 0 \\ 0 & 0 & 0 \end{bmatrix} \quad (\text{E.1b})$$

$$\Phi = m \begin{bmatrix} -\omega_z^2/2 & 0 & 0 \\ 0 & -\omega_z^2/2 & 0 \\ 0 & 0 & \omega_z^2 \end{bmatrix} \quad (\text{E.1c})$$

where we define the true cyclotron frequency $\omega_c = eB_0/m$ and the axial frequency $\omega_z = \sqrt{2e\phi_0/m}$. The eigenvectors obtained from solving the QEP are

$$q_+ = \frac{1}{\sqrt{2}} \begin{bmatrix} 1 \\ -i \\ 0 \end{bmatrix}, \quad q_- = \frac{1}{\sqrt{2}} \begin{bmatrix} 1 \\ -i \\ 0 \end{bmatrix}, \quad q_z = \begin{bmatrix} 0 \\ 0 \\ 1 \end{bmatrix} \quad (\text{E.2})$$

and these correspond to the positive eigenvalues, ω_+ , ω_- and ω_z , where

$$\omega_{\pm} = \frac{\omega_c \pm \sqrt{\omega_c^2 - 2\omega_z^2}}{2} \quad (\text{E.3})$$

The general solution for $r(t)$ can then be written as

$$r(t) = \text{Re}(\rho_+ q_+ e^{-i\omega_+ t} + \rho_- q_- e^{-i\omega_- t} + \rho_z q_z e^{-i\omega_z t}) \quad (\text{E.4})$$

which gives with the substitution $\rho_+ = r_+ e^{-i\delta_+}$, $\rho_- = r_- e^{-i\delta_-}$, $\rho_z = r_z e^{-i\delta_z}$,

$$x = \frac{r_+}{\sqrt{2}} \cos(\omega_+ t + \delta_+) + \frac{r_-}{\sqrt{2}} \cos(\omega_- t + \delta_-) \quad (\text{E.5a})$$

$$y = -\frac{r_+}{\sqrt{2}} \sin(\omega_+ t + \delta_+) - \frac{r_-}{\sqrt{2}} \sin(\omega_- t + \delta_-), \quad (\text{E.5b})$$

$$z = r_z \cos(\omega_z t + \delta_z), \quad (\text{E.5c})$$

QUANTUM REGIME

With the generalised position operators defined as x , y , and z , the conjugate momentum operators can be defined as

$$p_x = m(\dot{x} - \frac{\omega_c}{2} y) \quad (\text{E.6a})$$

$$p_y = m(\dot{y} + \frac{\omega_c}{2} x) \quad (\text{E.6b})$$

$$p_z = m\dot{z} \quad (\text{E.6c})$$

The normalised eigenvectors, frequencies and constant pre-factors used to form the creation and annihilation operators for the phonon modes can again be calculated by following the procedure described in Appendix B. Explicitly,

$$\gamma_+ = \frac{1}{\sqrt{2}} \begin{bmatrix} 1 \\ -i \\ 0 \end{bmatrix}, \quad \omega_+ = \frac{\omega_c + \sqrt{\omega_c^2 - 2\omega_z^2}}{2}, \quad \zeta_+ = im\Omega\gamma_+, \quad c_+ = \frac{1}{\sqrt{2\hbar m\Omega}} \quad (\text{E.7a})$$

$$\gamma_- = \frac{1}{\sqrt{2}} \begin{bmatrix} 1 \\ i \\ 0 \end{bmatrix}, \quad -\omega_- = -\frac{\omega_c - \sqrt{\omega_c^2 - 2\omega_z^2}}{2}, \quad \zeta_- = im\Omega\gamma_-, \quad c_- = \frac{1}{\sqrt{2\hbar m\Omega}} \quad (\text{E.7b})$$

$$\gamma_z = \begin{bmatrix} 0 \\ 0 \\ 1 \end{bmatrix}, \quad \omega_z, \quad \zeta_z = im\omega_z\gamma_z, \quad c_z = \frac{1}{\sqrt{2\hbar m\omega_z}} \quad (\text{E.7c})$$

This yields

$$a_+^\dagger = \sqrt{\frac{1}{4\hbar m\Omega}}(p_x - ip_y) + i\sqrt{\frac{m\Omega}{4\hbar}}(x - iy) \quad (\text{E.8a})$$

$$a_+ = \sqrt{\frac{1}{4\hbar m\Omega}}(p_x + ip_y) - i\sqrt{\frac{m\Omega}{4\hbar}}(x + iy) \quad (\text{E.8b})$$

$$a_-^\dagger = \sqrt{\frac{1}{4\hbar m\Omega}}(p_x + ip_y) + i\sqrt{\frac{m\Omega}{4\hbar}}(x + iy) \quad (\text{E.8c})$$

$$a_- = \sqrt{\frac{1}{4\hbar m\Omega}}(p_x - ip_y) - i\sqrt{\frac{m\Omega}{4\hbar}}(x - iy) \quad (\text{E.8d})$$

$$a_z^\dagger = \sqrt{\frac{1}{2\hbar m\omega_z}}p_z + i\sqrt{\frac{m\omega_z}{2\hbar}}z \quad (\text{E.8e})$$

$$a_z = \sqrt{\frac{1}{2\hbar m\omega_z}}p_z - i\sqrt{\frac{m\omega_z}{2\hbar}}z \quad (\text{E.8f})$$

The three sets of creation and annihilation operators follow the standard commutation relations

$$[a_j, a_k] = 0 \quad (\text{E.9a})$$

$$[a_j^\dagger, a_k^\dagger] = 0 \quad (\text{E.9b})$$

$$[a_j, a_k^\dagger] = \delta_{jk} \quad (\text{E.9c})$$

for $j, k = z, +, -$.

Defining $r_0 = \sqrt{\hbar/4m\Omega}$ and $z_0 = \sqrt{\hbar/2m\omega_z}$, the position and momentum operators take the form

$$x = ir_0(a_+ - a_+^\dagger + a_- - a_-^\dagger) \quad (\text{E.10a})$$

$$y = r_0(a_+ + a_+^\dagger - a_- - a_-^\dagger) \quad (\text{E.10b})$$

$$z = iz_0(a_z - a_z^\dagger) \quad (\text{E.10c})$$

$$p_x = m\Omega r_0(a_+ + a_+^\dagger + a_- + a_-^\dagger) \quad (\text{E.10d})$$

$$p_y = -im\Omega r_0(a_+ - a_+^\dagger - a_- + a_-^\dagger) \quad (\text{E.10e})$$

$$p_z = m\omega_z z_0(a_z + a_z^\dagger) \quad (\text{E.10f})$$

The total Hamiltonian can be written in second quantised form as

$$H = \hbar\omega_+(a_+^\dagger a_+^\dagger + \frac{1}{2}) - \hbar\omega_-(a_-^\dagger a_-^\dagger + \frac{1}{2}) + \hbar\omega_z(a_z^\dagger a_z^\dagger + \frac{1}{2}) \quad (\text{E.11})$$

F

Normal Modes of Linear Chains

Consider a linear chain of identical Penning traps, each containing a single ion (of the same species), along one of the radial coordinate axes, say x . If the quadrupole potential at each trap j is of the cylindrically symmetric form $V_j = \phi_0(z^2 - (x^2 + y^2)/2)$, the matrix V takes the diagonal form

$$V = m \begin{bmatrix} -\omega_z^2/2 \cdot \mathbb{I}_N & \mathbb{O}_N & \mathbb{O}_N \\ \mathbb{O}_N & -\omega_z^2/2 \cdot \mathbb{I}_N & \mathbb{O}_N \\ \mathbb{O}_N & \mathbb{O}_N & \omega_z^2 \cdot \mathbb{I}_N \end{bmatrix}, \quad (\text{F.1})$$

where we define $\omega_z = \sqrt{2e\phi_0/m}$

If $\mathbf{B} = B_0 \hat{z}$,

$$W = eB_0 \begin{bmatrix} \mathbb{O}_N & \mathbb{I}_N & \mathbb{O}_N \\ -\mathbb{I}_N & \mathbb{O}_N & \mathbb{O}_N \\ \mathbb{O}_N & \mathbb{O}_N & \mathbb{O}_N \end{bmatrix} \quad (\text{F.2})$$

The equilibrium positions of the ions in such a system naturally all lie along this axis, meaning for any pair of ions j and k , $\mathbf{R}_{jk0} = R_{jk0} \hat{x}$ and hence

$$\begin{aligned} R_{jk0}^x &= R_{jk0} \\ R_{jk0}^y &= 0 \\ R_{jk0}^z &= 0 \end{aligned} \quad (\text{F.3})$$

As a result all off-diagonal sub-matrices $K^{xx}, K^{xy}, K^{yx}, K^{xz}, K^{zx}, K^{yz},$ and K^{zy} equate to \mathbb{O}_N and K has the much simplified form

$$K = \begin{bmatrix} K^{xx} & \mathbb{O}_N & \mathbb{O}_N \\ \mathbb{O}_N & -K^{xx}/2 & \mathbb{O}_N \\ \mathbb{O}_N & \mathbb{O}_N & -K^{xx}/2 \end{bmatrix} \quad (\text{F.4})$$

At this point it becomes convenient to write down the equations of motion for the vectors along each rectangular coordinate axis $x = [x_1 \dots x_N]^T$, $y = [y_1 \dots y_N]^T$, and $z = [z_1 \dots z_N]^T$ so that equation [num] can be split into the following three

$$m\ddot{x} - eB_0\dot{y} - \frac{m\omega_z^2}{2}x + K^{xx}x = 0 \quad (\text{F.5a})$$

$$m\ddot{y} + eB_0\dot{x} - \frac{m\omega_z^2}{2}y - \frac{K^{xx}}{2}y = 0 \quad (\text{F.5b})$$

$$m\ddot{z} + m\omega_z^2z - \frac{K^{xx}}{2}z = 0 \quad (\text{F.5c})$$

Defining $\omega_c = eB_0/m$ and dividing the equations by the mass m ,

$$\ddot{x} - \omega_c\dot{y} - \frac{\omega_z^2}{2}x + \frac{K^{xx}}{m}x = 0 \quad (\text{F.6a})$$

$$\ddot{y} + \omega_c\dot{x} - \frac{\omega_z^2}{2}y - \frac{K^{xx}}{2m}y = 0 \quad (\text{F.6b})$$

$$\ddot{z} + \omega_z^2z - \frac{K^{xx}}{2m}z = 0 \quad (\text{F.6c})$$

Since the matrix K^{xx}/m is real, symmetric and positive semidefinite, its eigenvalues are real and non-negative. Then, for an eigenpair $\{\Omega_\lambda^2, q_\lambda\}$ of K^{xx}/m ,

$$\frac{K^{xx}}{m}q_\lambda = \Omega_\lambda^2q_\lambda \quad (\text{F.7a})$$

$$q_\lambda^T \frac{K^{xx}}{m} = \Omega_\lambda^2q_\lambda^T \quad (\text{F.7b})$$

Taking the inner product with q_λ , we get

$$q_\lambda^T \ddot{x} - \omega_c q_\lambda^T \dot{y} - \frac{\omega_z^2}{2} q_\lambda^T x + \Omega_\lambda^2 q_\lambda^T x = 0 \quad (\text{F.8a})$$

$$q_\lambda^T \ddot{y} + \omega_c q_\lambda^T \dot{x} - \frac{\omega_z^2}{2} q_\lambda^T y - \frac{\Omega_\lambda^2}{2} q_\lambda^T y = 0 \quad (\text{F.8b})$$

$$q_\lambda^T \ddot{z} + \omega_z^2 q_\lambda^T z - \frac{\Omega_\lambda^2}{2} q_\lambda^T z = 0 \quad (\text{F.8c})$$

Defining the new coordinates $X_\lambda = q_\lambda^T x = \sum_{j=1}^N q_{\lambda j} x_j$, $Y_\lambda = q_\lambda^T y = \sum_{j=1}^N q_{\lambda j} y_j$, and $Z_\lambda = q_\lambda^T z = \sum_{j=1}^N q_{\lambda j} z_j$, these equations transform into the equations of a motion like those of a single ion with coordinates $(X_\lambda, Y_\lambda, Z_\lambda)$

$$\ddot{X}_\lambda - \omega_c \dot{Y}_\lambda - \left(\frac{\omega_z^2}{2} - \Omega_\lambda^2\right) X_\lambda = 0 \quad (\text{F.9a})$$

$$\ddot{Y}_\lambda + \omega_c \dot{X}_\lambda - \left(\frac{\omega_z^2}{2} + \frac{\Omega_\lambda^2}{2}\right) Y_\lambda = 0 \quad (\text{F.9b})$$

$$\ddot{Z}_\lambda + \left(\omega_z^2 - \frac{\Omega_\lambda^2}{2}\right) Z_\lambda = 0 \quad (\text{F.9c})$$

The axial motion is decoupled from the radial degrees of freedom. Substituting the ansatz $Z_\lambda = Z_{\lambda 0} e^{-i\omega_{z\lambda} t}$,

$$-\omega_{z\lambda}^2 Z_{\lambda 0} + \left(\omega_z^2 - \frac{\Omega_\lambda^2}{2}\right) Z_{\lambda 0} = 0, \quad (\text{F.10})$$

giving

$$\omega_{z\lambda}^2 = \left(\omega_z^2 - \frac{\Omega_\lambda^2}{2}\right) \quad (\text{F.11})$$

With this definition, the radial equations transform to

$$\ddot{X}_\lambda - \omega_c \dot{Y}_\lambda - \frac{\omega_{z\lambda}^2}{2} (1 - \epsilon_\lambda) X_\lambda = 0 \quad (\text{F.12a})$$

$$\ddot{Y}_\lambda + \omega_c \dot{X}_\lambda - \frac{\omega_{z\lambda}^2}{2} (1 + \epsilon_\lambda) Y_\lambda = 0, \quad (\text{F.12b})$$

with $\epsilon_\lambda = 3\Omega_\lambda^2/2\omega_{z\lambda}^2$. These are the equations of motion for the so-called elliptical Penning trap, where the ‘ellipticity’ ϵ_λ reflects the breaking of radial symmetry due to Coulomb repulsion. Again these equations can be solved using the ansatz $X_\lambda = X_{\lambda 0} e^{-i\omega_\lambda t}$ and $Y_\lambda = Y_{\lambda 0} e^{-i\omega_\lambda t}$, yielding

$$-\omega_\lambda^2 X_{\lambda 0} + i\omega_c \omega_\lambda Y_{\lambda 0} - \frac{\omega_{z\lambda}^2}{2} (1 - \epsilon_\lambda) X_{\lambda 0} = 0 \quad (\text{F.13a})$$

$$-\omega_\lambda^2 Y_{\lambda 0} - i\omega_c \omega_\lambda X_{\lambda 0} - \frac{\omega_{z\lambda}^2}{2} (1 + \epsilon_\lambda) Y_{\lambda 0} = 0 \quad (\text{F.13b})$$

For non-trivial solutions, we require

$$\begin{vmatrix} \omega_\lambda^2 + \omega_{z\lambda}^2(1 - \epsilon_\lambda)/2 & -i\omega_c \omega_\lambda \\ i\omega_c \omega_\lambda & \omega_\lambda^2 + \omega_{z\lambda}^2(1 + \epsilon_\lambda)/2 \end{vmatrix} = 0 \quad (\text{F.14})$$

The radial frequencies are then given by

$$\omega_{\lambda\pm} = \sqrt{\frac{\omega_c^2 - \omega_{z\lambda}^2 \pm \sqrt{\omega_c^2(\omega_c^2 - 2\omega_{z\lambda}^2) + \omega_{z\lambda}^4 \epsilon_\lambda^2}}{2}} \quad (\text{F.15})$$

For a two ion chain with equilibrium distance d ,

$$\frac{K^{xx}}{m} = \begin{bmatrix} \frac{2k_e e^2}{md^3} & -\frac{2k_e e^2}{md^3} \\ -\frac{2k_e e^2}{md^3} & \frac{2k_e e^2}{md^3} \end{bmatrix} \quad (\text{F.16})$$

such that the two eigenvalues are $\Omega_1^2 = 0$ and $\Omega_2^2 = 4k_e e^2 / md^3$.

Then the two axial frequencies are $\omega_{z1} = \omega_z$, which corresponds to the COM frequency and the stretch frequency $\omega_{z2} = \sqrt{\omega_z^2 - 2k_e e^2 / md^3}$. Likewise the radial frequencies are

$$\omega_{\pm 1} = \omega_{\pm} \quad (\text{F.17a})$$

$$\omega_{\pm 2} = \sqrt{\frac{\omega_c^2 - \omega_{z2}^2 \pm \sqrt{\omega_c^2(\omega_c^2 - 2\omega_{z2}^2) + \omega_{z2}^4 \epsilon_2^2}}{2}} \quad (\text{F.17b})$$

When the ions are sufficiently far apart, we can approximate

$$\begin{aligned} \omega_{z2} &\approx \omega_z \left(1 - \frac{k_e e^2}{m\omega_z^2 d^3}\right) \\ &= \omega_z - \frac{k_e e^2}{m\omega_z d^3} \end{aligned} \quad (\text{F.18})$$

Thus we can define the exchange frequency for the axial modes

$$\Omega_{ex}^z \equiv \omega_{z2} - \omega_z \approx \frac{e^2}{4\pi\epsilon_0 m\omega_z d^3} \quad (\text{F.19})$$

Similarly,

$$\begin{aligned}
\omega_{\pm 2} &= \sqrt{\frac{\omega_c^2 - \omega_{z2}^2 \pm \sqrt{\omega_c^2(\omega_c^2 - 2\omega_{z2}^2) + 9\Omega_2^4/4}}{2}} \\
&\approx \sqrt{\frac{\omega_c^2 - \omega_{z2}^2 \pm \sqrt{\omega_c^2(\omega_c^2 - 2\omega_{z2}^2)}}{2}} \\
&= \frac{\omega_c \pm \sqrt{\omega_c^2 - 2\omega_{z2}^2}}{2} \\
&= \frac{\omega_c \pm \sqrt{\omega_c^2 - 2\omega_z^2 + 4k_e e^2/md^3}}{2} \\
&\approx \frac{\omega_c}{2} \pm \frac{1}{2}\sqrt{\omega_c^2 - 2\omega_z^2} \left\{ 1 + \frac{2k_e e^2}{md^3(\omega_c^2 - 2\omega_z^2)} \right\} \\
&= \omega_{\pm} \pm \frac{k_e e^2}{md^3\sqrt{\omega_c^2 - 2\omega_z^2}} \\
&= \omega_{\pm} \pm \frac{k_e e^2}{m(\omega_+ - \omega_-)d^3}
\end{aligned} \tag{F.20}$$

Thus we define for the radial modes a similar exchange frequency given by

$$\Omega_{ex}^{\pm} \equiv \omega_{\pm 2} - \omega_{\pm} \approx \pm \frac{e^2}{4\pi m \epsilon_0 (\omega_+ - \omega_-) d^3} \tag{F.21}$$

For a linear chain along the trapping axis we could do a similar analysis. The K matrix simplifies to

$$K = \begin{bmatrix} -K^{zz}/2 & \mathbb{O}_N & \mathbb{O}_N \\ \mathbb{O}_N & -K^{zz}/2 & \mathbb{O}_N \\ \mathbb{O}_N & \mathbb{O}_N & K^{zz} \end{bmatrix} \tag{F.22}$$

while all other matrices are the same as above.

$$\ddot{x} - \omega_c \dot{y} - \frac{\omega_z^2}{2} x - \frac{K^{zz}}{2m} x = 0 \tag{F.23a}$$

$$\dot{y} + \omega_c \dot{x} - \frac{\omega_z^2}{2} y - \frac{K^{zz}}{2m} y = 0 \tag{F.23b}$$

$$\ddot{z} + \omega_z^2 z + K^{zz} m z = 0 \tag{F.23c}$$

The matrix K^{zz}/m is real, symmetric and positive semidefinite. If

$$\frac{K^{zz}}{m} q_{\lambda} = \Omega_{\lambda}^2 q_{\lambda} \tag{F.24a}$$

$$q_\lambda^T \frac{K^{zz}}{m} = \Omega_\lambda^2 q_\lambda^T \quad (\text{F.24b})$$

then taking the inner product with q_λ , and again defining $X_\lambda = q_\lambda^T x = \sum_{j=1}^N q_{\lambda j} x_j$, $Y_\lambda = q_\lambda^T y = \sum_{j=1}^N q_{\lambda j} y_j$, and $Z_\lambda = q_\lambda^T z = \sum_{j=1}^N q_{\lambda j} z_j$,

$$\ddot{X}_\lambda - \omega_c \dot{Y}_\lambda - \left(\frac{\omega_z^2}{2} + \frac{\Omega_\lambda^2}{2} \right) X_\lambda = 0 \quad (\text{F.25a})$$

$$\ddot{Y}_\lambda + \omega_c \dot{X}_\lambda - \left(\frac{\omega_z^2}{2} + \frac{\Omega_\lambda^2}{2} \right) Y_\lambda = 0 \quad (\text{F.25b})$$

$$\ddot{Z}_\lambda + (\omega_z^2 + \Omega_\lambda^2) Z_\lambda = 0 \quad (\text{F.25c})$$

The axial motion is decoupled from the radial degrees of freedom. With the ansatz $Z_\lambda = Z_{\lambda 0} e^{-i\omega_{z\lambda} t}$,

$$-\omega_{z\lambda}^2 Z_{\lambda 0} + (\omega_z^2 + \Omega_\lambda^2) Z_{\lambda 0} = 0, \quad (\text{F.26})$$

giving

$$\omega_{z\lambda}^2 = (\omega_z^2 + \Omega_\lambda^2) \quad (\text{F.27})$$

The radial equations are simply

$$\ddot{X}_\lambda - \omega_c \dot{Y}_\lambda - \frac{\omega_{z\lambda}^2}{2} X_\lambda = 0 \quad (\text{F.28a})$$

$$\ddot{Y}_\lambda + \omega_c \dot{X}_\lambda - \frac{\omega_{z\lambda}^2}{2} Y_\lambda = 0, \quad (\text{F.28b})$$

which are just the equations of motion for a cylindrically symmetric Penning trap. It is then straightforward to show from the previous analysis for a single ion that there are two radial frequencies

$$\omega_{\lambda\pm} = \frac{\omega_c \pm \sqrt{\omega_c^2 - 2\omega_{z\lambda}^2}}{2} \quad (\text{F.29})$$

Again for two ions separated by an equilibrium distance d along the z -axis, $\omega_{z1} = \omega_z$ and $\omega_{\pm 1} = \omega_\pm$ while the exchange frequencies are given by

$$\Omega_{ex}^z \equiv \omega_{z2} - \omega_z \approx \frac{e^2}{2\pi\epsilon_0 m \omega_z d^3} \quad (\text{F.30})$$

and

$$\Omega_{ex}^\pm \equiv \omega_{\pm 2} - \omega_\pm \approx \pm \frac{e^2}{2\pi\epsilon_0 m (\omega_+ - \omega_-) d^3}, \quad (\text{F.31})$$

which are twice the values for the planar configuration.

G

Doppler Cooling

A quantitative analysis of Doppler cooling a system of N ions in an array of Penning traps begins, in the semi-classical limit, by finding the change in amplitude of each mode before and after a photon scattering event due to the laser-ion interaction.

The general solution for the collective motion of the ions can be written in terms of the normal mode vectors and frequencies as

$$\begin{aligned} r(t) &= \sum_{\lambda=1}^{3N} \text{Re}[\rho_{\lambda} q_{\lambda} e^{-i\omega_{\lambda} t}] \\ &= \frac{1}{2} \sum_{\lambda=1}^{3N} \left\{ \rho_{\lambda} q_{\lambda} e^{-i\omega_{\lambda} t} + \rho_{\lambda}^* q_{\lambda}^* e^{i\omega_{\lambda} t} \right\} \end{aligned} \quad (\text{G.1})$$

where ρ_{λ} are complex constants, and for the sake of simplicity all ω_{λ} are assumed to be positive. Then the velocity vector is given by

$$\dot{r}(t) = \frac{1}{2} \sum_{\lambda=1}^{3N} \left\{ -i\omega_{\lambda} \rho_{\lambda} q_{\lambda} e^{-i\omega_{\lambda} t} + i\omega_{\lambda} \rho_{\lambda}^* q_{\lambda}^* e^{i\omega_{\lambda} t} \right\} \quad (\text{G.2})$$

We can extract the amplitude of a single mode of motion λ from the ion positions and velocities as

$$\begin{aligned}
q_\lambda^H \{(-i\omega_\lambda M - W)r + M\dot{r}\} &= \frac{1}{2} \sum_{\lambda'=1}^{3N} \rho_{\lambda'} e^{-i\omega_{\lambda'} t} \{-i\omega_\lambda q_\lambda^H M q_{\lambda'} - q_\lambda^H W q_{\lambda'} - i\omega_{\lambda'} q_\lambda^H M q_{\lambda'}\} \\
&+ \frac{1}{2} \sum_{\lambda'=1}^{3N} \rho_{\lambda'}^* e^{i\omega_{\lambda'} t} \{-i\omega_\lambda q_\lambda^H M q_{\lambda'}^* - q_\lambda^H W q_{\lambda'}^* - i\omega_{\lambda'} q_\lambda^H M q_{\lambda'}^*\} \\
&= -\frac{i}{2} \sum_{\lambda'=1}^{3N} \rho_{\lambda'} e^{-i\omega_{\lambda'} t} \{(\omega_\lambda + \omega_{\lambda'}) q_\lambda^H M q_{\lambda'} + q_\lambda^H (-iW) q_{\lambda'}\} \\
&- \frac{i}{2} \sum_{\lambda'=1}^{3N} \rho_{\lambda'}^* e^{i\omega_{\lambda'} t} \{(\omega_\lambda - \omega_{\lambda'}) q_\lambda^H M q_{\lambda'}^* + q_\lambda^H (-iW) q_{\lambda'}^*\} \\
&= -\frac{i}{2\omega_\lambda} (\omega_\lambda^2 q_\lambda^H M q_\lambda + q_\lambda^H \Phi q_\lambda) \rho_\lambda e^{-i\omega_\lambda t} \\
&= -i\epsilon_\lambda \rho_\lambda e^{-i\omega_\lambda t}
\end{aligned} \tag{G.3}$$

where we have used relations from Appendix [] and defined the real quantity $\epsilon_\lambda = (\omega_\lambda^2 q_\lambda^H M q_\lambda + q_\lambda^H \Phi q_\lambda)/2\omega_\lambda$. Taking the complex conjugate of the previous equation, we get

$$q_\lambda^{*H} \{(i\omega_\lambda M - W)r + M\dot{r}\} = i\epsilon_\lambda \rho_\lambda^* e^{i\omega_\lambda t} \tag{G.4}$$

Splitting the eigenvector into its real and imaginary parts,

$$q_\lambda = \bar{q}_\lambda + i\tilde{q}_\lambda \tag{G.5}$$

we get

$$\frac{q_\lambda + q_\lambda^*}{2} = \bar{q}_\lambda \tag{G.6a}$$

$$\frac{q_\lambda - q_\lambda^*}{2} = i\tilde{q}_\lambda \tag{G.6b}$$

$$\frac{q_\lambda^H + q_\lambda^{*H}}{2} = \bar{q}_\lambda^H = \bar{q}_\lambda^T \tag{G.6c}$$

$$\frac{q_\lambda^H - q_\lambda^{*H}}{2} = -i\tilde{q}_\lambda^H = -i\tilde{q}_\lambda^T \tag{G.6d}$$

Then adding together equations G.3 and G.4 or subtracting equation G.3 from equation G.4 yields respectively

$$\omega_\lambda \tilde{q}_\lambda^T M r + \bar{q}_\lambda^T W r - \bar{q}_\lambda^T M \dot{r} = \epsilon_\lambda r_\lambda \sin(\omega_\lambda t + \delta_\lambda) \tag{G.7a}$$

$$\omega_\lambda \bar{q}_\lambda^T M r - \tilde{q}_\lambda^T W r + \tilde{q}_\lambda^T M \dot{r} = \epsilon_\lambda r_\lambda \cos(\omega_\lambda t + \delta_\lambda) \tag{G.7b}$$

where we have substituted $\rho_\lambda = r_\lambda e^{-i\delta_\lambda}$.

Squaring and adding these two we get the expression for the amplitude of each mode in terms of the position and velocity vectors as

$$r_\lambda^2 = \frac{1}{\epsilon_\lambda^2} \left\{ (\omega_\lambda \tilde{q}_\lambda^T M r + \bar{q}_\lambda^T W r - \bar{q}_\lambda^T M \dot{r})^2 + (\omega_\lambda \bar{q}_\lambda^T M r - \tilde{q}_\lambda^T W r + \tilde{q}_\lambda^T M \dot{r})^2 \right\} \quad (\text{G.8})$$

It can also be useful to re-express the position and velocity vectors as

$$r(t) = \sum_{\lambda=1}^{3N} \left\{ r_\lambda \bar{q}_\lambda \cos(\omega_\lambda t + \delta_\lambda) + r_\lambda \tilde{q}_\lambda \sin(\omega_\lambda t + \delta_\lambda) \right\} \quad (\text{G.9})$$

$$\dot{r}(t) = \sum_{\lambda=1}^{3N} \left\{ -\omega_\lambda r_\lambda \bar{q}_\lambda \sin(\omega_\lambda t + \delta_\lambda) + \omega_\lambda r_\lambda \tilde{q}_\lambda \cos(\omega_\lambda t + \delta_\lambda) \right\} \quad (\text{G.10})$$

At a time t just before a photon absorption event, we have

$$\omega_\lambda \tilde{q}_\lambda^T M r(t) + \bar{q}_\lambda^T W r(t) - \bar{q}_\lambda^T M \dot{r}(t) = \epsilon_\lambda r_\lambda \sin(\omega_\lambda t + \delta_\lambda) \quad (\text{G.11a})$$

$$\omega_\lambda \bar{q}_\lambda^T M r(t) - \tilde{q}_\lambda^T W r(t) + \tilde{q}_\lambda^T M \dot{r}(t) = \epsilon_\lambda r_\lambda \cos(\omega_\lambda t + \delta_\lambda) \quad (\text{G.11b})$$

while at the time t' just after the photon is re-emitted,

$$\omega_\lambda \tilde{q}_\lambda^T M r(t') + \bar{q}_\lambda^T W r(t') - \bar{q}_\lambda^T M \dot{r}(t') = \epsilon_\lambda r'_\lambda \sin(\omega_\lambda t' + \delta'_\lambda) \quad (\text{G.12a})$$

$$\omega_\lambda \bar{q}_\lambda^T M r(t') - \tilde{q}_\lambda^T W r(t') + \tilde{q}_\lambda^T M \dot{r}(t') = \epsilon_\lambda r'_\lambda \cos(\omega_\lambda t' + \delta'_\lambda) \quad (\text{G.12b})$$

If the photon scattering event is instantaneous and leaves the position unchanged but the ion interacting with the photon gets a momentum kick, the position and velocity vectors at times t and t' are related as $r(t') = r(t)$ and $\dot{r}(t') - \dot{r}(t) = \Delta v$. Subtracting G.11a from G.12a, and G.11b from G.12b,

$$-\bar{q}_\lambda^T M \Delta v = \epsilon_\lambda (r'_\lambda \sin(\omega_\lambda t' + \delta'_\lambda) - r_\lambda \sin(\omega_\lambda t + \delta_\lambda)) \quad (\text{G.13a})$$

$$\tilde{q}_\lambda^T M \Delta v = \epsilon_\lambda (r'_\lambda \cos(\omega_\lambda t' + \delta'_\lambda) - r_\lambda \cos(\omega_\lambda t + \delta_\lambda)) \quad (\text{G.13b})$$

and hence

$$\epsilon_\lambda r'_\lambda \sin(\omega_\lambda t' + \delta'_\lambda) = \epsilon_\lambda r_\lambda \sin(\omega_\lambda t + \delta_\lambda) - \bar{q}_\lambda^T M \Delta v \quad (\text{G.14a})$$

$$\epsilon_\lambda r'_\lambda \cos(\omega_\lambda t' + \delta'_\lambda) = \epsilon_\lambda r_\lambda \cos(\omega_\lambda t + \delta_\lambda) + \tilde{q}_\lambda^T M \Delta v \quad (\text{G.14b})$$

Squaring and adding equations G.14a and G.14b,

$$\epsilon_\lambda^2 r_\lambda'^2 = \epsilon_\lambda^2 r_\lambda^2 + (\bar{q}_\lambda^T M \Delta v)^2 - 2(\bar{q}_\lambda^T M \Delta v) \epsilon_\lambda r_\lambda \sin(\omega_\lambda t + \delta_\lambda) + (\tilde{q}_\lambda^T M \Delta v)^2 + 2(\tilde{q}_\lambda^T M \Delta v) \epsilon_\lambda r_\lambda \cos(\omega_\lambda t + \delta_\lambda) \quad (\text{G.15})$$

and the change in the amplitude of mode λ due to a single laser-ion interaction event is given by

$$\begin{aligned}\Delta r_\lambda^2 &\equiv r_\lambda'^2 - r_\lambda^2 \\ &= \frac{1}{\epsilon_\lambda^2} \left\{ (\tilde{q}_\lambda^T M \Delta v)^2 + (\tilde{q}_\lambda^T M \Delta v)^2 - 2(\tilde{q}_\lambda^T M \Delta v) \epsilon_\lambda r_\lambda \sin(\omega_\lambda t + \delta_\lambda) + 2(\tilde{q}_\lambda^T M \Delta v) \epsilon_\lambda r_\lambda \cos(\omega_\lambda t + \delta_\lambda) \right\}\end{aligned}\quad (\text{G.16})$$

In the low intensity limit, the average rate of change in the mode amplitudes can be found by multiplying the change in amplitude with each scattering event by the photon incidence rate and the scattering cross section and then averaging over the mode amplitudes, phases and scattering directions.

For a laser with uniform intensity I over the extent of the ion motion, the number of photons incident per unit time per unit area is $I/\hbar\omega$, while the cross-section takes the velocity dependent form

$$\sigma(\omega, \mathbf{v}) = \frac{\sigma_0(\Gamma/2)^2}{(\omega_0 + \mathbf{k} \cdot \mathbf{v} + R/\hbar - \omega)^2 + (\Gamma/2)^2} \quad (\text{G.17})$$

where ω_0 and Γ are respectively the frequency and natural linewidth of the cooling transition used, ω and \mathbf{k} are respectively the frequency and wave vector of the laser and σ_0 is a constant pertaining to the transition. Assuming the ion has already been somehow cooled so that the velocity is small,

$$\sigma(\omega, \mathbf{v}) \approx \frac{\sigma_0(\Gamma/2)^2}{\delta^2 + (\Gamma/2)^2} \left\{ 1 + \frac{2\delta \mathbf{k} \cdot \mathbf{v}}{\delta^2 + (\Gamma/2)^2} \right\} \quad (\text{G.18})$$

where $\delta = \omega - \omega_0$ is the detuning of the laser.

Considering the interaction of the laser with the j th ion, the change in velocity of the ion due to the absorption of a photon with momentum $\hbar\mathbf{k}$ and spontaneous emission of a photon with momentum $\hbar\mathbf{k}_s$ can be quantified as

$$\Delta \mathbf{v}_j = \mathbf{v}'_j - \mathbf{v}_j = \frac{\hbar(\mathbf{k} - \mathbf{k}_s)}{m_j} \quad (\text{G.19})$$

through the conservation of momentum, so that the Cartesian components are given as

$$\Delta v_j^\mu = \frac{\hbar(k^\mu - k_s^\mu)}{m_j}, \quad \mu = x, y, z \quad (\text{G.20})$$

Using this result,

$$\tilde{q}_\lambda^T M \Delta v = m_j \sum_\mu \tilde{q}_{\lambda j}^\mu \Delta v_j^\mu = \hbar \sum_\mu \tilde{q}_{\lambda j}^\mu (k^\mu - k_s^\mu) \quad (\text{G.21a})$$

$$\tilde{q}_\lambda^T M \Delta v = m_j \sum_\mu \tilde{q}_{\lambda j}^\mu \Delta v_j^\mu = \hbar \sum_\mu \tilde{q}_{\lambda j}^\mu (k^\mu - k_s^\mu) \quad (\text{G.21b})$$

and

$$(\bar{q}_\lambda^T M \Delta v)^2 = \hbar^2 \sum_\mu (\bar{q}_{\lambda_j}^\mu)^2 (k^\mu - k_s^\mu)^2 + \sum_{\mu \neq \nu} \bar{q}_{\lambda_j}^\mu \bar{q}_{\lambda_j}^\nu (k^\mu - k_s^\mu)(k^\nu - k_s^\nu) \quad (\text{G.22a})$$

$$(\tilde{q}_\lambda^T M \Delta v)^2 = \hbar^2 \sum_\mu (\tilde{q}_{\lambda_j}^\mu)^2 (k^\mu - k_s^\mu)^2 + \sum_{\mu \neq \nu} \tilde{q}_{\lambda_j}^\mu \tilde{q}_{\lambda_j}^\nu (k^\mu - k_s^\mu)(k^\nu - k_s^\nu) \quad (\text{G.22b})$$

The cross-section can be approximated as

$$\sigma(\omega, \mathbf{v}_j) \approx \frac{\sigma_0 (\Gamma/2)^2}{(\Gamma/2)^2 + \delta^2} \left\{ 1 + 2\delta \frac{\sum_{\rho, \lambda} (-\omega_\lambda r_\lambda k^\mu \bar{q}_{\lambda_j}^\mu \sin(\omega_\lambda t + \delta_\lambda) + \omega_\lambda r_\lambda k^\mu \tilde{q}_{\lambda_j}^\mu \cos(\omega_\lambda t + \delta_\lambda))}{(\Gamma/2)^2 + \delta^2} \right\} \quad (\text{G.23})$$

by substituting

$$\begin{aligned} \mathbf{k} \cdot \mathbf{v}_j &= \sum_\mu k^\mu v_j^\mu \\ &= \sum_{\mu, \lambda} \left\{ -\omega_\lambda r_\lambda k^\mu \bar{q}_{\lambda_j}^\mu \sin(\omega_\lambda t + \delta_\lambda) + \omega_\lambda r_\lambda k^\mu \tilde{q}_{\lambda_j}^\mu \cos(\omega_\lambda t + \delta_\lambda) \right\} \end{aligned} \quad (\text{G.24})$$

Defining

$$\gamma_s \equiv \frac{I}{\hbar \omega} \cdot \frac{\sigma_0 (\Gamma/2)^2}{(\Gamma/2)^2 + \delta^2} \quad (\text{G.25})$$

we get the rate equation for the amplitude of mode λ as

$$\begin{aligned} \frac{\Delta r_\lambda^2}{\Delta t} &= \frac{\gamma_{sj}}{\epsilon_\lambda^2} \left\{ (\bar{q}_\lambda^T M \Delta v)^2 + (\tilde{q}_\lambda^T M \Delta v)^2_{(1)} - 2(\bar{q}_\lambda^T M \Delta v) \epsilon_\lambda r_\lambda \sin(\omega_\lambda t + \delta_\lambda)_{(2)} + 2(\tilde{q}_\lambda^T M \Delta v) \epsilon_\lambda r_\lambda \cos(\omega_\lambda t + \delta_\lambda)_{(3)} \right\} \\ &\cdot \left\{ 1_{(a)} + \frac{2\delta}{(\Gamma/2)^2 + \delta^2} \sum_{\mu, \lambda'} (-\omega_{\lambda'} A_{\lambda'} k^\mu \bar{q}_{\lambda_j}^\mu \sin(\omega_{\lambda'} t + \delta_{\lambda'})_{(b)} + \omega_{\lambda'} A_{\lambda'} k^\mu \tilde{q}_{\lambda_j}^\mu \cos(\omega_{\lambda'} t + \delta_{\lambda'})_{(c)}) \right\} \end{aligned} \quad (\text{G.26})$$

We now average each sub-product over the phases $\{\delta_{\lambda'}\}$

$$\langle (1) \cdot (a) \rangle_{\{\delta_{\lambda'}\}} = (\bar{q}_\lambda^T M \Delta v)^2 + (\tilde{q}_\lambda^T M \Delta v)^2 \quad (\text{G.27a})$$

$$\langle (1) \cdot (b) \rangle_{\{\delta_{\lambda'}\}} = 0 \quad (\text{G.27b})$$

$$\langle (1) \cdot (c) \rangle_{\{\delta_{\lambda'}\}} = 0 \quad (\text{G.27c})$$

$$\langle (2) \cdot (a) \rangle_{\{\delta_{\lambda'}\}} = 0 \quad (\text{G.27d})$$

$$\langle (2) \cdot (b) \rangle_{\{\delta_{\lambda'}\}} = \sum_\mu \epsilon_\lambda \omega_\lambda A_\lambda^2 k^\mu \bar{q}_{\lambda_j}^\mu (\bar{q}_\lambda^T M \Delta v) \quad (\text{G.27e})$$

$$\langle (2) \cdot (c) \rangle_{\{\delta_{\lambda'}\}} = 0 \quad (\text{G.27f})$$

$$\langle\langle(3) \cdot (a)\rangle\rangle_{\{\delta_{\lambda'}\}} = 0 \quad (\text{G.27g})$$

$$\langle\langle(3) \cdot (b)\rangle\rangle_{\{\delta_{\lambda'}\}} = 0 \quad (\text{G.27h})$$

$$\langle\langle(3) \cdot (c)\rangle\rangle_{\{\delta_{\lambda'}\}} = \sum_{\mu} \epsilon_{\lambda} \omega_{\lambda} A_{\lambda}^2 k^{\mu} \tilde{q}_{\lambda_j}^{\mu} (\tilde{q}_{\lambda}^T M \Delta v) \quad (\text{G.27i})$$

Averaging over the scattering directions, and using the relations $\langle k_s^{\mu} \rangle_{\hat{k}_s} = 0$, $\langle k_s^{\mu} k_s^{\nu} \rangle_{\hat{k}_s} = 0$, $\mu \neq \nu$ and $\langle (k_s^{\mu})^2 \rangle_{\hat{k}_s} = k^2 f_s^{\mu}$

$$\langle \tilde{q}_{\lambda}^T M \Delta v \rangle_{\hat{k}_s} = \hbar \sum_{\mu} \tilde{q}_{\lambda_j}^{\mu} k^{\mu} \quad (\text{G.28a})$$

$$\langle \tilde{q}_{\lambda}^T M \Delta v \rangle_{\hat{k}_s} = \hbar \sum_{\mu} \tilde{q}_{\lambda_j}^{\mu} k^{\mu} \quad (\text{G.28b})$$

$$\langle (\tilde{q}_{\lambda}^T M \Delta v)^2 \rangle_{\hat{k}_s} = (\hbar \sum_{\mu} \tilde{q}_{\lambda_j}^{\mu} k^{\mu})^2 + \hbar^2 \sum_{\mu} (\tilde{q}_{\lambda_j}^{\mu})^2 k^2 f_s^{\mu} \quad (\text{G.28c})$$

$$\langle (\tilde{q}_{\lambda}^T M \Delta v)^2 \rangle_{\hat{k}_s} = (\hbar \sum_{\mu} \tilde{q}_{\lambda_j}^{\mu} k^{\mu})^2 + \hbar^2 \sum_{\mu} (\tilde{q}_{\lambda_j}^{\mu})^2 k^2 f_s^{\mu} \quad (\text{G.28d})$$

Finally, averaging over the amplitude of motion, we get the rate equation of the Doppler cooled mode

$$\begin{aligned} \frac{d}{dt} \langle r_{\lambda}^2 \rangle &= \frac{\gamma_s}{\epsilon_{\lambda}^2} \left\{ (\hbar \sum_{\mu} \tilde{q}_{\lambda_j}^{\mu} k^{\mu})^2 + (\hbar \sum_{\mu} \tilde{q}_{\lambda_j}^{\mu} k^{\mu})^2 + \hbar^2 \sum_{\mu} \{(\tilde{q}_{\lambda_j}^{\mu})^2 + (\tilde{q}_{\lambda_j}^{\mu})^2\} k_j^2 f_s^{\mu} \right. \\ &\quad \left. + \frac{2\delta \epsilon_{\lambda} \omega_{\lambda}}{(\Gamma/2)^2 + \delta^2} \{ \hbar (\sum_{\mu} \tilde{q}_{\lambda_j}^{\mu} k^{\mu})^2 + \hbar (\sum_{\mu} \tilde{q}_{\lambda_j}^{\mu} k^{\mu})^2 \} \langle r_{\lambda}^2 \rangle \right\} \end{aligned} \quad (\text{G.29})$$

Defining

$$F_{\lambda_j} = (\hbar \sum_{\mu} \tilde{q}_{\lambda_j}^{\mu} k^{\mu})^2 + (\hbar \sum_{\mu} \tilde{q}_{\lambda_j}^{\mu} k^{\mu})^2 \quad (\text{G.30})$$

$$F_{\lambda_s j} = \hbar^2 \sum_{\mu} \{(\tilde{q}_{\lambda_j}^{\mu})^2 + (\tilde{q}_{\lambda_j}^{\mu})^2\} k_j^2 f_s^{\mu} \quad (\text{G.31})$$

we can write the equation more succinctly as

$$\frac{d}{dt} \langle r_{\lambda}^2 \rangle = \frac{\gamma_s}{\epsilon_{\lambda}^2} \left\{ F_{\lambda_j} + F_{\lambda_s j} + \frac{2\delta \epsilon_{\lambda} \omega_{\lambda} F_{\lambda_j} / \hbar}{(\Gamma/2)^2 + \delta^2} \langle r_{\lambda}^2 \rangle \right\} \quad (\text{G.32})$$

If all ions are of the same species and a uniform laser beam is incident on all ions, the total rate of cooling can be found by simply summing over all ions so that

$$\frac{d}{dt} \langle r_{\lambda}^2 \rangle = \sum_{j=1}^N \frac{\gamma_s}{\epsilon_{\lambda}^2} \left\{ F_{\lambda_j} + F_{\lambda_s j} + \frac{2\delta \epsilon_{\lambda} \omega_{\lambda} F_{\lambda_j} / \hbar}{(\Gamma/2)^2 + \delta^2} \langle r_{\lambda}^2 \rangle \right\} \quad (\text{G.33})$$

It is clear that the mode will be cooled if δ and ϵ_λ are of different signs. If this criterion is met, final amplitude reached in the steady state is given by

$$\langle r_\lambda^2 \rangle = \hbar \frac{(\Gamma/2)^2 + \delta^2}{2|\delta \epsilon_\lambda| \omega_\lambda} \frac{\sum_j (F_{\lambda j} + F_{\lambda s j})}{\sum_j F_{\lambda j}} \quad (\text{G.34})$$

which is minimised for the detuning $|\delta| = \Gamma/2$.

H

Spin-Spin Coupling

The derivation in this Appendix follows closely the methodology from ref.¹⁹.
An ODF leads to the interaction term

$$H_{\text{ODF}} = - \sum_{j=1}^N E_O \cos(\mathbf{k}_R \cdot \mathbf{R}_j - \mu_R t) \sigma_j^z \quad (\text{H.1})$$

Expanding about the equilibrium positions,

$$\cos(\mathbf{k}_R \cdot \mathbf{R}_j - \mu_R t) = \cos(\mathbf{k}_R \cdot \mathbf{R}_{j0} - \mu_R t + \mathbf{k}_R \cdot \mathbf{r}_j) \quad (\text{H.2})$$

Dropping the term with no \mathbf{r}_j dependence and in the Lamb-Dicke regime,

$$H_{\text{ODF}} \approx \sum_{j=1}^N E_O \mathbf{k}_R \cdot \mathbf{r}_j \sin(\mathbf{k}_R \cdot \mathbf{R}_{j0} - \mu_R t) \sigma_j^z \quad (\text{H.3})$$

Then the effective spin Hamiltonian is given by

$$H_{\text{SPIN}} = \frac{i}{2\hbar} [W_I(t), V_I(t)] \quad (\text{H.4})$$

where

$$V_I(t) = e^{iH_{\text{PH}}t/\hbar} H_{\text{ODF}}(t) e^{-iH_{\text{PH}}t/\hbar} \quad (\text{H.5})$$

$$W_I(t) = \int_0^t V_I(t') dt' \quad (\text{H.6})$$

and

$$H_{\text{PH}} = \sum_{\lambda=1}^{3N} \hbar \omega_{\lambda} (a_{\lambda}^{\dagger} a_{\lambda} + \frac{1}{2}) \quad (\text{H.7})$$

In terms of operators,

$$\mathbf{k}_R \cdot \mathbf{r}_j = -i \hbar \sum_{\nu} k_R^{\nu} \sum_{\lambda=1}^{3N} (\alpha_{\lambda j \nu}^* a_{\lambda}^{\dagger} - \alpha_{\lambda j \nu} a_{\lambda}) \quad (\text{H.8})$$

Then

$$H_{\text{ODF}} = -i \hbar E_O \sum_{j=1}^N \sin(\mathbf{k}_R \cdot \mathbf{R}_{j0} - \mu_R t) \sum_{\nu} k_R^{\nu} \sum_{\lambda=1}^{3N} (\alpha_{\lambda j \nu}^* a_{\lambda}^{\dagger} - \alpha_{\lambda j \nu} a_{\lambda}) \sigma_j^z \quad (\text{H.9})$$

and

$$V_I(t) = -i \hbar E_O \sum_{j=1}^N \sin(\mathbf{k}_R \cdot \mathbf{R}_{j0} - \mu_R t) \sum_{\nu} k_R^{\nu} \sum_{\lambda=1}^{3N} (\alpha_{\lambda j \nu}^* e^{iH_{\text{PH}}t/\hbar} a_{\lambda}^{\dagger} \sigma_j^z e^{-iH_{\text{PH}}t/\hbar} - \alpha_{\lambda j \nu} e^{iH_{\text{PH}}t/\hbar} a_{\lambda} \sigma_j^z e^{-iH_{\text{PH}}t/\hbar}) \quad (\text{H.10})$$

Using the B-C-H formula,

$$e^{iH_{\text{PH}}t/\hbar} a_{\lambda}^{\dagger} \sigma_j^z e^{-iH_{\text{PH}}t/\hbar} = e^{i\omega_{\lambda}t} a_{\lambda}^{\dagger} \sigma_j^z \quad (\text{H.11a})$$

$$e^{iH_{\text{PH}}t/\hbar} a_{\lambda} \sigma_j^z e^{-iH_{\text{PH}}t/\hbar} = e^{-i\omega_{\lambda}t} a_{\lambda} \sigma_j^z \quad (\text{H.11b})$$

and hence we get

$$\begin{aligned} V_I(t) &= -i \hbar E_O \sum_{j=1}^N \sin(\mathbf{k}_R \cdot \mathbf{R}_{j0} - \mu_R t) \sum_{\nu} k_R^{\nu} \sum_{\lambda=1}^{3N} (\alpha_{\lambda j \nu}^* e^{i\omega_{\lambda}t} a_{\lambda}^{\dagger} \sigma_j^z - \alpha_{\lambda j \nu} e^{-i\omega_{\lambda}t} a_{\lambda} \sigma_j^z) \\ &\equiv -\frac{\hbar E_O}{2} \sum_{j, \nu, \lambda} k_R^{\nu} (f_{\lambda j}(t) \alpha_{\lambda j \nu}^* a_{\lambda}^{\dagger} \sigma_j^z - g_{\lambda j}(t) \alpha_{\lambda j \nu} a_{\lambda} \sigma_j^z) \end{aligned} \quad (\text{H.12})$$

where we define the functions

$$f_{\lambda j}(t) \equiv e^{i\phi_j} e^{i(\omega - \mu_R)t} - e^{-i\phi_j} e^{i(\omega + \mu_R)t} \quad (\text{H.13a})$$

$$g_{\lambda j}(t) \equiv e^{i\phi_j} e^{-i(\omega + \mu_R)t} - e^{-i\phi_j} e^{-i(\omega - \mu_R)t} \quad (\text{H.13b})$$

$$\phi_j = \mathbf{k}_R \cdot \mathbf{R}_{j0} \quad (\text{H.13c})$$

Then

$$W_I(t) = -\frac{\hbar E_O}{2} \sum_{j, \nu, \lambda} k_R^{\nu} (\bar{f}_{\lambda j}(t) \alpha_{\lambda j \nu}^* a_{\lambda}^{\dagger} \sigma_j^z - \bar{g}_{\lambda j}(t) \alpha_{\lambda j \nu} a_{\lambda} \sigma_j^z) \quad (\text{H.14})$$

where

$$\bar{f}_{\lambda j}(t) \equiv \int_0^t f_{\lambda j}(t') dt' = \frac{e^{i\phi_j}}{i(\omega_{\lambda} - \mu_R)} (e^{i(\omega_{\lambda} - \mu_R)t} - 1) - \frac{e^{-i\phi_j}}{i(\omega_{\lambda} + \mu_R)} (e^{i(\omega_{\lambda} + \mu_R)t} - 1) \quad (\text{H.15a})$$

$$\bar{g}_{\lambda_j}(t) \equiv \int_0^t g_{\lambda_j}(t') dt' = -\frac{e^{i\phi_j}}{i(\omega_\lambda + \mu_R)}(e^{-i(\omega_\lambda + \mu_R)t} - 1) + \frac{e^{-i\phi_j}}{i(\omega_\lambda - \mu_R)}(e^{-i(\omega_\lambda - \mu_R)t} - 1) \quad (\text{H.15b})$$

Then

$$\begin{aligned} H_{\text{SPIN}} &= \frac{i}{2\hbar} \frac{\hbar^2 E_O^2}{4} \sum_{j,j'} \sum_{\nu,\nu'} \sum_{\lambda,\lambda'} k_R^\nu k_R^{\nu'} \alpha_{\lambda_j\nu}^* \alpha_{\lambda_{j'}\nu'}^* \bar{f}_{\lambda_j}(t) f_{\lambda_{j'}}(t) [a_\lambda^\dagger \sigma_j^z, a_{\lambda'}^\dagger \sigma_{j'}^z] \\ &\quad - \frac{i}{2\hbar} \frac{\hbar^2 E_O^2}{4} \sum_{j,j'} \sum_{\nu,\nu'} \sum_{\lambda,\lambda'} k_R^\nu k_R^{\nu'} \alpha_{\lambda_j\nu}^* \alpha_{\lambda_{j'}\nu'}^* \bar{f}_{\lambda_j}(t) g_{\lambda_{j'}}(t) [a_\lambda^\dagger \sigma_j^z, a_{\lambda'} \sigma_{j'}^z] \\ &\quad - \frac{i}{2\hbar} \frac{\hbar^2 E_O^2}{4} \sum_{j,j'} \sum_{\nu,\nu'} \sum_{\lambda,\lambda'} k_R^\nu k_R^{\nu'} \alpha_{\lambda_j\nu}^* \alpha_{\lambda_{j'}\nu'}^* \bar{g}_{\lambda_j}(t) f_{\lambda_{j'}}(t) [a_\lambda \sigma_j^z, a_{\lambda'}^\dagger \sigma_{j'}^z] \\ &\quad + \frac{i}{2\hbar} \frac{\hbar^2 E_O^2}{4} \sum_{j,j'} \sum_{\nu,\nu'} \sum_{\lambda,\lambda'} k_R^\nu k_R^{\nu'} \alpha_{\lambda_j\nu}^* \alpha_{\lambda_{j'}\nu'}^* \bar{g}_{\lambda_j}(t) g_{\lambda_{j'}}(t) [a_\lambda \sigma_j^z, a_{\lambda'} \sigma_{j'}^z] \end{aligned} \quad (\text{H.16})$$

The commutation relations are

$$[a_\lambda^\dagger \sigma_j^z, a_{\lambda'}^\dagger \sigma_{j'}^z] = 0 \quad (\text{H.17a})$$

$$[a_\lambda^\dagger \sigma_j^z, a_{\lambda'} \sigma_{j'}^z] = -\delta_{\lambda\lambda'} \sigma_j^z \sigma_{j'}^z \quad (\text{H.17b})$$

$$[a_\lambda \sigma_j^z, a_{\lambda'}^\dagger \sigma_{j'}^z] = \delta_{\lambda\lambda'} \sigma_j^z \sigma_{j'}^z \quad (\text{H.17c})$$

$$[a_\lambda \sigma_j^z, a_{\lambda'} \sigma_{j'}^z] = 0 \quad (\text{H.17d})$$

and hence

$$\begin{aligned} H_{\text{SPIN}} &= \frac{i\hbar E_O^2}{8} \sum_{j,j'} \sum_{\nu,\nu'} \sum_{\lambda} k_R^\nu k_R^{\nu'} (\alpha_{\lambda_j\nu}^* \alpha_{\lambda_{j'}\nu'} \bar{f}_{\lambda_j}(t) g_{\lambda_{j'}}(t) - \alpha_{\lambda_j\nu} \alpha_{\lambda_{j'}\nu'}^* \bar{g}_{\lambda_j}(t) f_{\lambda_{j'}}(t)) \sigma_j^z \sigma_{j'}^z \\ &= \frac{i\hbar E_O^2}{8} \sum_{j,j'} \sum_{\nu,\nu'} \sum_{\lambda} k_R^\nu k_R^{\nu'} \text{Re}(\alpha_{\lambda_j\nu}^* \alpha_{\lambda_{j'}\nu'}) (\bar{f}_{\lambda_j}(t) g_{\lambda_{j'}}(t) - \bar{g}_{\lambda_j}(t) f_{\lambda_{j'}}(t)) \sigma_j^z \sigma_{j'}^z \\ &\quad - \frac{\hbar E_O^2}{8} \sum_{j,j'} \sum_{\nu,\nu'} \sum_{\lambda} k_R^\nu k_R^{\nu'} \text{Im}(\alpha_{\lambda_j\nu}^* \alpha_{\lambda_{j'}\nu'}) (\bar{f}_{\lambda_j}(t) g_{\lambda_{j'}}(t) + \bar{g}_{\lambda_j}(t) f_{\lambda_{j'}}(t)) \sigma_j^z \sigma_{j'}^z \end{aligned} \quad (\text{H.18})$$

Explicitly,

$$\begin{aligned} \bar{f}_{\lambda_j}(t) g_{\lambda_{j'}}(t) &= \frac{e^{i(\phi_j + \phi_{j'})}}{i(\omega_\lambda - \mu_R)} (e^{-i2\mu_R t} - e^{-i(\omega_\lambda + \mu_R)t}) - \frac{e^{-i(\phi_j - \phi_{j'})}}{i(\omega_\lambda + \mu_R)} (1 - e^{-i(\omega_\lambda + \mu_R)t}) \\ &\quad - \frac{e^{i(\phi_j - \phi_{j'})}}{i(\omega_\lambda - \mu_R)} (1 - e^{-i(\omega_\lambda - \mu_R)t}) + \frac{e^{-i(\phi_j + \phi_{j'})}}{i(\omega_\lambda + \mu_R)} (e^{i2\mu_R t} - e^{-i(\omega_\lambda - \mu_R)t}) \end{aligned} \quad (\text{H.19a})$$

$$\begin{aligned}\bar{g}_{\lambda_j}(t)f_{\lambda_{j'}}(t) &= -\frac{e^{i(\phi_j+\phi_{j'})}}{i(\omega_\lambda+\mu_R)}(e^{-i2\mu_R t}-e^{i(\omega_\lambda-\mu_R)t})+\frac{e^{-i(\phi_j-\phi_{j'})}}{i(\omega_\lambda-\mu_R)}(1-e^{i(\omega_\lambda-\mu_R)t}) \\ &+ \frac{e^{i(\phi_j-\phi_{j'})}}{i(\omega_\lambda+\mu_R)}(1-e^{i(\omega_\lambda+\mu_R)t})+\frac{e^{-i(\phi_j+\phi_{j'})}}{i(\omega_\lambda-\mu_R)}(e^{i2\mu_R t}-e^{i(\omega_\lambda+\mu_R)t})\end{aligned}\quad (\text{H.19b})$$

The time-independent part of these functions is given by

$$\bar{f}_{\lambda_j}(t)g_{\lambda_{j'}}(t)+\bar{g}_{\lambda_j}(t)f_{\lambda_{j'}}(t)=\frac{4\mu_R\sin(\phi_j-\phi_{j'})}{\mu_R^2-\omega_\lambda^2}\quad (\text{H.20a})$$

$$\bar{f}_{\lambda_j}(t)g_{\lambda_{j'}}(t)-\bar{g}_{\lambda_j}(t)f_{\lambda_{j'}}(t)=-\frac{4\omega_\lambda i\cos(\phi_j-\phi_{j'})}{\mu_R^2-\omega_\lambda^2}\quad (\text{H.20b})$$

Thus, the static part of the effective spin Hamiltonian is

$$\begin{aligned}H_{\text{SPIN}} &= \frac{\hbar E_O^2}{8}\sum_{j,j'}\sum_{\nu,\nu'}\sum_{\lambda}\frac{4\omega_\lambda\cos(\phi_j-\phi_{j'})}{\mu_R^2-\omega_\lambda^2}k_R^\nu k_R^{\nu'}\text{Re}(\alpha_{\lambda_j\nu}^*\alpha_{\lambda_{j'}\nu'})\sigma_j^z\sigma_{j'}^z \\ &- \frac{\hbar E_O^2}{8}\sum_{j,j'}\sum_{\nu,\nu'}\sum_{\lambda}\frac{4\mu_R\sin(\phi_j-\phi_{j'})}{\mu_R^2-\omega_\lambda^2}k_R^\nu k_R^{\nu'}\text{Im}(\alpha_{\lambda_j\nu}^*\alpha_{\lambda_{j'}\nu'})\sigma_j^z\sigma_{j'}^z\end{aligned}\quad (\text{H.21})$$

The above is just the expression for an Ising-like spin Hamiltonian

$$H_{\text{SPIN}}=\sum_{jj'}J_{jj'}^0\sigma_j^z\sigma_{j'}^z,\quad (\text{H.22})$$

with the coupling terms given by

$$\begin{aligned}J_{jj'}^0 &= \frac{E_O^2}{2}\sum_{\nu,\nu'}\sum_{\lambda}\frac{\omega_\lambda^2}{m\omega_\lambda^2+\gamma_\lambda^H\Phi\gamma_\lambda}\frac{k_R^\nu k_R^{\nu'}}{\mu_R^2-\omega_\lambda^2}\cos(\phi_j-\phi_{j'})\text{Re}(\gamma_{\lambda_j\nu}^*\gamma_{\lambda_{j'}\nu'}) \\ &- \frac{E_O^2}{2}\sum_{\nu,\nu'}\sum_{\lambda}\frac{\omega_\lambda\mu_R}{m\omega_\lambda^2+\gamma_\lambda^H\Phi\gamma_\lambda}\frac{k_R^\nu k_R^{\nu'}}{\mu_R^2-\omega_\lambda^2}\sin(\phi_j-\phi_{j'})\text{Im}(\gamma_{\lambda_j\nu}^*\gamma_{\lambda_{j'}\nu'}).\end{aligned}\quad (\text{H.23})$$

where γ_λ is the normalised normal mode eigenvector corresponding to the frequency ω_λ , the indices ν, ν' run over x, y, z and the ion-dependent phases are defined as $\phi_j = \mathbf{k}_R \cdot \mathbf{R}_{j0}$.

References

- [1] IM Georgescu, Sahel Ashhab, and Franco Nori. Quantum simulation. *Reviews of Modern Physics*, 86(1):153, 2014.
- [2] Richard P Feynman. Simulating physics with computers. *International journal of theoretical physics*, 21(6):467–488, 1982.
- [3] Seth Lloyd. Universal quantum simulators. *Science*, pages 1073–1078, 1996.
- [4] Iulia Buluta and Franco Nori. Quantum simulators. *Science*, 326(5949):108–111, 2009.
- [5] Rainer Blatt and Christian F Roos. Quantum simulations with trapped ions. *Nature Physics*, 8(4):277–284, 2012.
- [6] Ch Schneider, Diego Porras, and Tobias Schaetz. Experimental quantum simulations of many-body physics with trapped ions. *Reports on Progress in Physics*, 75(2):024401, 2012.
- [7] Wolfgang Paul. Electromagnetic traps for charged and neutral particles. *Reviews of modern physics*, 62(3):531, 1990.
- [8] Jiehang Zhang, Guido Pagano, Paul W Hess, Antonis Kyprianidis, Patrick Becker, Harvey Kaplan, Alexey V Gorshkov, Z-X Gong, and Christopher Monroe. Observation of a many-body dynamical phase transition with a 53-qubit quantum simulator. *Nature*, 551(7682):601, 2017.
- [9] DJ Berkeland, JD Miller, James C Bergquist, Wayne M Itano, and David J Wineland. Minimization of ion micromotion in a paul trap. *Journal of applied physics*, 83(10):5025–5033, 1998.
- [10] Lowell S Brown and Gerald Gabrielse. Geonium theory: Physics of a single electron or ion in a penning trap. *Reviews of Modern Physics*, 58(1):233, 1986.
- [11] Wayne M Itano and DJ Wineland. Laser cooling of ions stored in harmonic and penning traps. *Physical Review A*, 25(1):35, 1982.
- [12] M König, G Bollen, H-J Kluge, T Otto, and J Szerypo. Quadrupole excitation of stored ion motion at the true cyclotron frequency. *International Journal of Mass Spectrometry and Ion Processes*, 142(1-2):95–116, 1995.
- [13] Joseph W Britton, Brian C Sawyer, Adam C Keith, C-C Joseph Wang, James K Freericks, Hermann Uys, Michael J Biercuk, and John J Bollinger. Engineered two-dimensional ising interactions in a trapped-ion quantum simulator with hundreds of spins. *Nature*, 484(7395):489–492, 2012.

- [14] Tobias Schätz, Axel Friedenauer, Hector Schmitz, Lutz Petersen, and Steffen Kahra. Towards (scalable) quantum simulations in ion traps. *Journal of Modern Optics*, 54(16-17):2317–2325, 2007.
- [15] Roman Schmied, Janus H Wesenberg, and Dietrich Leibfried. Optimal surface-electrode trap lattices for quantum simulation with trapped ions. *Physical review letters*, 102(23):233002, 2009.
- [16] John J Bollinger, Joseph W Britton, and Brian C Sawyer. Simulating quantum magnetism with correlated non-neutral ion plasmas. In *AIP Conference Proceedings*, volume 1521, pages 200–209. AIP, 2013.
- [17] RC Thompson and J Papadimitriou. Simple model for the laser cooling of an ion in a penning trap. *Journal of Physics B: Atomic, Molecular and Optical Physics*, 33(17):3393, 2000.
- [18] J Dalibard and Claude Cohen-Tannoudji. Dressed-atom approach to atomic motion in laser light: the dipole force revisited. *JOSA B*, 2(11):1707–1720, 1985.
- [19] Joseph Wang. Phonon-mediated quantum spin simulator employing a planar ionic crystal in a penning trap. *Physical Review A*, 87(1):013422, 2013.
- [20] DA Baiko. Coulomb crystals in the magnetic field. *Physical Review E*, 80(4):046405, 2009.
- [21] RJ Hendricks, ES Phillips, DM Segal, and RC Thompson. Laser cooling in the penning trap: an analytical model for cooling rates in the presence of an axializing field. *Journal of Physics B: Atomic, Molecular and Optical Physics*, 41(3):035301, 2008.
- [22] Sergio Blanes, Fernando Casas, JA Oteo, and José Ros. The magnus expansion and some of its applications. *Physics Reports*, 470(5-6):151–238, 2009.
- [23] C-C Joseph Wang and JK Freericks. Intrinsic phonon effects on analog quantum simulators with ultra-cold trapped ions. *Physical Review A*, 86(3):032329, 2012.
- [24] PJ Lee, KA Brickman, L Deslauriers, PC Haljan, LM Duan, and C Monroe. Phase control of trapped ion quantum gates. *Journal of Optics B: Quantum and Semiclassical Optics*, 7(10):S371, 2005.
- [25] Klaus Mølmer and Anders Sørensen. Multiparticle entanglement of hot trapped ions. *Physical Review Letters*, 82(9):1835, 1999.
- [26] A Bermudez, PO Schmidt, MB Plenio, and A Retzker. Robust trapped-ion quantum logic gates by continuous dynamical decoupling. *Physical Review A*, 85(4):040302, 2012.
- [27] J Chiaverini and WE Lybarger Jr. Laserless trapped-ion quantum simulations without spontaneous scattering using microtrap arrays. *Physical Review A*, 77(2):022324, 2008.
- [28] C Ospelkaus, U Warring, Y Colombe, KR Brown, JM Amini, D Leibfried, and DJ Wineland. Microwave quantum logic gates for trapped ions. *Nature*, 476(7359):181, 2011.

- [29] John Chiaverini, R Brad Blakestad, Joe Britton, John D Jost, Chris Langer, Dietrich Leibfried, Roee Ozeri, and David J Wineland. Surface-electrode architecture for ion-trap quantum information processing. *arXiv preprint quant-ph/0501147*, 2005.
- [30] Louis Deslauriers, S Olmschenk, D Stick, WK Hensinger, J Sterk, and C Monroe. Scaling and suppression of anomalous heating in ion traps. *Physical Review Letters*, 97(10):103007, 2006.
- [31] Dustin A Hite, Kyle S McKay, S Kotler, D Leibfried, David J Wineland, and David P Pappas. Measurements of trapped-ion heating rates with exchangeable surfaces in close proximity. *MRS Advances*, 2(41):2189–2197, 2017.
- [32] Jaroslaw Labaziewicz, Yufei Ge, Paul Antohi, David Leibbrandt, Kenneth R Brown, and Isaac L Chuang. Suppression of heating rates in cryogenic surface-electrode ion traps. *Physical review letters*, 100(1):013001, 2008.
- [33] FN Krauth, J Alonso, and JP Home. Optimal electrode geometries for 2-dimensional ion arrays with bi-layer ion traps. *Journal of Physics B: Atomic, Molecular and Optical Physics*, 48(1):015001, 2014.
- [34] Manuel Mielenz, Henning Kalis, Matthias Wittmer, Frederick Hakelberg, Ulrich Warring, Roman Schmied, Matthew Blain, Peter Maunz, David L Moehring, Dietrich Leibfried, et al. Arrays of individually controlled ions suitable for two-dimensional quantum simulations. *Nature communications*, 7:ncomms11839, 2016.
- [35] Simcha Korenblit, Dvir Kafri, Wess C Campbell, Rajibul Islam, Emily E Edwards, Zhe-Xuan Gong, Guin-Dar Lin, LM Duan, Jungsang Kim, Kihwan Kim, et al. Quantum simulation of spin models on an arbitrary lattice with trapped ions. *New Journal of Physics*, 14(9):095024, 2012.
- [36] Françoise Tisseur and Karl Meerbergen. The quadratic eigenvalue problem. *SIAM review*, 43(2):235–286, 2001.
- [37] Steve Barnett. Matrix polynomials (i. gohberg, p. lancaster and l. rodman), 1983.